ON LATTICE TOPOLOGICAL FIELD THEORIES WITH FINITE GROUPS

N.J.B. AZA AND F. DORESTY F.

Abstract. The approach of Lattice Topological Field Theories is used to describe quantities which are independent of manifolds, and the same time Lattice Gauge Theories are important to renormalize continuous theories. Therefore, the natural connection between both theories can be made to understand physical topological theories. In this work, we review the basic concepts of each theory and study gauge theories coupled with matter fields in two-dimensional manifolds. In order to proceed, we first describe a formalism in two and three dimensions which is based on the idea of Kuperberg of defining a topological invariant in three dimensions using Hopf algebras and Heegaard diagrams. This formalism is useful in the context of our analysis because it allows to easily identify topological limits without solving the model. Furthermore, we write the gauge model with matter fields choosing the unitary gauge, working with finite groups, in particular with the abelian group $\mathbb{Z}_n$ and explaining the $\mathbb{Z}_2$ case in detail. We calculate partition functions and Wilson loops for this group in different topological limits. We show that there were cases in which the results depended on the triangulation although in a trivial way, these cases are called quasi-topological.

Contents

Date: June 02, 2014.

1. Introduction

In recent years, Topological Field Theories (TFT) have been advantageous for understanding the non-perturbative structure of continuous models, such as string theories to quantize gravity [GSW87a, GSW87b, Wit88]. Witten uses the Jones polynomials to show the relevance of topological theories in physics, in particular in connection with Quantum Field Theory (QFT) [Jon87, Wit89], which in turn can be described as a lattice model when the continuum limit is taken. In such models gravity is quantized following the prescriptions of loop quantum gravity [Reg61, Iwa95, BDR11]. A relation between lattice models and topological theories have been developed by Fukuma, Hosono, Kawai, Chung and Shapere (FHKCS) in [FHK94, CFS94] , where the authors formulate a Lattice Topological Field Theories (LTFT) in two and three dimensions. Moreover, it has been shown that their ideas can be generalized [CKS98], being possible to go to a higher number of dimensions. Thanks to the fact that on the lattice all scales are equivalent, the use of a LTFT allows the study of the geometry and the algebraic structure of the corresponding TFT even without recurring to the limiting procedure from discrete to continuum.

Topological invariants in physics or mathematics have direct relevance to topological theories, they represent in fact quantities that can be calculated on a manifold $\mathscr{M}$ independently of the metric or discretization used [Wit89] (in phys such quantities correspond generally to the partition function). In the lattice there are several ways to define topological invariants, such as: the Dijkgraaf-Witten invariants [DW90], the Turaev-Viro invariants [TV92] and invariants constructed from Hopf algebras, via Kuperberg method [Kup91], which is the case of the invariants that we use in this paper. While Kuperberg defined topological invariants using Hopf algebras for the three-dimensional case when the Hopf algebra is involutory, he later introduced a generalization for the non-involutory case [Kup96]. Kuperberg invariants for triangulations are represented by Heegard diagrams [PS97, Joh], and FHKCS [FHK94, CFS94] showed that there exist a one to one relation between these and semisimple algebras in the two-dimensional case and involutory Hopf algebras in the three-dimensional case. Hopf algebras then connect Kuperberg invariants and LTFT.

For a partition function Z over a manifold $\mathscr{M}$ to be topological invariant, it has to be independent of the discretization or "triangulation" of the manifold $\mathscr{M}$. This means that for two different triangulations $\mathscr{T}_1$ and $\mathscr{T}_2$ the value found for the partition function is the same, i.e., $Z(\mathscr{M}, \mathscr{T}_1) = Z(\mathscr{M}, \mathscr{T}_2)$. When this happens, the theory is called a TFT. Since the manifold is the same for both triangulations, there must exist some way to go from one triangulation to the other in a finite number of steps, a requirement satisfied by the Pachner moves [Pac78, Pac91, Rob05, DH12] that need to be taken into account in the construction of a LTFT. Finally, if Z trivially depends on the size of the lattice it is said that the theory is a Quasi-Topological Field Theory (QTFT) [YTSM09, Yok05, FPTS12, Ber12, Aza13].

On the other hand, we look back to Lattice Gauge Theories (LGT). These appeared for the first time when Wegner wanted generalize the Ising model by placing the spin variables, $\sigma(l)$, on the links of the lattice [Weg71]. Using this procedure, it was shown that in this model there was no spontaneous magnetization and the phase diagrams of the theory were not trivial [Kog79]. To distinguish the phases of the model, Wegner introduced a gauge invariant quantity, $W_\ell = \prod_{l\in\ell} \sigma(l)$ around a closed loop ℓ and it was enough to show the called area's and perimeter's law for different energy regimes [GP96]. Formally, LGT were proposed by Wilson in [Wil74], using the idea of lattice regularization of non-abelian gauge theory of a continuum theory. One of his first results was that in a pure gauge theory (without matter fields) the quarks are confined. This means that the energy to separate two charges increases linearly with the distance between them making therefore impossible to create single charges [FM83]. On the other hand, without gauge fields, the theory is topological [Bou97]. In the case when gauge and matter fields are present, Wilson's basic ideas can not predict the existence of charges and consequently different methods in condensed matter were developed, such as the recent ones by Wen [Wen04, Wen03] and others. In particular to classify the differents states of the matter at temperature 0°K, via topological order and quantum order, which are general propierties of states to this temperature [LW05, LW06, BPT13].

As mentioned, LGT can generalize Ising models and methods of statistical mechanics can be used for solving them. At the same time, we know that despite the formal simplicity of the Ising model, it is extremely difficult to find analytical solutions for it. In the one-dimensional case the exact analytic value of the partition function (with and without external magnetic field) is known [Sal10], however, when more dimensions are considered an analytical value is not known, except for the two-dimensional case without external magnetic field for which an exact solution is available [Sei82]. In the presence of a magnetic field, the Ising model in two dimensions is dual to a gauge theory coupled to matter fields. Finally, the three-dimensional Ising model, is dual to a gauge theory with gauge group $\mathbb{Z}_2$ [YT07].

For the gauge-Higgs model in the two-dimensional case, with finite gauge group G, the parameter space in the topological limit is represented by the figure 1. This

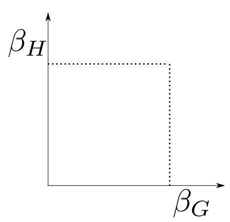

FIGURE 1. Parameter space.

diagram corresponds to coupling constants with positive sign and the dotted boundaries represent the limits $\beta_{G,H} \to \infty$. It is known that on the solid and dotted lines, an exact value for the partition function exists corresponding to the topological and quasi-topological limits of the theory respectively.

Our purpose in this paper is to review lattice topological theories for finite groups and apply it to extend the phase diagram of figure 1 using the gauge group $\mathbb{Z}_2$, for a two-dimensional, orientable, connected and closed manifold $\mathscr{M}$. We will make this based in LTFT and LGT analyzing first the case of negative coupling constants in

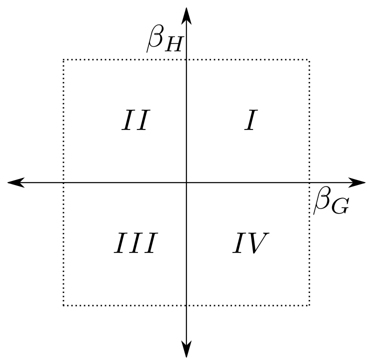

FIGURE 2. Parameter space. Cases where the partition function and the Wilson loops are calculable.

the topological limits. Then, we will observe what happens when coupling constants with different sign are considered also in topological limits, a case that has not been studied before. The resulting full phase diagram is shown in figure 2. We will get an exact value for the partition functions and the expectation value of observables, Wilson loops, in both the solid and dotted lines.

This paper is organized as follows.

In section 2 we review what is a lattice gauge theory in two and three dimensions for finite groups. We recall which are the gauge transformations when gauge fields are coupled with matter fields. We will also make a particular choice of gauge called unitary gauge. We do this for the gauge group $\mathbb{Z}_n$ and we write a gauge-Higgs action for this instance. Making use of the formalism of Kuperberg [Kup91], we represent two-dimensional and three-dimensional lattices in terms of curves.

In section 3 we discuss Lattice Topological Field Theories (LTFT). We describe the formalism provided by FHKCS [FHK94, CFS94], for two-dimensional and three-dimensional manifolds. We write the partition function and Wilson loops in terms of contractions of certain tensors M, Δ and S, and we define the topological and quasi-topological theories. In particular, the partition function coincides with the one provided by Kuperberg. We show topological invariance in the language of curves, i.e., we show the invariance by Pachner moves for the case where a two-dimensional gauge theory is coupled with a matter field.

In section 4 we use character expansions to describe the gauge model for a general finite group, in particular the dihedral group D_6 and for $\mathbb{Z}_n$ we find the curve that describe the parameter space of the model. We show that for $\mathbb{Z}_2$ the coefficients describing the pure gauge model γ^0_G and γ^1_G, are related by the hiperbola-equation $\gamma^0_G\gamma^1_G = 1$, which is represented by the dotted curve in figure 3. The values where the partition function is calculated correspond to the dotted line, $\beta_G = 0$ and solid lines, $\beta_G \to \pm\infty$. A similar graph is obtained for the pure Higgs model. We will see that the parameter space of figure 3 can be extended for negative values of the parameters γ^0_G and γ^1_G, for the $\mathbb{Z}_2$ case. Thus, the partition function and the

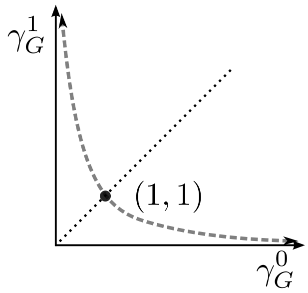

FIGURE 3. Parameter space. Cases where the partition function and the Wilson loops are calculable.

Wilson loops can also be calculated in regions of the parameter space which do not correspond to any physical model and only carry a mathematical meaning.

Finally, in section 5 we summarize the results found for partition functions and Wilson loops were found. Thanks to the diagrammatic and algebraic formalism developed here and from other works in the same field, we expect that the methods presented in this work lead to find interesting applications in the near future.

2. Lattice Gauge Theory

In this section, our goal is to explain the basis of the formalism introduced by Wegner and Wilson in [Weg71] and [Wil74], respectively. First, we state the basic definition of a lattice gauge theory taking the gauge group as finite. We present the action of the theory when we consider gauge fields associated to matter fields. Furthermore, we study the gauge transformations which satisfy the fact that the action is gauge invariant. We define the expected value of observables, which are constructed like gauge invariants and called Wilson loops. In the following subsection, we define a gauge-Higgs model for the discrete gauge group $\mathbb{Z}_n$, using a particular gauge. Finally, we discuss about the formalism of colored curves for two-dimensional manifolds, who is based in Heegaard diagrams, which are a tool for studying three-dimensional manifolds.

2.1. **Basic properties of a lattice gauge theory.** A lattice is a discretization of a manifold $\mathscr{M}$ composed by vertices v, links e and faces f. The vertices can be thought as a finite set of points on the manifold, the links as lines that connect two different points and the faces as surfaces that are bounded by a set of links joined between them via vertices. In accordance with this, every link e has two vertices in its boundary called $\{v_1, v_2\}$. In the same way, every face f has in its boundary a sequence of links $(e_1, \ldots, e_k)$, such that every link e_i has one vertex in common with the preceding link e_{i-1} and the other vertex in common is the link e_{i+1}. It is said that the link e is oriented if it is possible to distinguish the initial vertex $s(e)$ and the final vertex $t(e)$. Furthermore, it is said that the face f is oriented if it is possible to choose a sequence of links in its boundary in a cyclic form [Rob05], see figure 4(a). Finally, we say that the lattice is oriented when it is oriented in links and faces at the same time. In order to define a gauge configuration, we consider a group G where each link e_i will be associated to the variable $g_{e_i} \in \mathsf{G}$, as shown in 4(b). We recognize g_{e_i} as the parallel transport operator of $s(e_i)$ to $t(e_i)$ [Wit91]. We now define the holonomy for the face f by ordering the links $(e_1, \ldots, e_n)$ at the boundary ∂ of f [BDHK13]. We multiply the group elements associated to every link

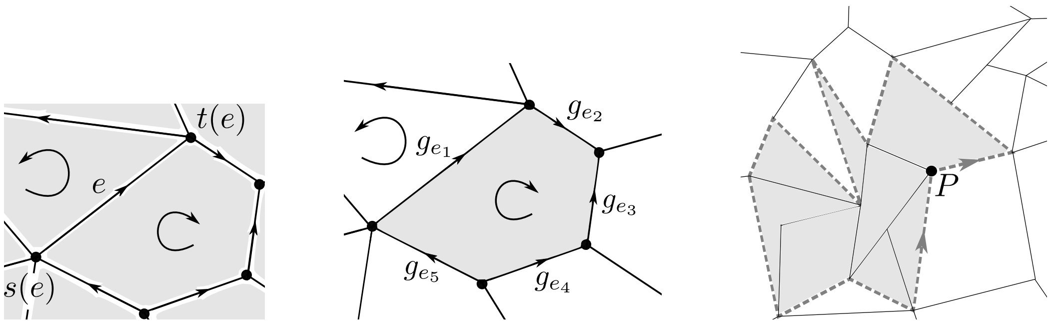

(a) Oriented link e, with inicial vertex $v_1(e) = s(e)$ and final vertex $v_2(e) = t(e)$.

(b) Gauge configuration.

(c) Loop with inicial point P.

FIGURE 4. Construction of a discrete gauge theory.

$(g_{e_1}, \ldots, g_{e_n})$ according to the cyclic order. The orientation of the links is induced by the orientation of the face (and $g_e = g_{e^{-1}}^{-1}$ where e^{-1} is the link with opposite orientation to the link e) [BDR11]. We take the relative orientation face-link by $o_i(f, e_i) = \pm 1$ for every link e_i around the face f. Explicitly, an holonomy is defined as

$$U_f \equiv \prod_{e_i \in \partial^2 f} g_{e_i}^{o_i(f,e_i)}. \tag{1}$$

When this is written, we choose an initial vertex to make a proper sequence of the cyclical ordering of links.
Holonomies can be calculated also for composed polygons of many plaquetes as follows (figure 4(c)): we choose some initial point P in the lattice such that it coincides with the end point of a path. We take a particular direction through each link where each one of these has associated an element of the group G. Then, we note that the holonomy depends on the relative orientation path-link in expression (1).

Let us now recall that the group G is divided into conjugacy classes by the following relation: we say that x is in the same class of y if there is a $g \in \mathsf{G}$ such that $y = gxg^{-1}$ and we write $x \sim y$, because this is an equivalence relation. Using the last sentence, we define $\psi : \mathsf{G} \to \mathbb{C}$ as a class function $\psi(x) = \psi(y)$ where x and y are conjugate elements of G. An important point about holonomies is that for a class function $\psi : U_f \to \mathbb{C}$, ψ is invariant under the set of gauge transformations, as we will discuss in the subsection 2.2. The physical configuration of any gauge theory can be described uniquely and faithfully by their holonomies. Indeed, holonomies can offer a popular geometric structure of work for all fundamental forces of nature. Each equivalence class of closed curves is called loop [GP96].

Clearly, when we define the action of the theory, this should be an invariant function by cyclic permutations of the links, furthermore the action will be a function of the holonomy, since the holonomy over each face is calculated without taking into account the order of links on the boundary, because the initial vertex can be anyone.

In addition, the action must be invariant by the conjugation of elements of the group; without this condition, the action is not invariant by gauge transformations (subsection 2.2). For this action, the orientation of the plaquete must be invariant due to the fact that it has to be irrelevant, i.e., by changing the orientation of a plaquete or link, the action should remain unchanged. Finally, the action must also be independent of the initial and final links when we expect to calculate the numerical value of each holonomy for each plaquete. With the conditions above, the action for finite groups is defined as

$$S_{\text{conf. faces}} = \sum_{f\in\mathscr{F}} (\psi(U_f) + \psi(U_f^{-1})), \tag{2}$$

where it is required that $\psi \to \mathbb{C}$ be a class function. However, it is clear that for abelian groups all the functions are class functions [CO83].

Note that the action of the model (2) is trivially invariant by inversion of faces, i.e., by changing the orientation of a face f by its inverse, we obtain that the holonomy U_f changes to U_f^{-1}. However, this term is considered in expression (2), so that the numeric value does not change due to holonomies. Since $\psi(U_f)$ is a class function, it is certain that it is invariant by cyclic permutations, i.e.

$$\psi(xyz) = \psi(x^{-1}(xyz)x) = \psi(yzx) = \psi(y^{-1}(yzx)y) = \psi(zxy),$$

for all x, y and $z \in \mathsf{G}$. Thus, the holonomy over every face can be calculated starting from any link around the boundary.

Let ρ be an unitary representation of G on a field F, i.e. a homomorphism ρ that sends G to $\mathsf{G}L(n, F)$, for any n, where the dimension of ρ is the integer n[1]. We can redefine the action (2) as

$$S_{\text{conf. faces}} = -\beta \sum_{f\in\mathscr{F}} (\alpha(\operatorname{tr}(\rho(U_f)) + \operatorname{tr}(\rho(U_f^{-1}))) + \gamma), \tag{3}$$

with $\rho(g)^{-1} = \rho(g^{-1}) = \rho(g)^{\dagger}$[2] [JL01], β the coupling constant, α a nonnegative real number and γ a real number, where α and γ have units such that their product with β gives dimensionless. For $\mathsf{G} = \mathbb{Z}_2$ with $\alpha = \frac{1}{2}, \gamma = 0$ we have the spin-gauge action [Bha81] and for $\alpha = -\frac{\gamma}{2} = \frac{1}{2}$ the Wilson action [ID91].

Vertex variables or matter fields can be introduced in the following way [Sei82]: the variable v_i is a map which associates the site i of the lattice with some unitary

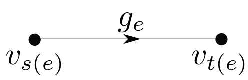

FIGURE 5. Matter fields defined on the vertices of the lattice.

vectorial space V_H of finite size, which is an unitary representation of the gauge group G (figure 5). The action for matter fields or Higgs fields, is defined as

$$S_{\text{conf. links}} = -\beta_H \sum_{\{s(e),t(e)\}} \langle v_{s(e)}, \rho(g_e)v_{t(e)}\rangle, \tag{4}$$

[1] $\mathsf{G}L(n, F)$ denotes the group of invertible matrices $n \times n$ with entries in F.
[2] The matrix $A^{\dagger}$ references the conjugate transpose of the matrix A.

where β_H is the interaction term associated with the Higgs field and $\langle v_1, v_2\rangle = \Re(\mathrm{tr}(v_1^\dagger v_2)) \in \mathbb{R}$ is the inner product. The symbol $\{s(e), t(e)\}$ in (4), refers to nearest neighbors.
Therefore, the full action is the sum of (3) and (4)

$$S_{\text{conf.}} = -\beta_G \sum_{f\in\mathscr{F}} (\alpha(\mathrm{tr}(\rho(U_f)) + \mathrm{tr}(\rho(U_f^{-1}))) + \gamma) - \beta_H \sum_{\{s(e),t(e)\}} \langle v_{s(e)}, \rho(g_e)v_{t(e)}\rangle, \tag{5}$$

where the indices G and H distinguish the gauge and Higgs fields respectively. Adding terms, the partition function for finite groups has the form

$$Z = \sum_{\text{conf.}} \mathrm{e}^{S_{\text{conf.}}}. \tag{6}$$

2.2. **Gauge transformations.** As in gauge theories in the continuum it can be also defined a gauge transformation in the lattice [BDR11, Rob05, Mor83]. This is given by a mapping $\vartheta : \mathscr{V} \to \mathsf{G}$, that assignes an element h of the group G to each vertex v. The gauge transformation for the links is defined as

$$g_e \longrightarrow h_{s(e)} g_e h_{t(e)}^{-1}, \tag{7}$$

where h_v are the gauge group elements associated to the vertices of the lattice (remember that $s(e)$ is the initial vertex of link e and $t(e)$ its final vertex). The invariant gauge information is contained in the conjugacy class of U_f. For an "oriented polygon", a loop with initial point P of n links, we choose one direction as in figure 6(a). Then we associate each link with g_{e_i} and each vertex with h_{e_i}, with the constraint $h_{e_{n+1}} = h_{e_1}$. We assume that all links are oriented, so each link has an inicial vertex and a final vertex. We see that when the orientation coincides (not coincides) with the orientation of the loop ℓ, the signal $o_i(\ell, e_i)$ in (1) on

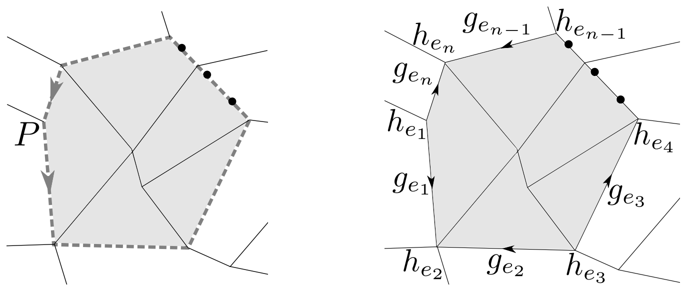

(a) Loop ℓ.

(b) Oriented links with labeled vertices.

FIGURE 6. Figure 6(a). Loop ℓ with some orientation. Figure 6(b). Oriented links in the lattice.

the orientation of the loop-link is positive (negative). Therefore, the initial vertex (with respect to loop) will be always found to the left of the transformation (7) (for example if the orientation of the loop coincides with the orientation of some link, $\{e_i\}_{i=1}^n$, then $(h_{e_i} g_{e_i} h_{e_{i+1}}^{-1})^1 = h_{e_i} g_{e_i} h_{e_{i+1}}^{-1}$. On the other hand, for inverse orientation

$(h_{e_{i+1}} g_{e_i} h_{e_i}^{-1})^{-1} = h_{e_i} g_{e_i}^{-1} h_{e_{i+1}}^{-1})$. Consequently, when the two elements associated with two consecutive links are multiplied, the result is

$$g_{e_1}^{o_1(\ell,e_1)} g_{e_2}^{o_2(\ell,e_2)} \to (h_{e_1,e_2} g_{e_1} h_{e_2,e_1}^{-1})^{o_1(\ell,e_1)} (h_{e_2,e_3} g_{e_2} h_{e_3,e_2}^{-1})^{o_2(\ell,e_2)}.$$

Additionally, $t(e_1)$ must coincide with $s(e_2)$ because both links are united. Then

$$g_{e_1}^{o_1(\ell,e_1)} g_{e_2}^{o_2(\ell,e_2)} \to h_{e_1} g_{e_1}^{o_1(\ell,e_1)} g_{e_2}^{o_2(\ell,e_2)} h_{e_3}^{-1}.$$

By induction we obtain for $1 \leqslant j \leqslant n$ that

$$\prod_{e_i \in \ell} g_{e_i}^{o_i(\ell,e_i)} \to h_{e_1} \left(\prod_{e_i \in \ell} g_{e_i}^{o_i(\ell,e_i)} \right) h_{e_{j+1}}^{-1} \text{ for } 1 \leqslant i \leqslant j.$$

Working for all links of the loop, $h_{e_{n+1}} = h_{e_1}$, we prove the following lemma [ID91]

2.1. Lemma.
The product of fields along a closed curve $\ell = e_1 e_2 \cdots e_n e_1$ drawn on the lattice

$$U_\ell = U_{e_1 e_2} U_{e_2 e_3} \cdots U_{e_n e_1}$$

is transformed like

$$U_\ell \to h_{e_1} U_\ell h_{e_1}^{-1}.$$

That is, it remains in the same conjugation class of the group.

2.2. Corollary.
For one oriented plaquete we take the orientation of the loop as the same of the plaquete. The gauge transformation $U_f \to h_{e_1} U_f h_{e_1}^{-1}$ makes that for one class function ψ

$$\psi(U_f') = \psi(U_f).$$

I.e., the necessary condition for the invariance of the action that depends on the faces (2).

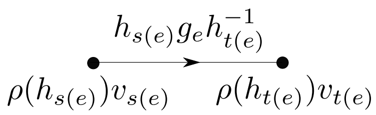

Figure 7. Gauge transformation with Higgs field.

For the Higgs field we take the gauge transformation as (figure 7)

$$v_{i(e)} \to \rho(h_{i(e)}) v_{i(e)}, \text{ for all } i(e) = s(e) \text{ or } t(e),$$

and since ρ and $v_{i(e)}$ are unitary representations, it is easy to see (using (7)), that the Higgs field associated is invariant

$$\begin{aligned}
\langle v'_{s(e)}, \rho(g'_e) v'_{t(e)} \rangle &= v'^{\dagger}_{s(e)} \rho(g'_e) v'_{t(e)} \\
&= (\rho(h_{s(e)}) v_{s(e)})^\dagger \rho(h_{s(e)} g_e h_{t(e)}^{-1}) (\rho(h_{t(e)}) v_{t(e)}) \\
&= v_{s(e)}^\dagger \left(\rho(h_{s(e)})^\dagger \rho(h_{s(e)}) \right) \rho(g_e) \left(\rho(h_{t(e)}^{-1}) \rho(h_{t(e)}) \right) v_{t(e)} \\
&= v_{s(e)}^\dagger \rho(g_e) v_{t(e)} \\
&= \langle v_{s(e)}, \rho(g_e) v_{t(e)} \rangle.
\end{aligned}$$

Summarizing, the gauge invariance is valid when the gauge transformations are [Cre80, OHZ06]

$$g_e \;\rightarrow\; h_{s(e)} g_e h_{t(e)}^{-1}, \tag{8a}$$

$$v_{i(e)} \;\rightarrow\; \rho(h_{i(e)}) v_{i(e)}, \text{ for all } i(e) = s(e) \text{ or } t(e), \tag{8b}$$

as shown above.

2.3. **Wilson loops.** Observables in gauge theories need to be gauge invariant. Therefore, it is useful to introduce a set of quantities in terms of which any gauge invariant can be written. These objects are called Wilson loops which are gauge invariant constructed, considering a closed loop ℓ and defining

$$\langle W(\ell)\rangle = \frac{\sum\limits_{\text{conf}} W(\ell)\mathrm{e}^{S_{\text{conf.}}}}{\sum\limits_{\text{conf}} \mathrm{e}^{S_{\text{conf.}}}}, \tag{9}$$

where $W(\ell) = \chi_r(U_\ell)$. χ_r are the characters, that means, the traces of the corresponding matrices in the irreducible representation. U_ℓ in (9) is the holonomy of the link variables around the closed curve ℓ.

In a pure gauge theory, for very large loops ℓ, there are two possible limit behaviors [GP96, OHZ06][3]

(1) Area law. $\langle W(\ell)\rangle \sim \mathrm{e}^{-K\times \text{area}(\ell)}$, for $\beta_G \ll 1$
(2) Perimeter law. $\langle W(\ell)\rangle \sim \mathrm{e}^{-K'\times \text{perimeter}(\ell)}$, for $\beta_G \gg 1$.

2.4. **The gauge-Higgs model.** The gauge action with Higgs fields ($\alpha = \frac{1}{2}$, $\gamma = 0$ in the expression (3)) can be written as

$$\begin{aligned} S_{\text{gauge-Higgs}} &= -\beta_G \sum_{f\in\mathscr{F}} \left(\frac{1}{2}\left(\mathrm{tr}(\rho_r(U_f)) + \mathrm{tr}\left(\rho_r\left(U_f^{-1}\right)\right)\right)\right) \\ &\quad -\beta_H \sum_{\{s(e),t(e)\}} \Re(\mathrm{tr}(v_{s(e)}^{\dagger}\rho_r(g_e)v_{t(e)})). \end{aligned}$$

For $\mathsf{G} = \mathbb{Z}_n$, the n irreducible representations denoted by $\{\rho_r\}_{0\leqslant r\leqslant n-1}$ in $\mathbb{C}$ are [JL01]

$$\rho_r(\omega^k) = \mathrm{e}^{\frac{2rk\pi}{n}\mathrm{i}} \;\; (0 \leqslant k \leqslant n-1 \text{ e } \omega = \mathrm{e}^{\frac{2\pi}{n}\mathrm{i}}).$$

Furthermore, as stated in the previous section, each link e of each face f has an associated member of the group $\mathbb{Z}_n$, therefore the representation is given by

$$\rho_r(U_f) = \exp\left(\frac{2rk_1\pi}{n}\mathrm{i}\right)\exp\left(\frac{2rk_2\pi}{n}\mathrm{i}\right)\cdots\exp\left(\frac{2rk_{N_{e_f}}\pi}{n}\mathrm{i}\right), \tag{10}$$

with N_{e_f} the number of links of the face f. In (10) 1 makes reference to the first link where the holonomy begins to be calculated and N_{e_f} to the last link of the

[3] In general Wilson loops have two fundamental properties [GP96]

- The Mandelstam identities: these are relations between Wilson loops which reflect the structure of a given gauge group.
- The reconstruction property: it can be reconstructed all the gauge invariant information of a theory from the Wilson Loops.

face. Since the irreducible representations have dimension 1×1, the character of the representation, $\mathrm{tr}(\rho_r(\omega^k)) = \chi_r(\omega^k)$ coincides with the representation. Hence, we have that

$$\chi_r(U_f) + \chi_r(U_f^{-1}) = 2\cos\left(\frac{2r(k_1 + \cdots + k_{N_{e_f}})\pi}{n}\right).$$

In this work, we use the faithful representation from the previous expression[4], i.e., $r = 1$. Given that each face has a certain number of links, the action is written as

$$S_{\text{gauge-Higgs}} = -\beta_G \sum_f \cos\left(\frac{2\pi}{n}\sum_{i=1}^{N_{e_f}} k_i\right) - \beta_H \sum_{\{s(e),t(e)\}} \Re(\mathrm{tr}(v^\dagger_{s(e)} \mathrm{e}^{\frac{2k\pi}{n}\mathrm{i}} v_{t(e)})).$$

It follows that Higgs fields at the vertices represented by v_i must be a matrix of size 1×1 and also the gauge transformation $v_{i(e)} \to \rho(h_{i(e)})v_{i(e)}$ must be satisfied. We choose $v_{i(e)} = \rho(h_{i(e)})^{-1}$ such that the field at each vertex be the unity. This gauge fixation is equivalent to a pure gauge theory coupled to a field which is not gauge invariant with coupling constant β_H. This choice is called unitary gauge [Cre80]. We represent this as in figure 8. The "new" term of matter field can be written now

$$\bullet \xrightarrow{\;h_{s(e)} g_e h^{-1}_{t(e)}\;} \bullet$$

FIGURE 8. Configuration without matter fields at vertices.

as $\mathrm{e}^{\frac{2k_1\pi}{n}\mathrm{i}}\mathrm{e}^{\frac{2k\pi}{n}\mathrm{i}}\mathrm{e}^{-\frac{2k_2\pi}{n}\mathrm{i}}$, where k_1 and k_2 are integers $(0 \leqslant k_1, k_2 \leqslant n-1)$. By cyclicity, it is clear that this new term belongs to $\mathbb{Z}_n$, then the complete action is

$$S_{\text{gauge-Higgs}} = -\beta_G \sum_f \cos\left(\frac{2\pi}{n}\sum_{i=1}^{N_{e_f}} k_i\right) - \beta_H \sum_l \cos\left(\frac{2k_l\pi}{n}\right). \tag{11}$$

For a two-dimensional manifold with gauge group $\mathbb{Z}_2$ decomposed into triangles, the partition function was exactly calculated $\beta_H = 0$, and it can be shown that this quantity depends only on the number of triangles with which the manifold is discretized [Weg71, YT07]. The general case for $\mathbb{Z}_2$ is dual to the Ising model with external field [Weg71, Kog79, Sav80], and it is well known than an exact value is still elusive. Overall for the group $\mathbb{Z}_n$ the analytic value is not known even for $\beta_H = 0$. However, for $\beta_G = 0$ the value is easily found and the model is considered topologically trivial [Bou97]. On the other hand, approaches by the Monte Carlo method in the general case were found in various articles of the text [Reb83], and it is shown that for $n \to \infty$ the behavior of the model is very similar to the $U(1)$. Our purpose is to find numerical values of the partition function and the Wilson loops for $\beta_H \neq 0$. For this reason, we consider the methods used in [YT07, FPTS12, Aza13, BPT13], where there are some techniques for calculating the partition function of three-dimensional manifolds, not for the general case $\beta_{G,H} \neq 0$, but within the limits

[4] In the case that each element of the group matches a distinct transformation, one says that the representation is faithful [Tun85].

$\beta_{G,H} \to \pm\infty$ and other points. In this work, we aim for topological limits of the gauge theory coupled with matter fields only for the two-dimensional case, because the study for the three-dimensional case is more complicated and it is not studied here.

2.5. **Colored diagrams and Heegaard diagrams.** Consider a triangularized two-dimensional manifold $\mathscr{M}$. We choose a plaquete oriented triangulation at faces as links, figure 9(a). We associated each face with a closed black curve and each

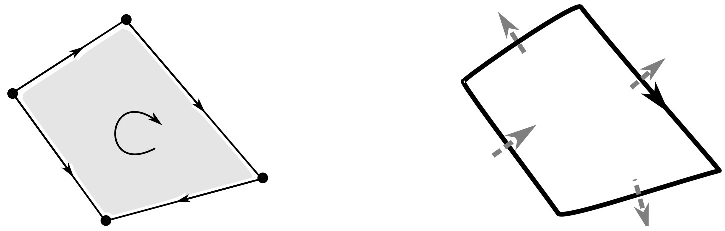

(a) Oriented plaquete in faces and links.

(b) Association of colors to plaquetes. Face, black closed curve. Gray closed curve.

FIGURE 9. Association of colors to faces and links for a triangulation.

link with a closed gray curve perpendicular to the link, figure 9(b). The relative orientation between the face and each link is determined by the intersection of their respective curves (this will be explained in detail in the section 3). Thus, we have a

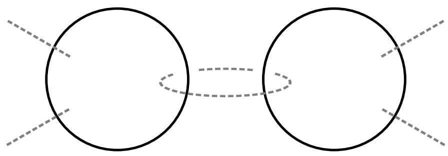

FIGURE 10. Two triangles connected by a link without representing the orientations of faces and links. We note that the gray curve which connects the two triangles seems to be in 3D. However, it was drawn in this way in order to show that the curve is closed.

set of curves for faces and links denoted by b and g respectively. The rule for each set of black or gray curves is simple: any curve can be crossed by itself and two curves of the same color do not intersect. These two conditions are compatible with the fact that every face of a triangulation and every link do not cross the other face and any other link respectively. For representing two glued triangles (being homeomorphic a closed curve, as defined here, with a circle), we use circles connected by a link (figure 10). Note that each triangle has three gray curves to denote its links, and these in turn are connected to other black curves representing the neighboring faces.

For the three-dimensional case, we consider the triangulation $\mathscr{T}$ of the manifold $\mathscr{M}$, oriented, closed, compact and connected, see figure 11(a) [Ber12, Aza13, Ale01,

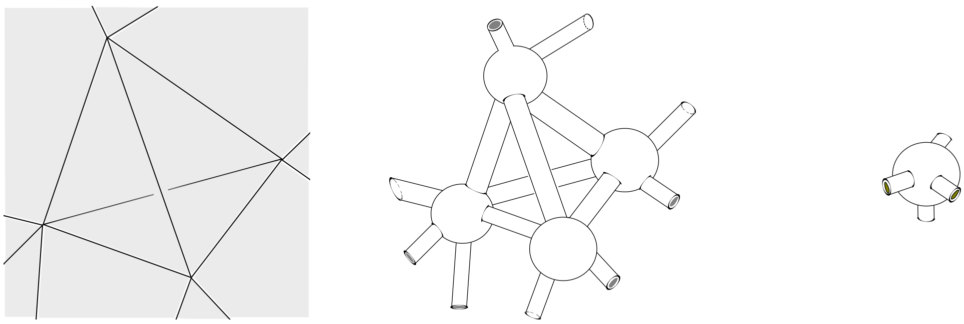

(a) (b) (c)

FIGURE 11. 11(a). Triangulation in 3D. 11(b). Regular neighborhood of a 1-skeleton, handlebody H_{g}. 11(c). Part of a regular neighborhood of a dual 1-skeleton, handlebody H_{b}. It is just a 3-ball of the dual 1-skeleton.

Joh, BPT13]. It is well known that a regular neighborhood of a 1-skeleton $\mathscr{S}$ in a three-manifold is a handlebody, H_{g} (figure 11(b))[Joh]. On the other hand, the dual 1-skeleton to $\mathscr{S}$, called $\mathscr{S}^*$, has also a regular neighborhood which is also a handlebody, this will be called H_{b} (figure 11(c)). Furthermore, there is a handlebody

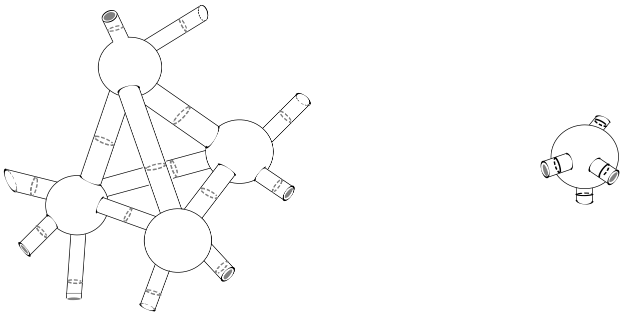

(a) (b)

FIGURE 12. 12(a). The handlebody H_{g} has associated finite set of closed curves, g. 12(b). The handlebody H_{b} has associated finite set of closed curves, b.

H of genus g, homeomorphic to H_{g} and H_{b} [Ale01, Joh]. Therefore, we note that there is a finite collection of disjoint 2-disks, $\{D_1, \ldots, D_g\}$ which are cut in a set of disjoint 3-balls. We use H_{g} to represent the boundaries of these discs by gray (dotted) curves (figure 12(a)). In a similar way, there is a finite collection of 2-disks, $\{D'_1, \ldots, D'_g\}$ which cuts H_{b} in a set of disjoint 3-balls. We represent the boundaries of these disks by black curves (figure 12(b)). The set of gray curves is denoted by $\mathsf{g} = \{\mathsf{g}_1, \ldots, \mathsf{g}_g\}$ and the set of black curves by $\mathsf{b} = \{\mathsf{b}_1, \ldots, \mathsf{b}_g\}$.
Now, since H is homeomorphic to H_{g} and H_{b} there is a function ϕ such that maps the gray closed curves g in H_{g}, in the handlebody H_{b}. The surface where both finite finite closed curves are living will be called Σ, figure 13(a). Also there is a

function φ such that maps the closed curves b in H_{b}, in the handlebody H_{g}. The

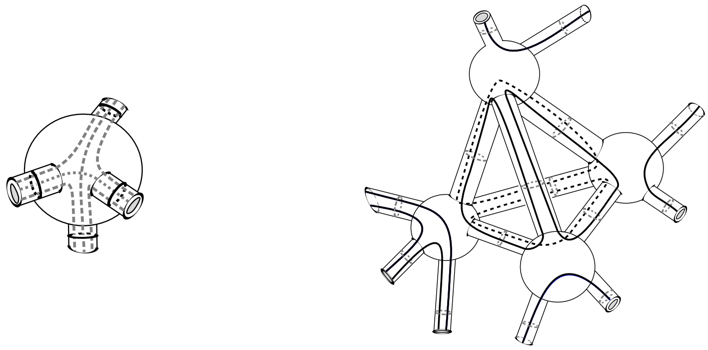

(a) (b)

FIGURE 13. 13(a). Heegaard diagram. 13(b). Dual Heegaard diagram.

surface where both finite closed curves are living will be called Σ', figure 13(b). The collections $\mathsf{b} = \{\mathsf{b}_1, \ldots, \mathsf{b}_g\}, \mathsf{g} = \{\mathsf{g}_1, \ldots, \mathsf{g}_g\}$ motivate the following definition [Ber12, Ale01, Joh]

2.1. **Definition** (Heegaard diagram)**.** A Heegaard diagram is a triple $D = (\Sigma, \mathsf{b}, \mathsf{g})$, where Σ is a surface of genus g closed, oriented and connected and

$$\mathsf{b} = \{\mathsf{b}_1, \ldots, \mathsf{b}_g\}, \mathsf{g} = \{\mathsf{g}_1, \ldots, \mathsf{g}_g\}$$

are two pairs of systems of disjoint closed curves on Σ such that the complements of $\cup_i \mathsf{b}_i$ and $\cup_i \mathsf{g}_i$ are connected. The curves b_i (resp. $\mathsf{g} = \{\mathsf{g}_k\}$) are called black curves (resp. gray) of the diagram. Note that the set $\mathsf{b} \cap \mathsf{g}$ is finite and it can be supposed that the curves meet transversely. The Heegaard diagram D is called oriented if all black and gray curves are oriented.

The advantage of using curves is that we can employ them to obtain simpler curves. For example, the Heegaard diagram 13(a) can be deformed continuously for obtaining the figure 14(a). We represent the Heegaard diagram without surface,

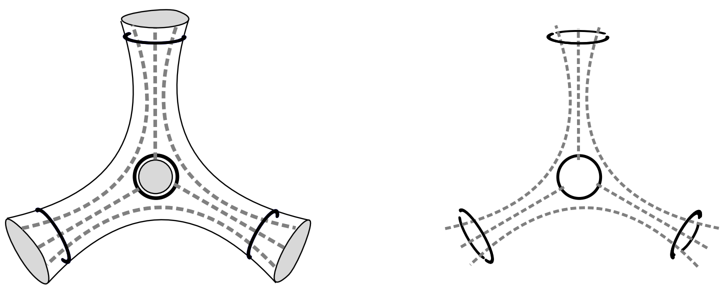

(a) (b)

FIGURE 14. 14(a). Modified Heegaard diagram. The regions of gray color are the holes in the surface. 14(b). Simplified Heegaard diagram.

like in figure 14(b). This diagram is called simplified Heegaard diagram. Diagrams corresponding to dual Heegaard diagram 13(b) can be obtained in a similar way. We can note, that in the Heegaard diagram, the black closed curves are relationed with the faces of the original triangulation and the gray closed curves with the links. This representation of a manifold can be used to describe a theory in three-dimensions [Kup91, BPT13].

As follows, we give the rules to know how the curves can be deformed. Formally, it is said that two colored diagrams (for the two-dimensional case) or Heegaard diagrams (for the three-dimensional case) are equivalent, if it is possible to obtain one from one another with a finite sequence of the following moves [Ale01]:

- Homeomorphism of the surface: Let $\mathscr{S}$ and $\mathscr{S}'$ be closed, connected and oriented surfaces. If $\mathscr{S}$ is homeomorphic to $\mathscr{S}'$, black curves (resp. gray) on $\mathscr{S}$ are homeomorphic to black curves (resp. gray) on $\mathscr{S}'$. The colors of the curves are equal.
- Orientation reversal: The orientation of black curves (resp. gray) is replaced by its inverse. The inverse of the black curve b_i is b_i^{-1}. Analogously, g_j^{-1} is the inverse of the gray curve g_j.
- Two point move: If the black curve intersects twice a gray curve, as in figure

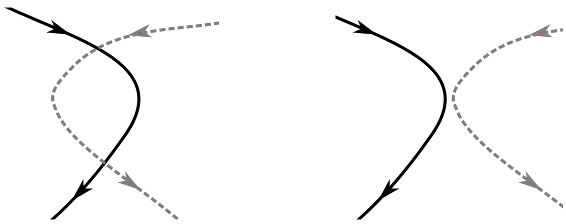

(a) Before. (b) After.

FIGURE 15. Two point move property.

15(a), one can eliminate the crossing as it is shown in figure 15(b). The color of each curve is invariant after separating them.
- Stabilization: Let $\mathscr{T}_1$ be a torus with genus one and let $\mathscr{T}_2$ be a torus of genus greater than or equal to one, both with their respective black and gray curves. If the black and gray curves of the two torus are disjoint, it can be added or removed the torus $\mathscr{T}_1$.
- Sliding: Let C_1 and C_2 be two closed curves of the same color in a colored diagram or Heegaard diagram over a surface $\mathscr{S}$. Let $b \in \mathscr{S}$ be the connection between C_1 and C_2 as in figure 16(a). The curve C_1 is replaced by the curve C_1'. The new curve C_2' is an isotopy of C_2. The curve C_1' (resp. C_2') has the same orientation of C_1 (resp. C_2) as it is shown in figure 16(b).

3. Topological and Quasi-Topological Theories

In mathematics, it is well known that each manifold $\mathscr{M}$ connected, closed and orientable, can be triangularized in different ways. In the particular case of one manifold with the topology of a torus, it may be sticked two triangles as it is shown in figure 17(a). However, we could also describe the same torus by gluing three

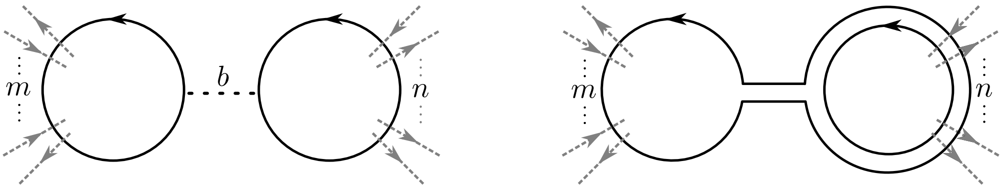

(a) Two curves of the same color glued by a ribbon.

(b) Sliding.

FIGURE 16. 16(a). The curve C_1 (resp. C_2) has m (resp. n) crosses with curves of different color. 16(b). After sliding the final curve C_1' (resp. C_2') has $m+n$ (resp. n) crosses with curves of different color.

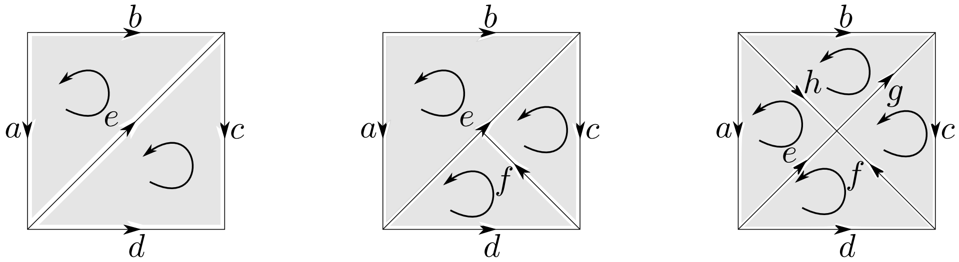

(a) Torus represented by two triangles.

(b) Torus represented by three triangles.

(c) Torus represented by four triangles.

FIGURE 17. Three equivalent ways to represent a torus. Note that we have to paste the links a and c, and also links b and d. All faces and links are properly oriented.

or four triangles (see figure 17(b) and 17(c)). On the other hand, it has physical interest to define invariant quantities of the topology, such as the partition functions which should not depend on the triangulation of the discretized manifold, because it is only a calculation tool. However, it is not necessarily so. It means that, the theory may depend on the number of constituents of triangulation, such as: links, triangles and tetrahedra. However, this dependence is trivial. In this section, we show how one can build a theory which in principle does not depend on the lattice details. To achieve this, we define topological theories and quasi-topological theories.

3.1. **Topological Theories.** Fukuma, Hosono, Kawai, Chung and Shapere provide a formalism to describe lattice topological field theories in two and three dimensions [FHK94, CFS94] and the basic ideas are described as follows: suppose a manifold $\mathscr{M}$ with triangulation $\mathscr{L}$. Let $\mathscr{L}$ be a lattice composed by a collection of oriented polygons with faces joined by hinges. Now, we color the lattice by associating to each face one element x of a set X (similar to the previous section where we associate a gauge group G with the faces of a lattice using the holonomy). When this is done, the rule which determines the weight for each polyhedron as a function of coloreds of the faces is established. The partition function is the total sum of these weights in all triangulations with their respective weights. In the three-dimensional

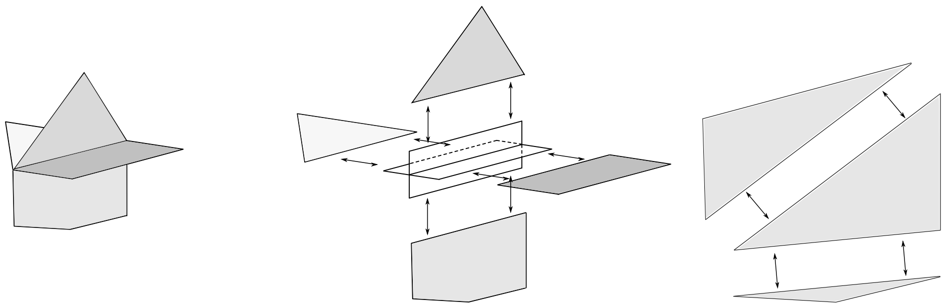

(a) Polygons glued. (b) Hinges where polygones are glued. (c) Polygon decomposed into triangles.

Figure 18. Decomposition of a tridimensional lattice into faces and hinges.

case many faces can be glued with a hinge, which is an open neighborhood of the line in which the faces stick together (see figure 18(a) and 18(b)). The theory is described assuming that each polygon can be decomposed into triangles (figure 18(c)). Therefore, we can simply specify which are the weights of the triangles by merely introducing the rule of gluing between triangles.

Now, we define the possible weight of a any face f: imagine a polygon as in figure 19(a). We associate t o each link of the polygon an element a_i of a group G which can be finite or infinite, and we associate to each polygon a symmetric tensor

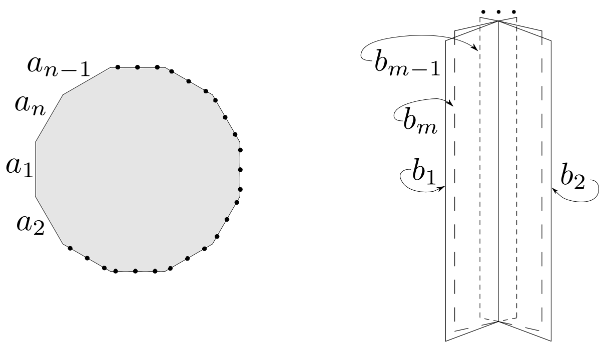

(a) Face with n links has associated a tensor $M_{a_1 a_2 \cdots a_{n-1} a_n}$. (b) Hinges with m polygons glued. They have associated a tensor $\Delta^{b_1 b_2 \cdots b_{m-1} b_m}$.

Figure 19. Diagramatic representation of a face and hinge.

$M_{a_1 a_2 \cdots a_{n-1} a_n}$, being n the number of links of the polygon. We choose a cyclic tensor M, i.e., $M_{a_1 a_2 \cdots a_{n-1} a_n} = M_{a_2 \cdots a_{n-1} a_n a_1} = \cdots = M_{a_n a_1 a_2 \cdots a_{n-1}}$; we perform a similar for each hinge h, as it is shown in figure 19(b), i.e., we associate the tensor $\Delta^{b_1 b_2 \cdots b_{m-1} b_m}$, where m is the number of polygons which are glued by the hinge. The tensor Δ is also cyclical, i.e., $\Delta^{b_1 b_2 \cdots b_{m-1} b_m} = \Delta^{b_2 \cdots b_{m-1} b_m b_1} = \cdots = \Delta^{b_m b_1 b_2 \cdots b_{m-1}}$.
Being able to decompose polygons into triangles is the first condition to construct a lattice topological theory. We have defined how polygons are glued and the two-dimensional case is a simple one as it is shown in following example

3.1. **Example.** Consider an oriented polygon of four links as shown in figure 20(a), with tensor M_{abcd} (figure 20(d)) associated with it. Due that we have four links, this

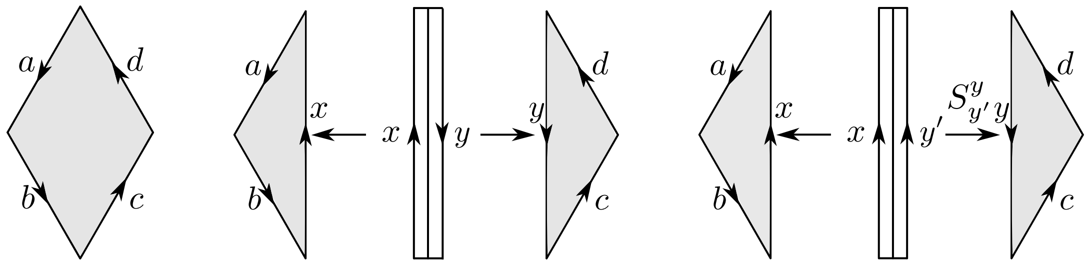

(a) Face with 4 links.

(b) Two glued faces with one hinge.

(c) Two glued faces with one hinge.

M_{abcd}

(d) Tensor associated to figure 20(a).

$M_{abx}\Delta^{xy}M_{ycd}$

(e) Tensor associated to figure 20(b).

$M_{abx}\Delta^{xy'}S^{y}_{y'}M_{ycd}$

(f) Tensor associated to figure 20(c).

FIGURE 20. The way to stick two polygons with their respective tensors.

polygon can be decomposed into two triangles which are glued by means of a hinge. Each triangle will have an associated tensor M with three indices and the hinge is represented by the tensor Δ with two indices. Therefore, the tensor M_{abcd} is written as $M_{abx}\Delta^{xy}M_{ycd}$ (figures 20(b) and 20(e)). Note that we are only contracting the tensors by using the rule of indices between lower and upper indices for M and Δ respectively. As it was stated, tensors M and Δ are cyclically symmetric. However, the relative orientation face-link must be taken into account when contracting tensors. For this reason, we introduce the operator S^y_x whose function is to change the direction of a link into a hinge. In figure 20(c), we change the orientation of a link and we associate the contraction of tensors $M_{abx}\Delta^{xy'}S^{y}_{y'}M_{ycd}$ represented by 20(f).

The same rules for gluing are used for three-dimensional polygons remembering that more than one face can be pasted on a hinge. When this is done, we define that the partition function[5] of the triangulation is $Z(\mathscr{M},\mathscr{T}) = \sum\prod M_{xyz}\Delta^{uv}S^{w}_{t}$, where the sum is over all the labels, and the product is for all the elements f, h and its orientations o. The partition function is topological invariant if it does not depend on the triangulation, because the triangulation is merely a helpful tool, and in turn, the results should not depend on it. Therefore, we have to connect in some way two different triangulations of the same manifold, then the concept of moves is used which satisfies all the mentioned requirements. These moves were discovered by Pachner in the general case of n-dimensional manifolds. These have the important property that if $\mathscr{T}_1$ and $\mathscr{T}_2$ are triangulations of the same manifold $\mathscr{M}$, by using a finite number of steps, we obtain the triangulation $\mathscr{T}_2$ starting from $\mathscr{T}_1$. In a similar way, it is possible to obtain $\mathscr{T}_1$ from $\mathscr{T}_2$ [CKS98, Pac78, Pac91, Rob05]. The moves

[5]This function was defined in a two-dimensional case, for the three-dimensional a similar expression will be defined.

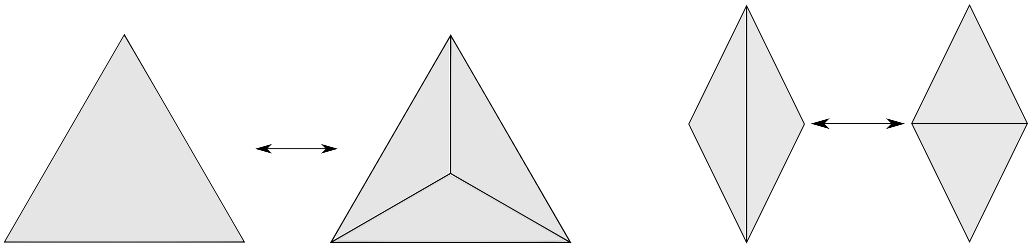

(a) Pachner move (1,3), (3,1). (b) Pachner move (2,2).

FIGURE 21. Pachner moves in two-dimensional manifolds.

for the two-dimensional case are shown in figures 21(a) and 21(b). These are called Pachner moves from (1,3) and (2,2), due to the number of triangles that are related. For the three-dimensional case, we have more complicated moves, however, these are not shown in this work because we are interested in a two-dimensional theory. Different moves in three-dimensional can be found in [Ber12, Pac78] and moves in four-dimensional are discussed in [CKS98, DH12].

Now, recall the formalism of colored curves provided in the previous section: each face corresponds to a black curve and every link to a gray curve. Thus, taking into account the number of faces and links, for the two-dimensional case, the Pachner

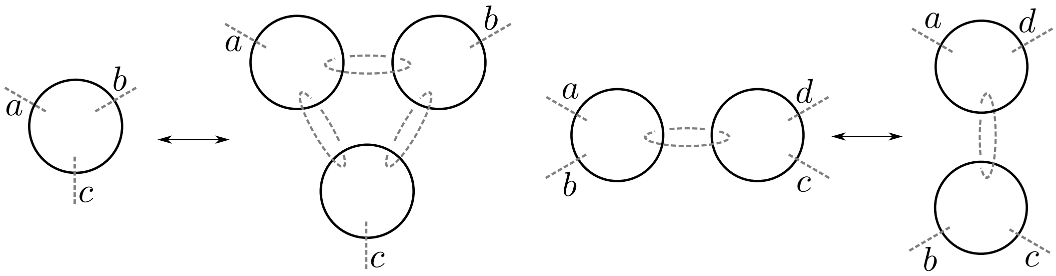

(a) Pachner move (1,3), (3,1). (b) Pachner move (2,2).

FIGURE 22. Pachner move like colored curves.

moves (1,3) and (2,2) are shown in figures 22(a) and 22(b). Note that the curves are not representing the orientations of any of them. As we mentioned in section 2, the Heegaard diagrams are the colored diagrams for the three-dimensional case and the Pachner moves are a slightly more complicated than 22(a) and 22(b), because these are based in glued multiple Heegaard diagrams. The basic Heegaard diagram used for it, is shown in figure 14(b), which corresponds to a polygon with four faces and six links.

As it was said before, in [FHK94, CFS94] and [CKS98] it can be found the traditional formalism to construct a lattice topological field theory. Basically, it is necessary to consider that the set of polygons and hinges which represent the triangulation $\mathscr{T}$ of a manifold $\mathscr{M}$ are cyclically symmetric, and that the Pachner moves are satisfied. That was the reason for introducing the tensors M and Δ besides the face-link orientation represented by the tensor S. However, in order to use the colored curves for our required computation of the partition function and Wilson loops, we will show in the following subsection that in fact the black and gray curves are symmetric, contain the information of the orientation, and in addition satisfy the Pachner moves.

3.2. **Diagramatic formalism and colored diagrams.** There is a one to one relation between an associative semisimple algebra and a lattice topological field theory in two dimensions while there is a one to one relation between an associative Hopf algebra and a lattice topological field theory in three dimensions [FHK94, CFS94, CKS98]. This shows a relation between topological invariance and Hopf algebras. In [Kup91, Kup96] Kuperberg defines invariants when the Hopf algebra is involutory ($S^2 = 1$) and non involutory ($S^2 \neq 1$), respectively. In this work we use the algebra as involutory. For the two-dimensional case we can use an involutory Hopf algebra because if $\mathrm{tr}(S^2) \neq 0$, the algebra is semisimple, see [LR95].

The basic properties of a Hopf algebra are explained as follows. We use the diagrammatic language provided by Kuperberg which is useful to represent the basic properties of such algebras [Kup91, KR99]. Once this is done, we diagrammatically define tensors M, Δ and S [BPT13, Ale01].

3.2.1. *Diagrammatic summary of Hopf algebras.* We consider a vectorial space $\mathscr{A}$ of finite dimension $\dim(\mathscr{A}) = n$, such that its basis is denoted by $\{\phi_g\}_{g=1}^n$. The dual vectorial space is written as $\mathscr{A}^*$, with finite dimension $\dim(\mathscr{A}^*) = n$ and basis denoted by $\{\phi^h\}_{h=1}^n$. The relation between the two basis is given by the pairing $\phi^h(\phi_g) = \delta_g^h$, for $g, h = 1, \dots, n$.

We recognize the product $m : \mathscr{A} \otimes \mathscr{A} \to \mathscr{A}$ (resp. coproduct $\Delta : \mathscr{A}^* \otimes \mathscr{A}^* \to \mathscr{A}^*$) associative (resp. coassociative), i.e. for elements of the basis $\phi_g, \phi_h, \phi_k \in \mathscr{A}$ (resp. $\phi^g, \phi^h, \phi^k \in \mathscr{A}^*$), we have

$$[m(m \otimes 1)](\phi_g \otimes \phi_h \otimes \phi_k) = [m(1 \otimes m)](\phi_g \otimes \phi_h \otimes \phi_k)$$

(resp. $[\Delta(1 \otimes \Delta)](\phi^g \otimes \phi^h \otimes \phi^k) = [\Delta(1 \otimes \Delta)](\phi^g \otimes \phi^h \otimes \phi^k)$). Furthermore, there is $e \in \mathscr{A}$ (resp. $\epsilon \in \mathscr{A}^*$), called the unity (resp. county), such that for all $\phi_g \in \mathscr{A}$ (resp. $\phi^g \in \mathscr{A}^*$), $m(\phi_g \otimes e) = m(e \otimes \phi_g) = \phi_g$ (resp. $(\phi^g \otimes \epsilon)\Delta = (\epsilon \otimes \phi^g)\Delta = \phi^g$). It is possible to write the product and coproduct using the basis ϕ_g through the structure constants m_{ij}^k and Δ_i^{jk}

$$\begin{aligned} m(\phi_i \otimes \phi_j) &= m_{ij}^k \phi_k, \\ \Delta(\phi_i) &= \Delta_i^{jk} \phi_j \otimes \phi_k. \end{aligned}$$

Therefore $m : \mathscr{A} \otimes \mathscr{A} \to \mathscr{A}$ and $\Delta : \mathscr{A} \to \mathscr{A} \otimes \mathscr{A}$. If additionally we have the relation

$$\begin{aligned} \Delta(m(\phi_i \otimes \phi_j)) &\equiv m(\Delta(\phi_i) \otimes \Delta(\phi_j)) \\ \to (\phi_i\phi_j)_1 \otimes (\phi_i\phi_j)_2 &\equiv (\phi_i)_1(\phi_j)_1 \otimes (\phi_i)_2(\phi_j)_2, \end{aligned} \tag{13}$$

we state that the algebra $\mathscr{A}$ is a bialgebra. Finally, if there is an element S, called the antipode, which satisfies for the product (resp. coproduct) $S(\phi_i \cdot \phi_j) = S(\phi_j)S(\phi_i)$ (resp. $S(\phi_i \otimes \phi_j) = S(\phi_j) \otimes S(\phi_i)$) and $m \circ (S \otimes 1) \circ \Delta = m \circ (1 \otimes S) \circ \Delta = e \circ \epsilon$, we invoked a Hopf algebra [CKS98, BJM10, LR88, GS96].

Graphically, the structure of a Hopf algebra $\mathscr{A}$ in a field $\mathbb{K}$ is provided by the product $m : \mathscr{A} \otimes \mathscr{A} \to \mathscr{A}$, the unity $e : \mathbb{K} \to \mathscr{A}$, the coproduct $\Delta : \mathscr{A} \to \mathscr{A} \otimes \mathscr{A}$, the counity $\epsilon : \mathscr{A} \to 1$, and the antipode $S : \mathscr{A} \to \mathscr{A}$. These are represented as in

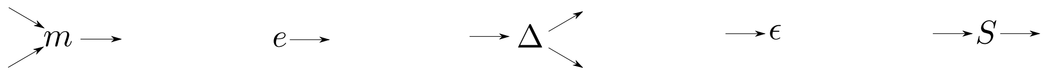

(a) (b) (c) (d) (e)

FIGURE 23. 23(a). Product. 23(b). Unity. 23(c). Coproduct. 23(d). Counity. 23(e). Antipode. Diagramatic formalism of the elements of a Hopf algebra.

figure 23. The outward arrows symbolize the product and are read counterclockwise and the inward arrows symbolize a coproduct and are read clockwise. The structure

(a) (b)

FIGURE 24. Representation of tensors m_{ij}^{k} and Δ_i^{jk}, in figures 24(a) and 24(b) respectively.

constants m_{ij}^{k} and Δ_i^{jk} for algebra and coalgebra are given by the figures 24(a) and

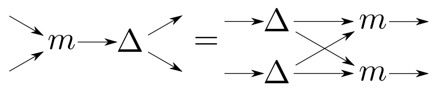

FIGURE 25. Relation between product and coproduct.

24(b). The relation of bialgebra, expression (13), is provided by figure 25. The properties of antipode are diagrammatically represented by figures 26(a) to 26(d). Hopf algebra properties can be shown using the diagrammatic formalism previously

(a) $m \circ (S \otimes 1) \circ \Delta = e \circ \epsilon$. (b) $m \circ (1 \otimes S) \circ \Delta = e \circ \epsilon$.

(c) $S(\phi_i \cdot \phi_j) = S(\phi_j)S(\phi_i)$. (d) $S(\phi_i \otimes \phi_j) = S(\phi_j) \otimes S(\phi_i)$.

FIGURE 26. Diagrammatic representation of antipode properties.

stated.
Let $(\rho(\phi_i))^b{}_a$ be the regular representation of one element ϕ_i of the basis of algebra; we write it as ϕ_i, in an abuse of notation. The trace is defined as $\mathrm{tr}(\phi_i) =$

(a) (b)

FIGURE 27. 27(a). Trace m_{ij}^{j}. 27(a). Cotrace Δ_i^{ij}.

$\sum_j m_{ij}^{j} = m_{ij}^{j}$ and it is diagrammatically represented in the figure 27(a). The cotrace $\operatorname{cotr}(\phi^j) = \sum_i \Delta_i^{ij} = \Delta_i^{ij}$, as in figure 27(b).

In this paper we use the following definition of the cointegral and integral elements of algebra [Kup91, KR99]:

3.1. **Definition** (Cointegral and integral)**.** The cointegral element $\lambda \in \mathscr{A}$ is defined as in the figure 28(a) and it can be a left or right cointegral. The figure 28(a)

(a) Cointegral λ. (b) Integral Λ.

FIGURE 28. Diagramatic representation of cointegral and integral elements of algebra.

represents the left cointegral. Analogously, the integral is an element $\Lambda \in \mathscr{A}^*$ such that the condition drawn in the figure is satisfied. In the figure 28(b) we represent the right integral.

For this work we use that the left and right cointegrals are equal [Kup91, LR88], in particular for an involutory Hopf algebra, $S^2 = 1$, λ is represented in terms

(a) Tensor λ. (b) Tensor Λ.

FIGURE 29. Diagramatic representation of cointegral and integral elements of algebra.

of the structure constants of the coproduct as in the figure 29(a). Similarly, Λ is represented in terms of the structure constants of the product as in the figure 29(b). The definition of cointegral, 29(a), and integral, 29(b), coincides with the definition of cotrace and trace as it is shown in figures 27(b) and 27(a), respectively.

3.1. Lemma.
In an involutory Hopf algebra the tensor $\Delta_i^{ij} m_{jk}^{k}$ is equal to the dimension of the algebra (see figure 30).

Proof. We note that the cointegral can be represented by figure 31(a). We use the integral property to obtain the figure 31(b). Placing the arrows with the same index

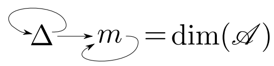

FIGURE 30. *Contraction* $\Delta_i^{ij} m_{jk}^{k}$.

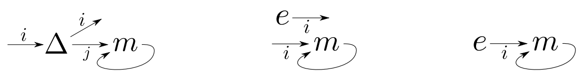

(a) (b) (c)

FIGURE 31. Proof of lemma 3.1.

we obtain the figure 31(c). Numerically, the last figure is $\sum_j e^i m_{ij}^{j} = \mathrm{tr}(\phi_e)$, where ϕ_e is the identity matrix. So, $\sum_j e^i m_{ij}^{j} = n = \dim(\mathscr{A})$ and thus we had proven the lemma. □

3.2.2. *Tensors associated to curves.* Through the associativity and coassociativity of algebra, the tensors $M_{a_1 a_2 \cdots a_n}$ and $\Delta^{b_1 b_2 \cdots b_m}$ can be defined diagrammatically as in

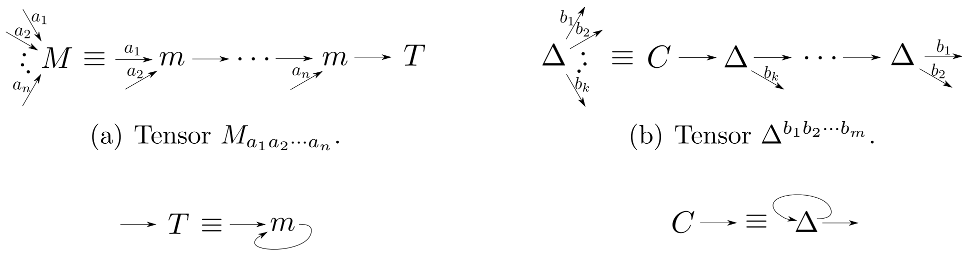

(a) Tensor $M_{a_1 a_2 \cdots a_n}$.

(b) Tensor $\Delta^{b_1 b_2 \cdots b_m}$.

(c) Trace m_{ij}^{j}.

(d) Cotrace Δ_i^{ij}.

FIGURE 32. Diagrammatic representation of tensors $M_{a_1 a_2 \cdots a_n}$ and $\Delta^{b_1 b_2 \cdots b_k}$.

diagrams 32(a) and 32(b), where there were defined the trace m_{ij}^{j} and the cotrace Δ_j^{ij} as in diagrams 32(c) and 32(d) [Kup91, KR99]. We note that combinations of several tensors M and Δ can be introduced by only placing the arrows according to the rules of contraction of tensors. In particular we have of following lemma:

3.2. Lemma (Relation between M, Δ and S).
In an involutory Hopf algebra, $S^2 = 1$, we have that the contraction between tensors M, Δ and S gives the dimension of algebra, figure 33.

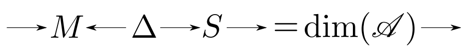

FIGURE 33. *Relation between tensors M, Δ and S.*

This proof can be found in [Kup91]. Based in this last relation, we can show the following results:

3.3. Lemma.
In an involutory Hopf algebra, $S^2 = 1$, the following identities are satisfied:

(1) $m^i_{ij} = m^j_{ij}$,

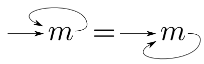

FIGURE 34. *Tensors m^i_{ij} and m^j_{ij} are equal.*

(2) $\Delta^{ij}_i = \Delta^{ij}_j$,

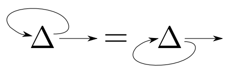

FIGURE 35. *Tensors Δ^{ij}_i and Δ^{ij}_j are equal.*

Proof. The basic idea is to use the above lemma. It is enough to proof the part 1 of it and the part 2 can be proven in a similar way. By the lemma 3.2, we note that the

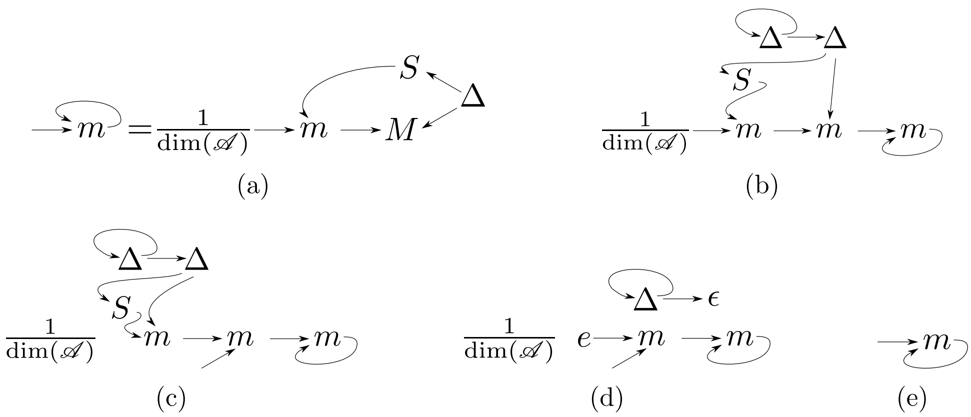

FIGURE 36. Diagrammatic proof to show that tensors m^i_{ij} and m^j_{ij} are equal.

left part of the identity can be represented as in figure 36(a). Using the definitions of tensors M and Δ we represent 36(a) as 36(b), and with the associativity of algebra we obtain the figure 36(c). However, with the property of the antipode, figure 26(b), we obtain the figure 36(d). Finally using the unity property and contracting the tensor Δ with the counity $\Delta^{ij}_i \to \epsilon_j = \dim(\mathscr{A})$, we have the figure 36(e). □

3.4. Lemma.
Tensors $M_{a_1\cdots a_n}$ and $\Delta^{b_1\cdots b_m}$ represented by 32(a) and 32(b) respectively, are cyclic symmetric.

Proof. The idea is to show that both tensors 32(a) and 32(b) can be represented by the diagrams 37(a) and 37(b), respectively. For tensor $M_{a_1a_2\cdots a_n}$, the proof is based on the associativity of the algebra, and we only need to note the sequence of diagrams 38(a) and 38(b). We see that the last arrow to the left is the same as the

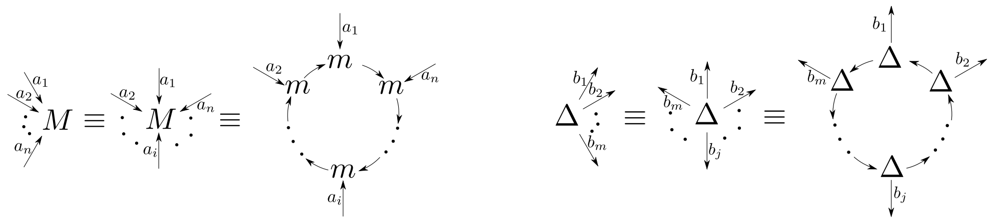

(a) Tensor $M_{a_1 a_2 \cdots a_n}$. (b) Tensor $\Delta^{b_1 b_2 \cdots b_k}$.

FIGURE 37. Another diagrammatic representation of tensors $M_{a_1 a_2 \cdots a_n}$ and $\Delta^{b_1 b_2 \cdots b_k}$.

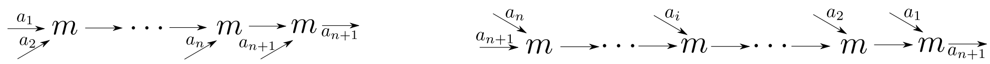

(a) Definition of trace. (b) Associativity of algebra.

FIGURE 38. Diagrammatic proof of invariance of tensor $M_{a_1 a_2 \cdots a_n}$ by cyclic permutations of their indices.

first one in figure 38(b). Joining these two arrows, we proved the desired lemma. For the tensor $\Delta^{b_1 b_2 \cdots b_k}$, we use a similar argument with the coassociative of the algebra. □

Using the two above lemmas, the associativity and coassociativity of algebra, it is easy to show the following result:

3.5. Corollary.

The orientation of arrows in the product leaves invariant the tensors M and Δ, see figures 39(a) and 39(b).

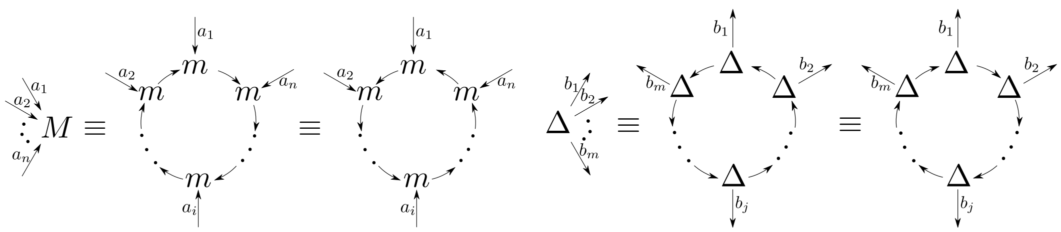

(a) *Tensor* $M_{a_1 a_2 \cdots a_n}$. (b) *Tensor* $\Delta^{b_1 b_2 \cdots b_k}$.

FIGURE 39. *The orientation of arrows leaves invariant the product and coproduct.*

It can be seen that the lemma 3.4 ensures that tensors M and Δ are cyclic, as we expect, to describe polygons and hinges as in the preceding section [Ale01]. With the tensorial notation previously defined, we can be provide a weight related to faces (black curves) and links (gray curves) of a colored diagram or Heegaard diagram. We naturally associate the tensor M to the black curves and Δ to the gray curves. Since every face and link are oriented, the black and gray curves should be also oriented.

The tensor $M_{a_1 \cdots a_n}$ associated with each black curve represents n crossings with gray curves. Similarly, it is defined a tensor $\Delta^{b_1 \cdots b_m}$ associated with each gray curve, with m the number of intersections with black curves. Note that M and Δ are cyclic, no matter the order of these crossings. Also, it is well known that the orientation of the faces and links should not change the value of the partition function. Now, we define how it is considered the relative orientation between black curves (faces) and gray curves (links): let P be the intersecting point between curves[6] and let $\vec{t}_{\mathsf{b}}$ and $\vec{t}_{\mathsf{g}}$ be the tangent vectors to the black and gray curves in P. If $\hat{n}$ is the normal vector to the surface ∂M, we have two possible cases for the vectorial product $\vec{t}_{\mathsf{b}} \times \vec{t}_{\mathsf{g}}$ and contractions of tensors between M and Δ:

(1) $\hat{n}$ and $\vec{t}_{\mathsf{b}} \times \vec{t}_{\mathsf{g}}$ are parallel according to the right hand rule, figure 40(a).
(2) $\hat{n}$ and $\vec{t}_{\mathsf{b}} \times \vec{t}_{\mathsf{g}}$ are antiparallel according to the right hand rule, figure 40(c).

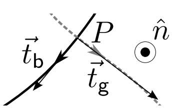

(a) Crossing.

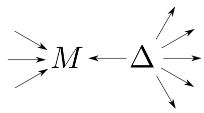

(b) Associated tensor.

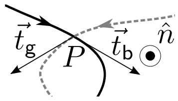

(c) Crossing.

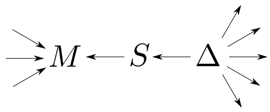

(d) Associated tensor.

FIGURE 40. 40(a), 40(b). Intersections of curves with parallel direction and contraction of tensors. 40(c), 40(d). Intersections of curves with antiparallel direction and contraction of tensors. We introduce the antipode.

Note that we introduce the tensor S in 40(d) to represent the relative orientation black-gray curve. In the case where the curves intersect twice as in figure 41(a), we use the diagrams 40(b) and 40(d) to write the tensor 41(b)[7].

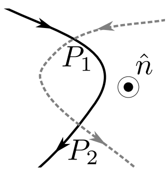

(a) Two crossings.

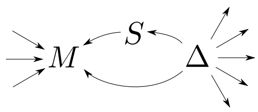

(b) Tensor associated to interlaced curves.

FIGURE 41. Crossings and contraction of tensors.

[6]Remember that two curves of the same color do not intersect.

[7]The number of inward arrows in M (going out Δ) is the number of gray curves (resp. black) crossing each black curve (resp. gray).

So far, we have seen how it is possible to describe a lattice topological theory, however, it has not been defined how is the contribution of tensors M and Δ. In [FHK94], Fukuma, Hosono, and Kawai showed that all the physical information is related to the center of the algebra considered. Let $\rho(\phi_i)^k{}_j$ be a regular representation of an element ϕ_i of the algebra which will represented, as previously mentioned, as ϕ_i. The tensor M is associated with the center of the algebra by the element z and the tensor Δ with the cocenter of the algebra denoted by ζ as follows

$$M_{a_1 a_2 \cdots a_n} = \mathrm{tr}(z\phi_{a_1}\phi_{a_2}\cdots\phi_{a_n}), \tag{14}$$

$$\Delta^{b_1 b_2 \cdots b_k} = \mathrm{cotr}(\zeta\phi^{b_1}\phi^{b_2}\cdots\phi^{b_m}), \tag{15}$$

with ϕ_i and ϕ^j the elements of the basis of $\mathscr{A}$ and its dual $\mathscr{A}^*$ respectively [BPT13]. The generalized tensors M and Δ provided by diagrams 32(a) and 32(b) are now

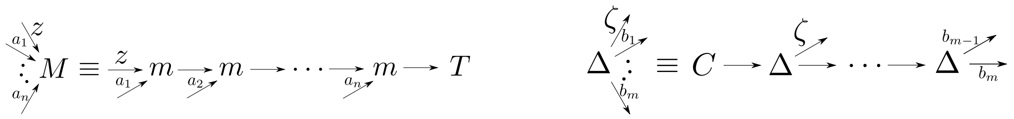

(a) General definition of M.

(b) General definition of Δ.

FIGURE 42. The tensors M and Δ are redefined using the center and cocenter of algebra.

represented by figure 42. For z (resp. ζ) being an element of the center (resp. cocenter), M (resp. Δ) is cyclically symmetric as expected when we build a Lattice Topological Field Theory.

3.3. **Partition function, Wilson Loops and topological invariance.** We are ready to define the partition function of the manifold $\mathscr{M}$. Due to the polygons are decomposed into triangles glued by hinges and each hinge can have pasted an arbitrary number of polygons, the partition function for the manifold $\mathscr{M}$ with triangulation $\mathscr{T}$ is naturally defined by

$$Z(\mathscr{M},\mathscr{T}) = \sum_{\mathrm{conf}}\prod_{\mathrm{f}}\prod_{\mathrm{e}}\prod_{\mathrm{o}} M_{abc}(\mathrm{f})\Delta^{b_1 b_2\cdots b_k}(\mathrm{e})S_x^y(\mathrm{o}), \tag{16}$$

where we use f and e to denote that the product is over all faces and links. The product "o" means the product of all crossings with different orientation from the normal vector to the surface $\partial\mathscr{M}$. We write the partition function in the same way followed in the three-dimensional case by Kuperberg [Kup91] and it is basically the same as Chung, Fukuma and Shapere [CFS94]. The difference regarding the two-dimensional case is that as it was described before hinges can be thought as links, which can only stick two polygons[8]. I.e., the tensor $\Delta^{b_1 b_2\cdots b_k}$ in (16) has only two indices: $\Delta^{b_1 b_2}$. Now, it is well known that the relevant physical quantities depend on the partition function, however, this one, for a manifold $\mathscr{M}$, written as we did above may or may not depend on the manifold of triangulation. We summarize this in two cases:

[8]Only two different faces can share the same link.

(1) Topological invariant: the partition function of each triangulation is equal for two different triangulations $\mathscr{T}_1, \mathscr{T}_2$ of the manifold $\mathscr{M}$, i.e., $Z(\mathscr{T}_1) = Z(\mathscr{T}_2)$. This can be done by selecting (or finding) the weights z and ζ on curves such that this condition is satisfied.

(2) Quasi-Topological invariant: the partition function depends on details of the triangulations $\mathscr{T}_1$ and $\mathscr{T}_2$ of the manifold $\mathscr{M}$. As in the topological invariant case, we choose (or find) the weights z and ζ associated to curves such that this condition is satisfied. In the quasi-topological case

$$Z(\mathscr{M}, \mathscr{T}_2) = \mathsf{f}(n_{\mathrm{e}_1} - n_{\mathrm{e}_2}, n_{\mathrm{f}_1} - n_{\mathrm{f}_2}, n_{\mathrm{t}_1} - n_{\mathrm{t}_2}) Z(\mathscr{M}, \mathscr{T}_1),$$

where n_{e_i}, n_{f_i} and n_{t_i} are the number of links, faces and tetrahedras (in the three-dimensional case) of triangulation $\mathscr{T}_i$ respectively, and f a factor that depends on the difference of the number of constituents for each triangulation. Note that for the topological case $\mathsf{f} \equiv 1$.

According to the paragraph above, the Wilson loops are now defined as follows

$$\langle W(\ell)\rangle = \frac{1}{Z(\mathscr{M}, \mathscr{T})} \sum_{\mathrm{conf}} \prod_{\mathrm{f}} \prod_{\mathrm{e}} \prod_{\mathrm{o}} W(\ell) M_{abc}(\mathrm{f}) \Delta^{b_1 b_2 \cdots b_m}(\mathrm{e}) S_x^y(\mathrm{o}), \tag{17}$$

where we take the partition function different from zero.

As it was stated, the invariance or quasi invariance of the partition function will be satisfied by taking the elements of the center (resp. cocenter) of the algebra of the group (resp. coalgebra). Thus, we associate a point to each black and gray curve to denote the relation with the center and cocenter of the algebra, respectively (figure 43). Since z is related with the black curves, this will provide information of gauge fields residing on their faces. On the other hand, ζ is related to matter fields or Higgs fields of section 2.4, where we choose the unitary gauge, $v_{i(e)} = \rho(h_{i(e)})^{-1}$,

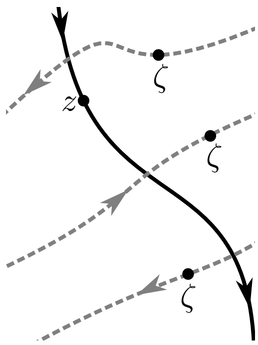

Figure 43. Curves with weights.

such that matter fields lying on the vertices vanish and now these lie on the links.

As expected, all the information in the triangulation is provided by tensors M, Δ and S which are built from a Hopf algebra. However, it is still needed to show that we can obtain a triangulation from another in a finite number of steps. As mentioned earlier for triangulations, Pachner showed that one only need some moves for this purpose. Then, we need to show that by using the language of colored curves we get a triangulation $\mathscr{T}_2$ with diagram $\mathscr{D}_2$ from a triangulation $\mathscr{T}_1$ with diagram $\mathscr{D}_1$

in a finite number of moves. By proving this, we are showing the invariance of the partition function.

In the previous section, we saw the conditions for two colored diagrams or Heegaard diagrams to be equivalent (see subsection 3.2 and the conditions on moves 2.5). Our goal is to show invariance and quasi invariance (unless scalar factors) of the partition function using these conditions [Kup91, Ale01]. We suppose that each black curve (resp. gray) has a weight associated with z (resp. ζ). However, it will not stand for simplicity this weight as a point but just as a gray curve (resp. black) in the diagrams and also in the statements of lemmas below.

3.6. Lemma (Homeomorphism of the surface).
Let $\mathscr{S}$ and $\mathscr{S}'$ be closed, connected and oriented surfaces. If $\mathscr{S}$ is homeomorphic to $\mathscr{S}'$, black curves (resp. gray) on $\mathscr{S}$ are homeomorphic to black curves (resp. gray) on $\mathscr{S}'$. The colors of the curves are equal.

This is equal to show that two homeomorphic surfaces have the same colored diagram or Heegaard diagram[9]. Clearly the partition function (16) is invariant with respect to this condition.

3.7. Lemma (Orientation reversal).
The orientation of black curves (resp. gray) is replaced by its inverse. The inverse of the black curve b_i is b_i^{-1}. Analogously g_j^{-1} is the inverse of the gray curve g_j.

Proof. The proof is based on the cyclicity of tensors M and Δ. Consider a black curve with three crossings with gray curves, as it is shown in figure 44(a) (a similar proof can be done for a gray curve). For n crossings the proof is trivial following the same procedure. The idea is to show that the tensor associated to figure 44(b) is

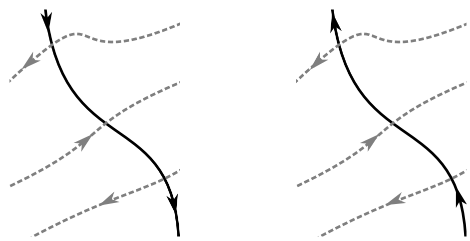

(a) First orientation. (b) Second orientation.

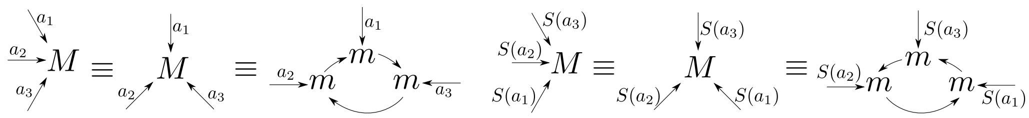

(c) Tensor $M_{a_1a_2a_3}$ associated to 44(a). (d) Tensor $M_{S(a_3)S(a_2)S(a_1)}$ associated to 44(b).

FIGURE 44. Intersection of curves with first and second orientations and diagram showing that $M_{a_1a_2a_3}$ and $M_{S(a_3)S(a_2)S(a_1)}$ are equal.

$M_{S(a_3)S(a_2)S(a_1)}$ (figure 44(d)) and this is equal to $M_{a_1a_2a_3}$ (figure 44(c)) which is the associated tensor to figure 44(a). The tensor $M_{a_1a_2a_3}$ in the figure 44(c) is equal to

[9]The proof of this effect can be found in [Joh] for Heegaard diagrams.

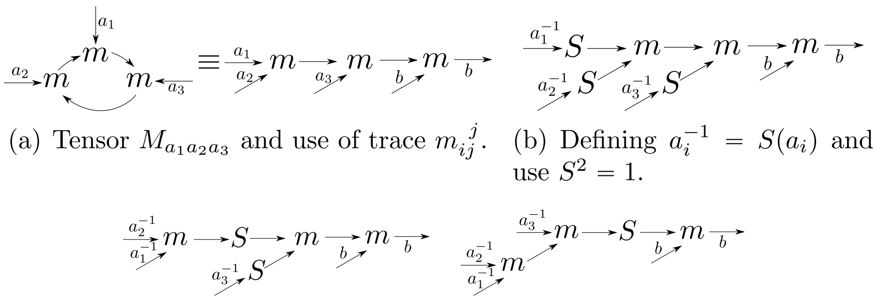

(a) Tensor $M_{a_1a_2a_3}$ and use of trace $m_{ij}^{\ j}$.

(b) Defining $a_i^{-1} = S(a_i)$ and use $S^2 = 1$.

(c) Use $S(ab) = S(b)S(a)$ for a_1 and a_2.

(d) Use $S(ab) = S(b)S(a)$ for $a_2^{-1}a_1^{-1}$ and a_3.

FIGURE 45. Proofs that tensors $M_{a_1a_2a_3}$ and $M_{S(a_3)S(a_2)S(a_1)}$ are equal.

the sequence of steps, from the figure 45(a) to the figure 46(d). Step by step, we use the facts that the algebra is associative and the antipode is an anti-homomorphism of the product. Finally, the corollary 3.5 states that the orientation of the product is invariant. So the tensors $M_{a_1a_2a_3}$ and $M_{S(a_3)S(a_2)S(a_1)}$ are equal. $\square$

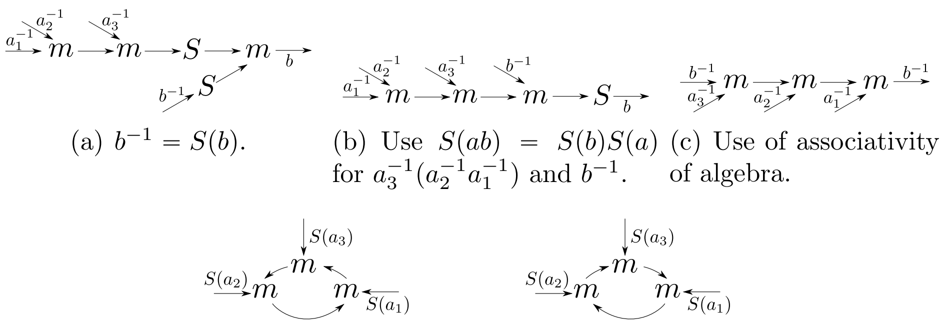

(a) $b^{-1} = S(b)$.

(b) Use $S(ab) = S(b)S(a)$ for $a_3^{-1}(a_2^{-1}a_1^{-1})$ and b^{-1}.

(c) Use of associativity of algebra.

(d) Joining the arrows in the ends $\rightarrow$ $M_{S(a_3)S(a_2)S(a_1)}$.

(e) Changing the orientation of the product.

FIGURE 46. Proofs that tensors $M_{a_1a_2a_3}$ and $M_{S(a_3)S(a_2)S(a_1)}$ are equal.

3.1. *Remark.*
Due that we are taking the weight z on the black curve (resp. gray) as a gray curve (resp. black), it seems that this is not taken into account. In this hypothesis we need that the antipode on the weight z (resp. ζ), i.e. $S(z)$ (resp. $S(\zeta)$) be equal to z (resp. ζ). We have the following result

3.8. Corollary.
Let z (resp. ζ) be the weight over a black curve (resp. gray), for topological invariance we need that $S(z) = z$ (resp. $S(\zeta) = \zeta$).

This ensures the invariance with respect to an orientation change. In the next section it is calculated the weight associated with the gauge model, and this will fulfill the mentioned condition.

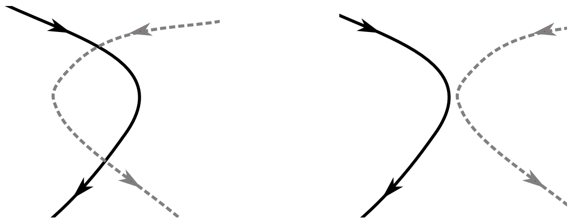

(a) *Before.* (b) *After.*

FIGURE 47. *Two point move property.*

3.9. Lemma (Two point move).

If the black curve intersects twice a gray curve, as in figure 15(a), one can eliminate the crossing as it is shown in figure 15(b). The color of each curve is invariant after separating them[10].

Proof. The diagram associated with the figure 47(a) is represented by diagram 48(a).

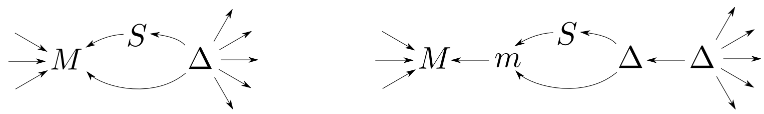

(a) Tensor associated with interlaced curves. (b) Definition of tensors M and Δ.

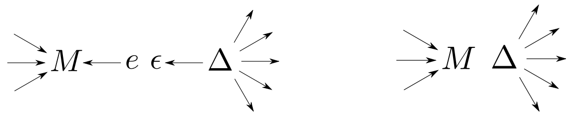

(c) Use $m \circ (S \otimes 1) \circ \Delta = e \circ \epsilon$. (d) Unity and counity.

FIGURE 48. Two point move proof.

Using the property of the antipode $m \circ (S \otimes 1) \circ \Delta = e \circ \epsilon$, diagram 26(a), we obtain diagrams 48(c) and 48(d) which are the tensors associated with the figure 47(b). □

3.10. Lemma (Stabilization).

Let $\mathscr{T}_1$ be a torus with genus one and let $\mathscr{T}_2$ be a torus of genus greater than or equal to one, both with their respective black and gray curves. If the black and gray curves of the two torus are disjoint, it can be added or removed the torus $\mathscr{T}_1$.

Proof. We consider the figure 49(a), which will be represented by the tensor 49(c). We expect to unite the torus with black and gray curves to the torus of genus $g \geqslant 1$. We write the tensors associated before and after of the union, these are equal. □

A more interesting result is that in which the cointegral (resp. integral) property is used.

[10]To say that the color of each curve is invariant is state that the weight of each curve does not change.

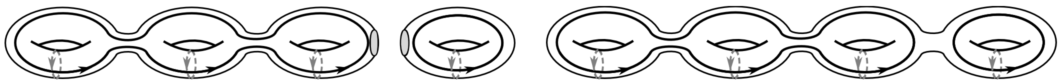

(a) Two torus which are separated by disjoint black and gray curves. (b) Two torus joined by black and gray curves.

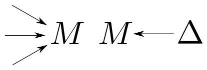

(c) Tensors associated with curves before and after the union of two torus, do not change.

FIGURE 49. Proof of stabilization, trivial.

3.11. Lemma (Cointegral (resp. integral) property).
Let be a black curve (resp. gray) whose weight is the cointegral (resp. integral) (figure 50(a)), crossed by any number of gray (resp. black) curves. The cointegral (resp. integral) can be replaced by a gray curve (resp. black), as shown in figure 50(b). We can separate the black curve (resp. gray) of other crosses, as in figure 50(c).

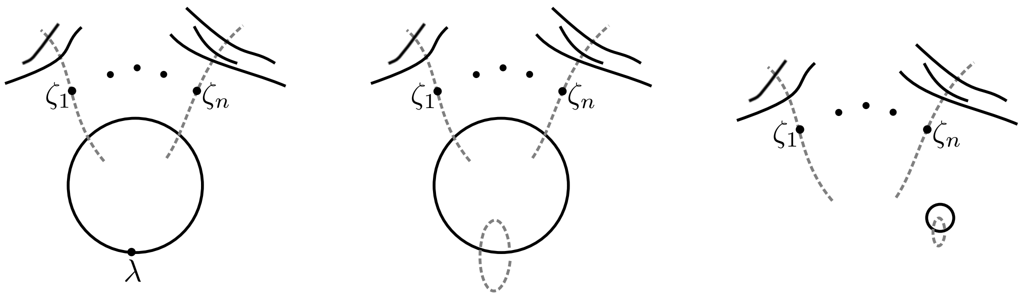

(a) *Black curve with weight the cointegral.* (b) *Gray curve crossing just one gray curve.* (c) *Use of cointegral property.*

FIGURE 50. *Cointegral property.*

Proof of cointegral property. By the definition of cointegral (definition 3.1), tensor 51(a), we have that it can be related to a gray curve, so we obtain the figure 50(b). Let $n+1$ be the number of crossings of the black curve with gray curves; the tensor associated to 50(b) is 51(b). By definition of M we have the tensor 51(c). Using the cointegral property (definition 3.1), we have the tensors 51(d) to 51(e). We observe that the tensor 51(e) is associated with the figure 50(c). To prove the integral property we use similar arguments. □

3.12. Corollary.
For the cointegral λ, the diagrammatic configuration shown in figure 52(a) can be represented as in figure 52(b).

Proof. We only apply the cointegral property on the black curve. □

3.13. Lemma (Sliding).
Let C_1 and C_2 be two closed curves of the same color in a colored diagram or Heegaard

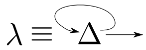

(a) Tensor λ, associated to gray curve.

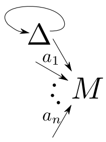

(b) Tensor M with $n+1$ inward arrows.

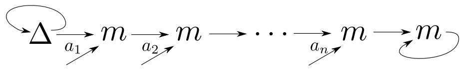

(c) Definition of M.

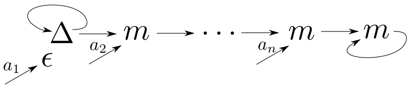

(d) Definition of the cointegral.

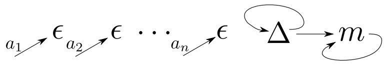

(e) Definition of the cointegral property repeatedly. Tensor associated to 50(c).

Figure 51. Proof of the cointegral property.

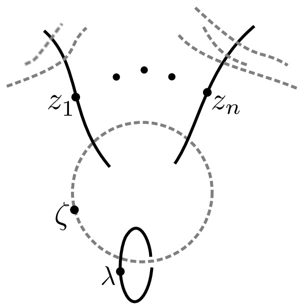

(a)

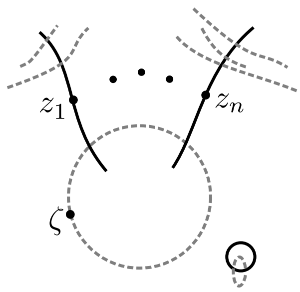

(b)

Figure 52. *Black curve with weight λ which intersects just one gray curve.*

diagram over a surface $\mathscr{S}$. Let $b \in \mathscr{S}$ be the connection between C_1 and C_2 as in figure 53(a). The curve C_1 is replaced by the curve C_1'. The new curve C_2' is an isotopy of C_2. The curve C_1' (resp. C_2') has the same orientation of C_1 (resp. C_2) figure 53(b).

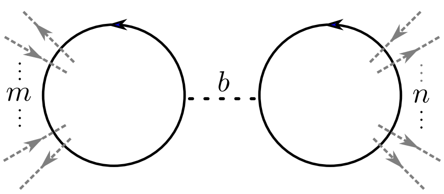

(a) *Two curves of the same color glued by a ribbon.*

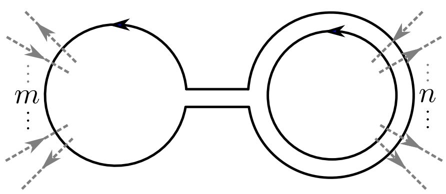

(b) *Sliding.*

Figure 53. *53(a). The curve C_1 (resp. C_2) has m (resp. n) crosses with curves of different color. 53(b). After sliding the final curve C_1' (resp. C_2') has $m+n$ (resp. n) crosses with curves of different color.*

Proof. The proof will be made for the basic case in which the weight of the curve to the right is trivial, i.e., $z = e$, the unity. In subsection 3.5 we show that there are other non-trivial weights with which we can also apply the sliding moves. It

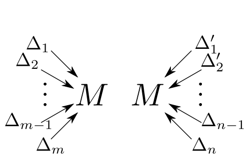

(a) Form of tensors of curves.

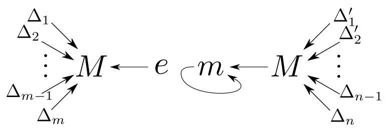

(b) Definition of M and unity e.

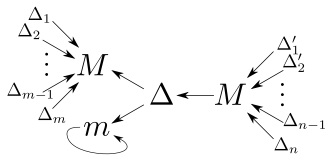

(c) Integral property.

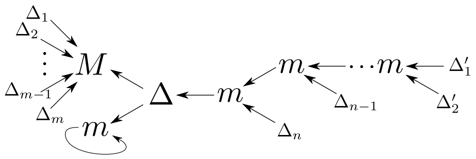

(d) Definition of M again.

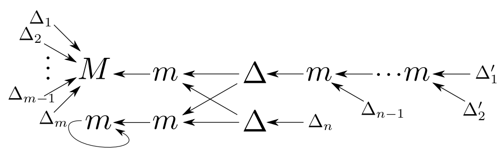

(e) Use of relation between product and coproduct.

FIGURE 54. First part of statement of the sliding property.

should follow diagrams 54(a) to 54(e), where there are used the definitions of the

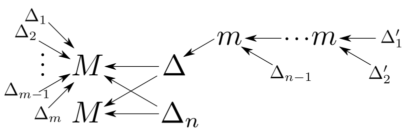

(a) Definition of M and Δ.

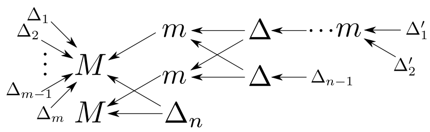

(b) Relation product and coproduct.

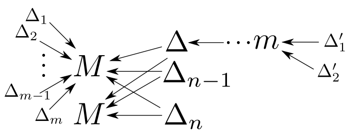

(c) Definition of Δ.

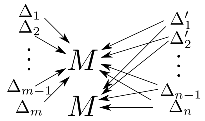

(d) Analogously by n crossings of the previous step.

FIGURE 55. Second part of the demonstration of the sliding property.

tensor M and unity e and also, the relation between product and coproduct. Now, in figures 55(a) to 55(d) it is used the Δ definition repeatedly. Furthermore, the relation between product and coproduct n times, where n is the number of crossings of the original curve to the right. □

3.4. **Topological invariance using curves.** It is well know that Pachner moves assure topological invariance. Therefore, our purpose is to show that these are satisfied at least for the two-dimensional case using the moves described in the previous subsection; a detailed demonstration for the three-dimensional case can be encountered in [Ber12]. At the end of this subsection, we shall give all details

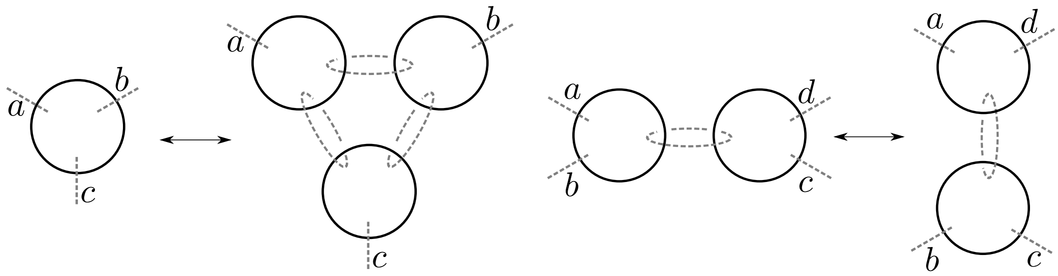

(a) Pachner move (1,3), (3,1). (b) Pachner move (2,2).

Figure 56. Relation between the two diagrams Pachner move like colored curves.

for the proof. Firstly, we merely show the relation between diagrams. Indeed, as stated before in this section, the corresponding diagrams in colored curves for the Pachner moves are represented by the figures 56(a) and 56(b). Using the moves for curves, we obtain that the association between diagrams (1,3), is shown in figure 57.

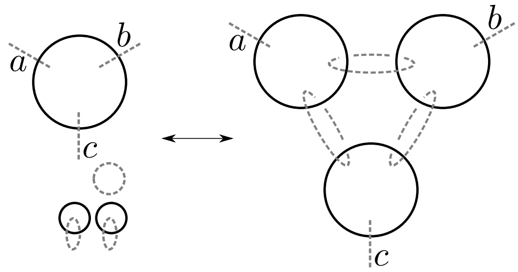

Figure 57. Pachner move (1,3), (3,1).

Note that we have three additional diagrams, in the left part of this figure, to relate both triangulations (two black curves crossing one gray curve and one isoloted gray curve), this will be discussed below. On the other hand, for the (2,2) move, it will

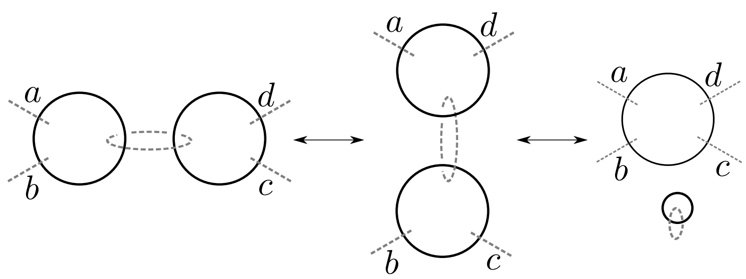

Figure 58. Pachner move (2,2).

be shown that the equivalence between figures is hold, see figure 58.

As it was shown, the relation between diagrams in figure 57 has three additional diagrams. These diagrams represent the difference in detail of both diagrams in figure 56(a). The diagram to the right has 6 links and 3 triangles, and the diagram to the left has 3 links and 1 triangle. Therefore, the additional three diagrams in the figure 57 represent the difference in details of both diagrams. This corresponds to a quasi-topological behavior of the model using the kind of moves shown in this work. To know the numeric value of the these isolated diagrams we remember that in subsections 3.2.2 and 3.3 we associate to each closed black curve the tensor M, and the tensor Δ to each closed gray curve; furthermore, we represent their weights z and ζ respectively by points. In figure 59(a) it is represented one black curve

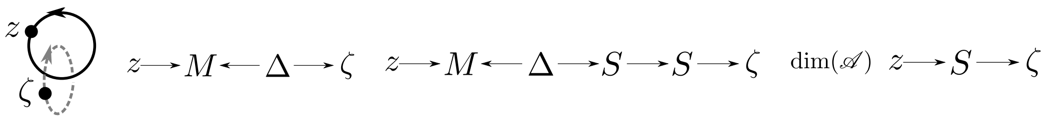

(a) (b) (c) (d)

FIGURE 59. Tensors associated with isolated curves with weight.

crossing just one gray curve, and its tensorial representation is given in figure 59(b), in which using that $S^2 = 1$ and the lemma 3.2, we obtain the figure 59(d). This last diagram has numeric value $\dim(\mathscr{A}) \sum_h z^h S(\zeta_h)$, however by corollary 3.8, $S(\zeta) = \zeta$, therefore the numeric value is $\dim(\mathscr{A}) \sum_h z^h \zeta_h$, where z^h and ζ_h are the coefficients that expand the center and cocenter respectively. On the other hand, by lemma 3.7 we know that by changing the orientation of one curve the partition function is the same. To know the numeric value of one black curve with weight z, we observe figures 60(a) and 60(b). The corresponding numeric value is $\sum_h z^h m_{hg}^{\ g}$ and

(a) (b) (c) (d)

FIGURE 60. Tensors associated with isolated curves with weight.

for one gray curve, figures 60(c) and 60(d), the numeric value is $\sum_h \zeta_h \Delta_g^{hg}$. Note that following the corollaries 3.5 and 3.8 the orientation of the curves is not important. This way, we proved the following lemma:

3.14. Lemma.
Each isolated curve, black or gray, and each pair of crossing curves, black with gray, has a numeric value independent of the orientation of each curve.

Following the definition of quasi-topological invariant in the partition function, two different triangulation $\mathscr{T}_1$ $\mathscr{T}_2$ of a manifold $\mathscr{M}$ are related by

$$Z(\mathscr{M}, \mathscr{T}_2) = \mathsf{f}(n_{e_1} - n_{e_2}, n_{f_1} - n_{f_2}, n_{t_1} - n_{t_2}) Z(\mathscr{M}, \mathscr{T}_1), \tag{18}$$

where n_{e_i}, n_{f_i} and n_{t_i} are the number of links, faces and tetrahedras (in the three-dimensional case) of triangulation $\mathscr{T}_i$ respectively, and f a factor that depends on the difference of the number of constituents for each triangulation. So, it is possible to take the function f according to paragraph above, as follows

$$\mathsf{f} = \gamma_1^{n_{e_2}-n_{e_1}} \gamma_2^{n_{f_2}-n_{f_1}}, \tag{19}$$

where γ_1, γ_2 real parameters, in principle non-negative. Therefore, the corresponding partition functions for two different triangulations are related for $\{\gamma_1, \gamma_2\} \neq 0$ by

$$Z(\mathscr{M}) = \frac{Z(\mathscr{M}, \mathscr{T}_2)}{\gamma_1^{n_{e_2}} \gamma_2^{n_{f_2}}} = \frac{Z(\mathscr{M}, \mathscr{T}_1)}{\gamma_1^{n_{e_1}} \gamma_2^{n_{f_1}}},$$

where $Z(\mathscr{M})$ is called topological partition function because it is independent of triangulation. For the three-dimensional case the topological partition function is given by the form [FPTS12, Ber12, BPT13, YTSB07]

$$Z(\mathscr{M}) = \frac{Z(\mathscr{M}, \mathscr{T}_2)}{\gamma_1^{n_{e_2}} \gamma_2^{n_{f_2}} \gamma_3^{-n_{t_2}}} = \frac{Z(\mathscr{M}, \mathscr{T}_1)}{\gamma_1^{n_{e_1}} \gamma_2^{n_{f_1}} \gamma_3^{-n_{t_1}}},$$

with $\gamma_1, \gamma_2, \gamma_3$ real parameters, in principle positives.

To complete this subsection, we prove the topological invariance under Pachner moves using the formalism of colored curves and their moves; in particular the two point move and the sliding move. On each black and gray curve, we do not represent the elements of the center and the cocenter of the algebra. However, each time we make the sliding move we assume that the element of the center or cocenter, allows this. Furthermore, we do not put the orientation because we are supposing that the lattice is oriented. The same technique is used to show topological invariance in more dimensions. However, we have to clarify that in dimensions higher than 3, the number of curves make very difficult to vefify topological invariance due to the number of Pachner moves that we need.

3.4.1. *Move (1,3).*

Proof. By definition, the Pachner move (1,3) is the reverse of move (3,1). Thus, we start from the triangulation which has three triangles and six links (figure 61(a)), denoted by $(3,6)$ and colored diagram 61(b), to another which has a triangle and three links, and it will be denoted by $(1,3)$, as in figure 61(c) and colored diagram 61(d). Firstly we use the sliding move, lemma 3.13, to the upper black curves, figure 62(a). We repeat the sliding move, but now on the lower black curve in the graph, figure 62(b). We use two point move and then we obtain the figure 62(c). We make move sliding on the lower gray curves and we have 62(d). We use two point move, and the gray curve is now in the black curve, as it is shown in figure 62(e). We do sliding between the two gray curves which intersect the same black curve, and then we can remove one of these, figure 62(f). We make now sliding of the gray curve crossing two black curves 63(a). Using two point move, we obtain the figure 63(b). Now, each gray curve crossing a black curve can move freely on the black curve as in figure 63(c). We make sliding over the gray curve crossing two black curves, figure 63(d). We use two point move to get the diagram 63(e). We note that in the last diagram there is a black curve which crosses only one gray curve. It can be removed from the diagram because it does not intersect with any other curve. Doing the same for other gray curve, we have the figure 63(f). We note that the final diagram is equivalent to a

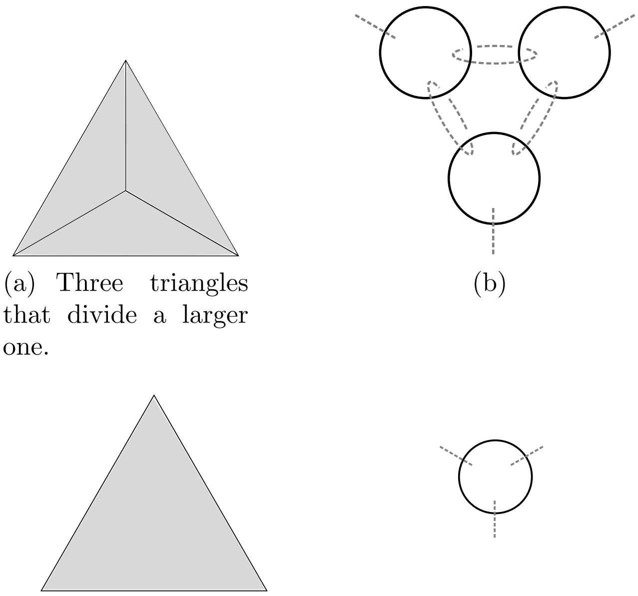

(a) Three triangles that divide a larger one.

(b)

(c) One triangle.

(d)

FIGURE 61. Representation of triangles 61(a) and 61(c) in colored curves.

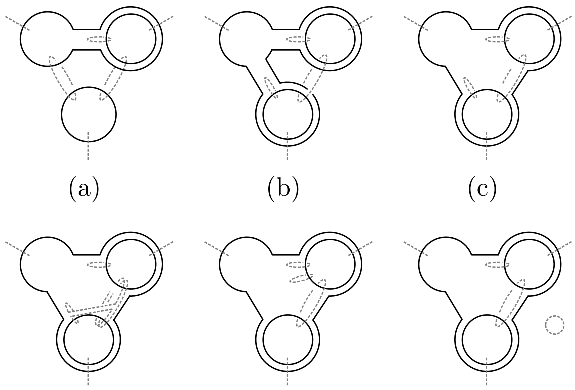

(a) (b) (c)

(d) (e) (f)

FIGURE 62. First part of the statement of Pachner moves (1,3) in colored curves.

triangle with three links: two black curves, each one crossed by a gray curve, and a gray curve. □

3.4.2. *Move (2,2).*

Proof. The proof is again based on sliding move. Considering the diagram 64(c) which is originated from diagram 64(a). First, we make a sliding move on the left black curve, figure 65(a). Then, we recall that the gray curve which intersects only a black curve can move freely through it, as in figure 65(b). We move the sliding between gray curves and we obtain the figure 65(c). Making two point move we find the figure 65(d). Making sliding again, it is removed the black curve which crosses only one gray curve. After that,

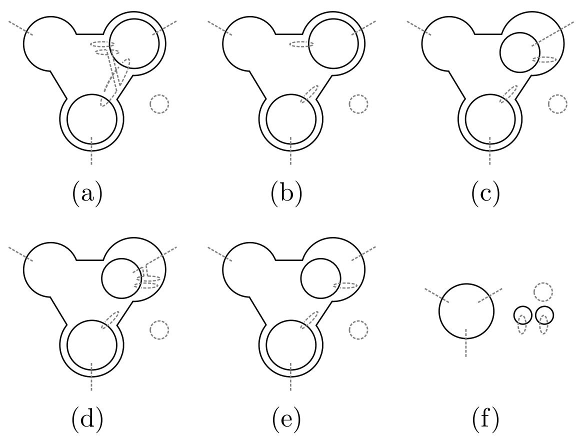

FIGURE 63. Second part of the statement of Pachner moves (1,3) in colored curves.

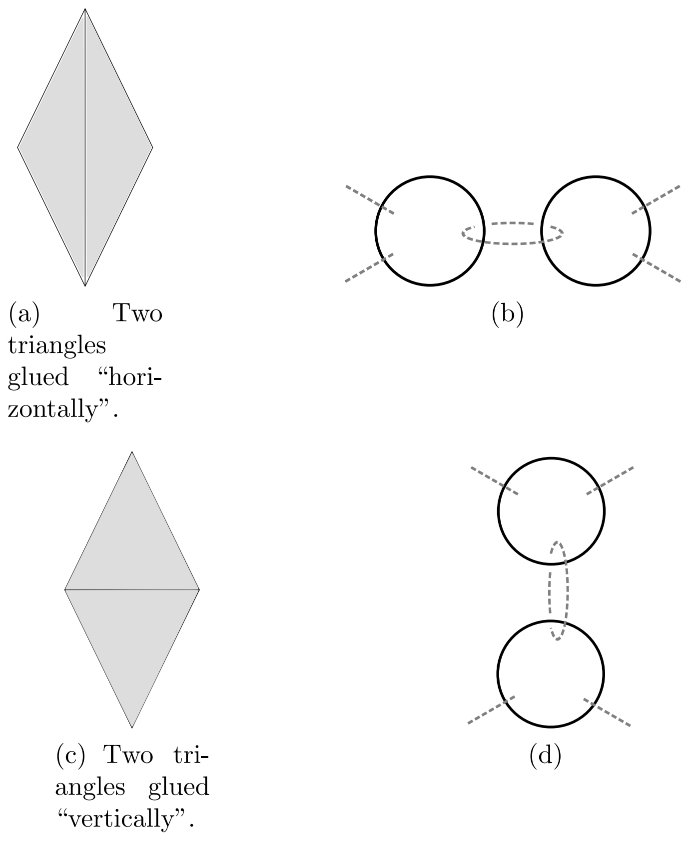

FIGURE 64. Representation of two triangles 64(a) and 64(c) glued together in colored curves 64(b) and 64(d).

we extract these curves and the figure 65(e) is obtained. The same steps are followed for the other triangulation, and as a result we have an equality between graphs. □

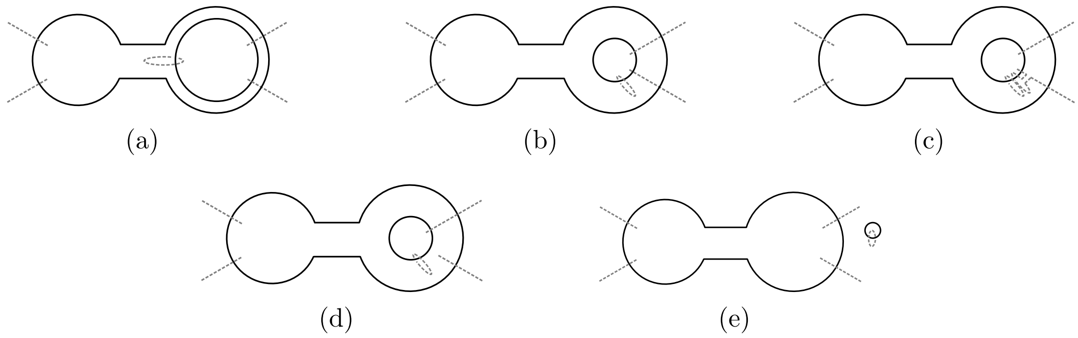

FIGURE 65. Diagrammatic proof of Pachner moves (2,2) in colored curves.

3.5. **Group algebra.** So far, we have the most general formalism for a topological theory. We only chose a Hopf algebra, $(A, m, \Delta, S, e, \epsilon)$ and we were able to show Pachner moves which imply topological invariance, except by multiplicative factors. However, the goal is to work with discrete groups, therefore it is natural introduce the group algebra defined below [JL01, pag. 53].

3.2. **Definition** (Group algebra)**.** Let G be a finite group whose elements are $g_1, \ldots, g_n$, and let F be a field ($\mathbb{R}$ or $\mathbb{C}$).
A vectorial space over F with $\phi_{g_1}, \ldots, \phi_{g_n}$ as a basis, is called vectorial space $F\mathsf{G}$. The elements of $F\mathsf{G}$ are all elements of the form $\sum\limits_{g \in \mathsf{G}} \lambda^g \phi_g = \lambda^g \phi_g$, where the rules of addition and multiplication by a scalar in $F\mathsf{G}$ are naturally given by: if

$$u = \lambda^i \phi_i \text{ and } v = \mu^i \phi_i$$

are elements of $F\mathsf{G}$, and $\lambda \in F$, then

$$u + v = (\lambda^i + \mu^i)\phi_i \text{ and } \lambda u = (\lambda \lambda^i)\phi_i.$$

Since G is a finite group of order n, $\dim F\mathsf{G} = n$.

The product of two elements ϕ_g, ϕ_h of the basis is provided by $\phi_g \phi_h = \phi_{gh}$, where the product gh is the same of the group G. For consistency, the structure constants of the product

$$m(\phi_g \otimes \phi_h) \equiv \phi_g \phi_h = m_{gh}^{\ \ k} \phi_k,$$

are given by $m_{gh}^{\ \ k} = \delta(gh, k)$. The identity element is written unambiguously as $e = \phi_e$, where $e \in \mathsf{G}$ is the identity of group G. The group algebra is a Hopf algebra if the following relations are satisfied

$$\begin{aligned}
(\phi_g \phi_h)\phi_k &= \phi_g(\phi_h \phi_k), \\
\Delta(\phi_g) &= \phi_g \otimes \phi_g, \\
\Delta(\phi_g \phi_h) &= \Delta(\phi_g)\Delta(\phi_h), \\
\epsilon(\phi_g \phi_h) &= \epsilon(\phi_g)\epsilon(\phi_h) \\
S(\phi_g) &= \phi_{g^{-1}}.
\end{aligned}$$

The structure constants of the coproduct and antipode are

$$\Delta_g^{hk} = \delta(g,h)\delta(g,k), \tag{20}$$

$$S_g^h = \delta(g,h^{-1}) \tag{21}$$

The diagram representing the property $\Delta(\phi_g) = \phi_g \otimes \phi_g$ corresponds to the figure

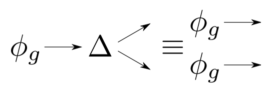

FIGURE 66. Homogeneous element aplied to the coproduct.

66, in which the element ϕ_g of the basis will be called an homogeneous element of the group algebra.

3.3. **Definition.** In the case of the group algebra $F\mathsf{G}$, the elements of the center of it will be provided by

$$Z(F\mathsf{G}) = \{z \in F\mathsf{G} : zr = rz \text{ for all } r \in F\mathsf{G}\},$$

with $z = t^g\phi_g$ for some coefficients $t^g \in F, \forall g \in \mathsf{G}$. It is easy to verify that if all t^g are equal to $t \in F$ then the element $t\sum\limits_{g\in\mathsf{G}}\phi_g$ belongs to $Z(F\mathsf{G})$. In the particular case $t = 1$, we are making reference to the cointegral element of the algebra, see definition 3.1 [BPT13].

3.15. Proposition.
Let ϕ_g be a homogeneous element of the group algebra and we define the diagram 67(a) for simplicity. Then Δ, can be modified as in figure 67(b).

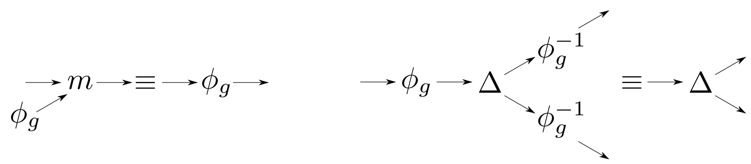

(a) *Definition $\to \phi_g \to$.* (b) Δ *modified.*

FIGURE 67. *Proposition.*

Proof. Considering the sequence of figures 68(a) to 68(e), we prove the desired result. □

3.6. **Abelian groups.** Let us contemplate show other useful properties for discrete abelian groups in the group algebra. Since we have a great interest in the $\mathbb{Z}_n$ group a "direct" application of it will be obtained in the following section.

We know that tensors M and Δ can be expressed in terms of the center z and cocenter ζ of an algebra, and we previously mentioned that these are represented by points on the black and gray curves. In the case of the group G be commutative, the Hopf algebra in the group algebra is commutative and cocommutative. Knowing that the move sliding implies topological invariance, we want to know what happens

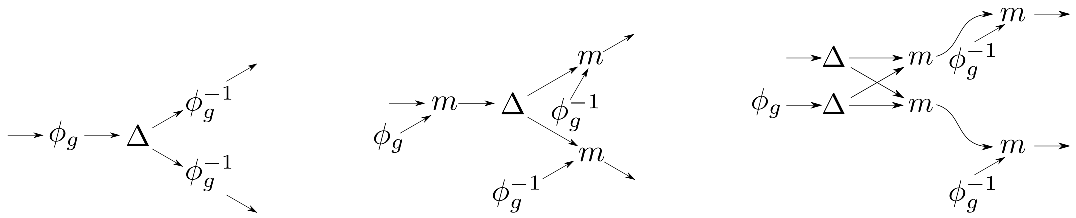

(a) (b) Definition $\to \phi_g \to$. (c) Relation product and co-product.

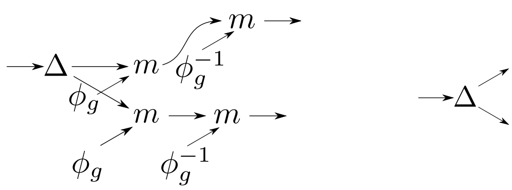

(d) Homogeneous element aplied to coproduct. (e) Associativity.

FIGURE 68. Proof of proposition 3.15.

with the weights of the curves after this move. The lemma 3.13 states that it is possible to make the sliding for curves of the same color when the weight of one of them is trivial. However, the following lemma is valid when the groups are abelian and the sliding move is applied over a black curve with weight, ϕ_g, a homogeneous element.

3.16. Lemma (Sliding over homogeneous elements).
Let G be an abelian group with $\phi_{g\in\mathsf{G}}$ the basis of the group algebra. Let C_1 and C_2 be two closed black curves with weights z and ϕ_g respectively, figure 69(a). The curve C_1 is replaced by the curve C_1' with weight $z\phi_g$. The new curve C_2' is an isotopy of C_2. The curve C_1' (resp. C_2') has the same orientation of C_1 (resp. C_2) figure 69(b).

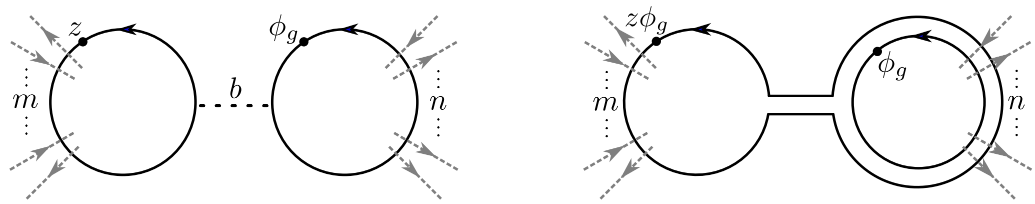

(a) *Two black curves connected by a ribbon.* (b) *Sliding.*

FIGURE 69. *69(a). The black curve C_1 (resp. C_2) has m (resp. n) crosses with gray curves (resp. black curves). 69(b). After sliding the final curve C_1' (resp. C_2') has $m+n$ (resp. n) crosses with gray curves (resp. black curves).*

Proof. The proof is similar to the sliding for the trivial case of the black curve to the right, lemma 3.13. However, in this situation the weights are represented as

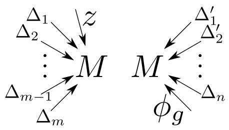

(a) Shape of tensors of curves.

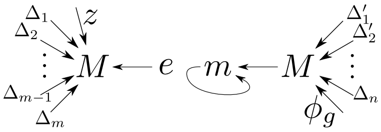

(b) Definition of M and counity e.

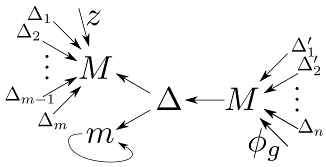

(c) Integral property.

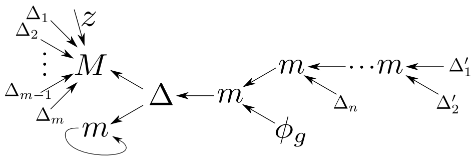

(d) Definition of M.

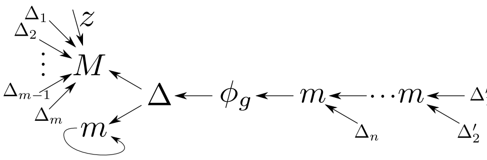

(e) Use of definition $\rightarrow \phi_g \rightarrow$.

FIGURE 70. First part of proof of sliding property.

points in the figures. Another difference is that for the proof of lemma 3.13, the center was considered as a gray curve. Now, the elements of the center are explicitly represented. We associate with each tensor M the element of the center as shown the figure 70(a) and then we follow the steps to figure 70(d). Finally we use the

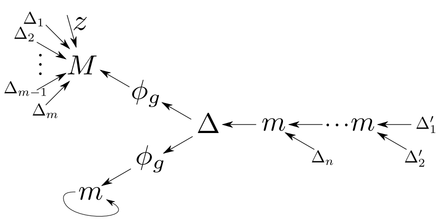

(a) Use proposition 3.15.

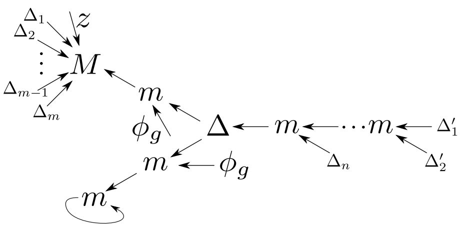

(b) Definition $\rightarrow \phi_g \rightarrow$.

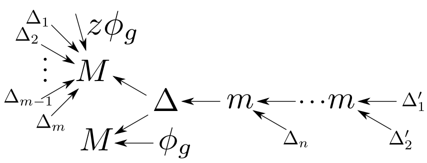

(c) Definition M.

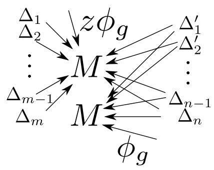

(d) Follow the steps in figure 55.

FIGURE 71. Second part of the statement of the sliding property.

proposition 67 from 71(a) to 71(d). □

Another property that can be shown is the following lemma:

3.17. Lemma.
Consider the diagrammatic configuration 72(a). It is equivalent to figure 72(b), here ζ is an element of cocenter of the algebra, which can be written as $\zeta = \sum_h \zeta_h \phi^h$. Thus, the element $\phi_g^{-1} \rightarrow \zeta$ is $\zeta_{g^{-1}}$.

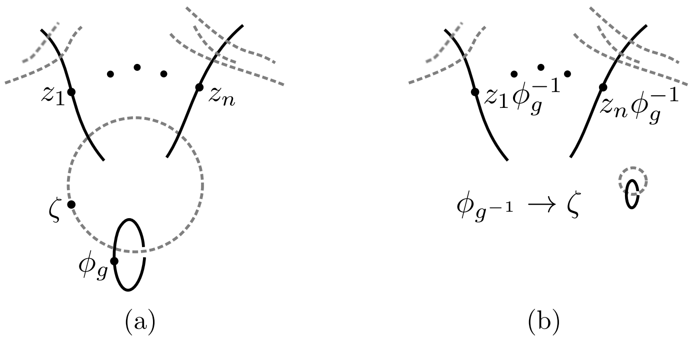

FIGURE 72. *Figure of lemma 3.17.*

Proof. To prove this lemma we write the tensor associated to each curve and then we use proposition 3.15. □

4. Gauge-Higgs model in the topological limits

In section 2 we described the traditional formalism when it is defined a gauge theory with matter fields. In this section, we use the unitary gauge which makes that the variables related with the matter field do not lie on the vertices, but in fact, lie on the links of the lattice of discretized manifold $\mathscr{M}$. Also, in section 3 we did a rundown of how a lattice topological theory can be constructed. We define tensors M and Δ which provide information of faces and links of the triangulation $\mathscr{T}$, and the tensor S which provides the relative orientation face-link in their crossings. Furthermore, we showed the invariance of the partition function in the representation of oriented black and gray curves, which are associated to faces and links respectively. But even defining the partition function and the Wilson loops, we did not calculate explicitly any of them.

In this section we calculate explicitly partition functions and Wilson loops of two-dimensional manifolds for the gauge-Higgs model with gauge group $\mathbb{Z}_2$. We do this remembering that the information of triangulation of the manifold $\mathscr{M}$ is contained in the weights of black and gray curves. As we mentioned, these weights are related to the center and cocenter of a Hopf algebra. We shall show that the weights associated to gray curves, which are in the cocenter of algebra, are related to the center of algebra, in such a way that we can replace this weight by one black curve with weight in the center of the algebra. Thus, by knowing only an expression of the center of the group, we can fully describe the gauge-Higgs model. As follows, we define what is a topological limit, and we see that for $\mathbb{Z}_2$, the partition function is topological or quasi-topological. Finally, we calculate the expected value of the observables, Wilson loops, using the formalism of curves shown here.

4.1. **Character expansions and center of group.**

In section 2 we state that for a finite group G, the action for a pure gauge model is given by expression (3)

$$S = -\beta \sum_{f\in\mathscr{F}} (\alpha(\mathrm{tr}(\rho(U_f)) + \mathrm{tr}(\rho(U_f^{-1}))) + \gamma),$$

where U_f is the holonomy for each face. Let r denote the representation in $\mathrm{tr}(\rho(U_f))$, such that the action can be written in terms of the character $\chi_r(U_f) = \mathrm{tr}(\rho(U_f))$. The weight associated with the partition function related with the gauge fields is (without loss of generality we take $\gamma = 0$)

$$W_{\text{gauge}}(\mathrm{f}) = \prod_f \mathrm{e}^{-\alpha\beta(\chi_r(U_f)+\overline{\chi_r(U_f)})}.$$

Let $M(U_f) = \mathrm{e}^{-\alpha\beta(\chi_r(U_f)+\overline{\chi_r(U_f)})}$ be the class function, i.e. $M(hU_fh^{-1}) = M(U_f)$ for all $h \in \mathsf{G}$. So, it is possible to expand $M(U_f)$ in terms of the k irreducible characters, $\chi_1, \ldots, \chi_k$ of the group G

$$M(U_f) = \sum_r M^r \chi_r(U_f), \tag{22}$$

where M^r are real numbers. In order to obtain these last terms, we use the following theorem (we take all irreducible representation as unitaries) [JL01, page 161]:

4.1. Theorem.
Let $\chi_1, \ldots, \chi_k$ be the irreducible characters of a finite group G. Let $g_1, \ldots, g_k$ be representatives of the conjugacy class of G. The following relations are satisfied for any $r, s \in \{1, \ldots, k\}$.

(1) *Ortogonality relation between rows:*

$$\sum_{i=1}^{k} \frac{\chi_r(g_i)\overline{\chi_s(g_i)}}{|C_{\mathsf{G}}(g_i)|} = \delta(r,s).$$

(2) *Ortogonality relation between columns:*

$$\sum_{i=1}^{k} \chi_i(g_r)\overline{\chi_i(g_s)} = \delta(r,s)|C_{\mathsf{G}}(g_r)|.$$

Where $C_{\mathsf{G}}(x)$ is the centralizer of x in G, this is, the set of elements $g \in G$ that commute with x.

On the other hand, we shall prove the following lemma [Fer14]:

4.1. Lemma.
Let $\chi_1, \ldots, \chi_k$ be the irreducible characters of a finite group G. The following relation is satisfied for all elements $f, h \in \mathsf{G}$

$$\sum_{g \in \mathsf{G}} \chi_r(gf)\overline{\chi_s(gh)} = n\delta_{rs}\chi_r(fh^{-1}). \tag{23}$$

Proof. We use the relation of ortogonality of irreducible unitary representation matrices $D(g)_i^{\ j}$ of the group G

$$\sum_{g \in \mathsf{G}} D_r(g)_i^{\ l}\overline{D_s(g)_j^{\ m}} = \frac{n}{d_r}\delta_{rs}\delta_{ij}\delta_{lm}, \tag{24}$$

where n and d_r are the dimension of the group and irreducible representation r, respectively [Ham89]. We write the expression (23) as

$$\sum_{g \in \mathsf{G}} \chi_r(gf)\overline{\chi_s(gh)} = \sum_{g,i,j} D_r(gf)_i^{\ i}\overline{D_s(gh)_j^{\ j}},$$

where we have used that $g \to gf$, so we write

$$\sum_{g\in\mathsf{G}} \chi_r(gf)\overline{\chi_s(gh)} = \sum_{g,i,j} D_r(g)_i^{\ i}\overline{D_s(gf^{-1}h)_j^{\ j}} = \sum_{g,i,j,k} D_r(g)_i^{\ i}\overline{D_s(g)_j^{\ k}}\,\overline{D_s(f^{-1}h)_k^{\ j}}.$$

Using the ortogonality relation (24) we obtain

$$\begin{aligned}\sum_{g\in\mathsf{G}} \chi_r(gf)\overline{\chi_s(gh)} &= \sum_{i,j,k} \frac{n}{d_r}\delta_{rs}\delta_{ij}\delta_{ik}\overline{D_s(f^{-1}h)_k^{\ j}} \\ &= \sum_i n\delta_{rs}\overline{D_s(f^{-1}h)_i^{\ i}} \\ &= n\delta_{rs}\chi_r(fh^{-1}),\end{aligned}$$

because the representation is unitary, and we had proven the lemma. □

With the above lemma we find the coefficients M^r in (22) to obtain

$$\sum_{U_f} M(U_f)\overline{\chi_s(U_f)} = \sum_{r,U_f} M^r\chi_r(U_f)\overline{\chi_s(U_f)} \to M^r = \frac{1}{n}\sum_{U_f} M(U_f)\overline{\chi_r(U_f)}. \tag{25}$$

For consistency, we note that $M(U_f)$ is the contraction between tensors $M_{a_1a_2\cdots a_{N_{e_f}}}|_{a_i\in\partial f}\Delta^{b_1b_2\cdots b_k}\prod_i S_{x_i}^{y_i}$ defined in (16), where for each link a_i we associate an element g of a group G, and there is an antipode when the relative orientation face-link is reversed.

We recall that the partition function in the formalism of Heegaard diagrams depends of weights on the faces and links (16). However, due to the weight of faces associated with black curves, this is associated with the center of the gauge group G. Since it is a finite group, every element of the center $z \in Z(F\mathsf{G})$ can be written as [JL01]

$$z = \sum_i z^i c_i, \text{ where } c_i = \sum_{g\in\mathscr{C}_i} \phi_g \tag{26}$$

with $\mathscr{C}_i$ the conjugacies class of the group G and z^i complex numbers. Also, as mentioned above, the contraction between tensors $M_{a_1a_2\cdots a_{N_{e_f}}}|_{a_i\in\partial f}\Delta^{b_1b_2\cdots b_k}\prod_i S_{x_i}^{y_i}$ (where a_i are links around the face f and each g_i is an element of the group G associated with the link) must coincide with $M(U_f)$. In the group algebra we have (expressions (14), (20) and (21))

$$\begin{aligned}M_{a_1a_2\cdots a_{N_{e_f}}}|_{a_i\in\partial f}\Delta^{b_1b_2\cdots b_k}\prod_i S_{x_i}^{y_i} &= \mathrm{tr}(z\phi_{g_1}\cdots\phi_{g_{N_{e_f}}})\Delta^{g_1g_1'}\cdots\Delta^{g_{N_{e_f}}g_{N_{e_f}}'}\prod_i S_{b_i'}^{y_i} \\ &= \mathrm{tr}\left(z\prod_i^{N_{e_f}}\phi_{g_i^{o_i(f,e_i)}}\right) \\ &= \mathrm{tr}(z\phi_{U_f}),\end{aligned}$$

with $U_f = \prod_i^{N_{e_f}} g_i^{o_i(f,e_i)}$ the holonomy around of the face f. Using the expression (26) we obtain

$$M_{a_1a_2\cdots a_{N_{e_f}}}|_{a_i\in\partial f}\Delta^{b_1b_2\cdots b_k}\prod_i S^{y_i}_{x_i} = \sum_i z^i \mathrm{tr}(c_i\phi_{U_f}) = \sum_i\sum_{g\in\mathscr{C}_i} z^i\mathrm{tr}(\phi_g\phi_{U_f}).$$

For the group algebra $\mathrm{tr}(\phi_g\phi_{U_f}) = \mathrm{tr}(\phi_{gU_f}) = n\delta(gU_f, e) = \chi_r(gU_f)$ for some representation r. Since $M_{a_1a_2\cdots a_{N_{e_f}}}|_{a_i\in\partial f}\Delta^{b_1b_2\cdots b_k}\prod_i S^{y_i}_{x_i} = M(U_f)$ we have

$$M(U_f) = \sum_i\sum_{g\in\mathscr{C}_i} z^i\chi_r(gU_f).$$

Multiplying both sides by $\overline{\chi_s(U_f)}$ and adding all the group elements we find

$$\begin{aligned}\sum_{U_f} M(U_f)\overline{\chi_s(U_f)} &= \sum_i\sum_{g\in\mathscr{C}_i} z^i\sum_{U_f}\chi_r(gU_f)\overline{\chi_s(U_f)}\\ &= \sum_i\sum_{g\in\mathscr{C}_i} z^i n\delta_{rs}\chi_r(g),\end{aligned}$$

where we used the lemma 4.1. In the last sum we can take a representative element $g_i \in \mathscr{C}_i$ such that the number of elements in the conjugacy class $\mathscr{C}_i$ is $|\mathscr{C}_i|$. So, we have

$$n\sum_{g_i\in\mathsf{G}} z^i|\mathscr{C}_i|\chi_r(g_i) = \sum_{U_f} M(U_f)\overline{\chi_r(U_f)}.$$

Multiplying both sides by $\overline{\chi_r(g_j)}$ and adding all the representative characters r

$$n\sum_{g_i\in\mathsf{G}} z^i|\mathscr{C}_i|\sum_r\chi_r(g_i)\overline{\chi_r(g_j)} = \sum_{U_f} M(U_f)\sum_r\chi_r(U_f^{-1})\overline{\chi_r(g_j)}.$$

Finally, we use the ortogonality relation for columns of theorem 4.1, where we note that U_f^{-1} must be in some conjugacy class such that the element g_k is its representative element

$$n\sum_{g_i\in\mathsf{G}} z^i|\mathscr{C}_i|\delta(i,j)|C_{\mathsf{G}}(g_j)| = \sum_{g_k} M(g_k^{-1})\delta(i,k)|C_{\mathsf{G}}(g_i)| = M(g_i^{-1})|\mathscr{C}_i||C_{\mathsf{G}}(g_i)|,$$

where in the last expression we have used the fact that M is a class function and that the number of elements in the conjugacy class $\mathscr{C}_k$ is $|\mathscr{C}_k|$. We obtain that the coefficients z^i are given by $z^i = \frac{1}{n}M(g_i^{-1})$. However $M(U_f) = M(U_f^{-1})$, therefore the coefficients are

$$z^i = \frac{1}{n}M(g_i). \tag{27}$$

This last expression gives the weight related with a pure gauge, for a general finite group such that $M(U_f) = \mathrm{e}^{-\alpha\beta(\chi_r(U_f)+\overline{\chi_r(U_f)})}$. For example, we know that the dihedral group [JL01]

$$G = D_6 = \langle a, b : a^3 = b^2 = 1, b^{-1}ab = a^{-1}\rangle$$

has elements, $g = \{1, a, a^2, b, ab, a^2b\}$, and the representative elements of its conjugacies classes are,

$$1^G = \{1\}, a^G = \{a, a^2\}, b^G = \{b, ab, a^2b\}.$$

Then, since the characters of D_6 are real numbers, see table 1, we have that the

	1	a	b
χ_1	1	1	1
χ_2	1	1	-1
χ_3	2	-1	0

Table 1. Characters for the group $G = D_6$.

coefficients which expand the center have the form ($\alpha = \frac{1}{2}\times$units such that their product with β gives dimensionless)

$$z^g_{D_6} = \frac{1}{6}\mathrm{e}^{-\beta\chi_r(g)}, \text{ such that } z = \sum_{i\in D_6} z^i \sum_{g\in\mathscr{C}_i} \phi_g.$$

Now, we know that D_6 has three irreducible characters, therefore we write the center for each one of these as

$$\begin{aligned} z &= \frac{1}{6}(\phi_1 + \phi_a + \phi_{a^2} + \phi_b + \phi_{ab} + \phi_{a^2b}); \text{ for } r = 1 \\ z &= \frac{1}{6}\mathrm{e}^{-\beta}\phi_1 + \frac{1}{6}\mathrm{e}^{-\beta}(\phi_a + \phi_{a^2}) + \frac{1}{6}\mathrm{e}^{\beta}(\phi_b + \phi_{ab} + \phi_{a^2b}); \text{ for } r = 2 \\ z &= \frac{1}{6}\mathrm{e}^{-2\beta}\phi_1 + \frac{1}{6}\mathrm{e}^{\beta}(\phi_a + \phi_{a^2}) + \frac{1}{6}(\phi_b + \phi_{ab} + \phi_{a^2b}); \text{ for } r = 3. \end{aligned}$$

We note that the first of the above expressions coincides with the definition of the cointegral multiplied by a constant given by the definition 3.3. The other two expressions for the center of the group for the particular action of gauge pure can be used to describe the theory, however, we use the second expression because it has each term dependent of β.

For the $\mathbb{Z}_n$ case, recalling the action for the gauge-Higgs field with gauge group found in section 2

$$S_{\text{gauge-Higgs}} = -\beta_G \sum_f \cos\left(\frac{2\pi}{n}\sum_{i=1}^{N_{e_f}} k_i\right) - \beta_H \sum_l \cos\left(\frac{2k_l\pi}{n}\right), \tag{28}$$

where every $k_i \in \{0, 1, \dots, n-1\}$. As previously mentioned, the term field spin-gauge is due to the holonomy in all faces. We recognize $M(U_f) = -\beta_G \cos\left(\frac{2\pi}{n}\sum_{i=1}^{N_{e_f}} k_i\right)$.

Following the expression (27), we find that the coefficients expanding the center are given by

$$z^h = \frac{1}{n}\mathrm{e}^{\beta\cos\left(\frac{2h\pi}{n}\right)}, \tag{29}$$

where h now corresponds to the representative element of each conjugacy class. I.e., the center is

$$z = \frac{1}{n} \sum_{h=0}^{n-1} \mathrm{e}^{\beta \cos\left(\frac{2h\pi}{n}\right)} \phi_h. \tag{30}$$

Taking the expression (25), the characters are given in terms of coefficients which expand the center of group

$$M^r = \sum_{h=0}^{n-1} z^h \omega^{-hr} = \frac{1}{n} \sum_{h=0}^{n-1} \mathrm{e}^{\beta \cos\left(\frac{2h\pi}{n}\right)} \omega^{-hr}. \tag{31}$$

We notice that this center z, associated to faces, has a similar relation in the case of links, by the expression (28). However, we have to be careful, because the information on the links is associated with the center of coalgebra or cocenter and not to the center. In the next subsection, we will show how to obtain the physical information, in the regular representation, of the triangularized manifold $\mathscr{M}$ using only the elements z of the center of group G.

4.1. *Remark.*
We can note that the coefficients describing the model, pure gauge or pure Higgs, are given by $\tilde{\gamma}^k = \frac{1}{n}\mathrm{e}^{\beta \cos\left(\frac{2k\pi}{n}\right)}$ for $k = \{0, 1, \dots, n-1\}$. So, the relation between them is found by multiplying these terms in order to obtain

$$\tilde{\gamma}^0 \tilde{\gamma}^1 \cdots \tilde{\gamma}^{n-1} = \frac{1}{n^n} \mathrm{e}^{\beta \sum\limits_{k=0}^{n-1} \cos\left(\frac{2k\pi}{n}\right)} = \frac{1}{n^n},$$

due to the fact that $\sum\limits_{k=0}^{n-1} \cos\left(\frac{2k\pi}{n}\right) = 0$. Normalizing, we take $\tilde{\gamma}^k = n\gamma^k$ and we have

$$\gamma^0 \gamma^1 \cdots \gamma^{n-1} = 1, \tag{32}$$

this is the expression which describes the model.

4.2. *Remark.*
In the remark 3.1 we assure that $S(z) = z$, to have topological invariance with respect to the orientation of the black curve b. We see this for our z which describes the gauge-Higgs model. Indeed, we can write z as expression (26)

$$z = \sum_i z^i c_i, \text{ where } c_i = \sum_{g \in \mathscr{C}_i} \phi_g,$$

such that z is written following the expression (27), $z^i = \frac{1}{n} M(g_i) = \frac{1}{n} M(g_i^{-1})$

$$z = \frac{1}{2n} \sum_i \left(M(g_i) \sum_{g \in \mathscr{C}_i} \phi_g + M(g_i^{-1}) \sum_{g^{-1} \in \mathscr{C}_i'} \phi_g \right).$$

Therefore, the antipode $S(z)$ for the group algebra is

$$\begin{aligned} S(z) &= \frac{1}{2n}\sum_i \left(M(g_i) \sum_{g\in\mathscr{C}_i} \phi_{g^{-1}} + M(g_i^{-1}) \sum_{g^{-1}\in\mathscr{C}_i'} \phi_{g^{-1}} \right) \\ &= \frac{1}{2n}\sum_i \left(M(g_i) \sum_{g^{-1}\in\mathscr{C}_i} \phi_{g} + M(g_i^{-1}) \sum_{g\in\mathscr{C}_i'} \phi_{g} \right), \end{aligned}$$

but this last expression coincides with z, then $S(z) = z$, which is the required condition.

4.2. **Partition function and Wilson loops with matter fields.** In order to study gauge fields coupled to matter, we have to check the relation between these two fields. In section 3 we stated that the information contained in gray curves, which are associated with the links, depends on the elements ζ of the cocenter of the algebra $\mathscr{A}$. However, the following lemma will show that it can be replaced the weight associated with a gray curve by one black curve which has a weight that belongs to center of the algebra.

4.2. Lemma.
Consider the group algebra $\mathscr{A}$, and a gray curve with weight $\zeta = \zeta_h \phi^h$ as in figure 73(a). The weight ζ can be replaced by a black curve with weight $z = z^h \phi_h$, as it is

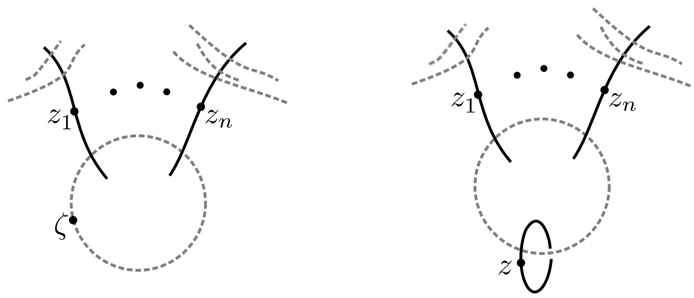

(a) *Gray curve with weight ζ.*

(b) *Gray curve with one additional black curve with weight z.*

FIGURE 73. *Equivalence between gray curves.*

shown in figure 73(b). The relation between the elements z^h of z and the coefficients ζ_h of ζ is given by $z^h = \frac{1}{\dim(\mathscr{A})}\zeta_{h^{-1}}$.

Before the proof of lemma 4.2, we will recall the meaning of the term diagrammatic, as follows: imagine a gray curve g with weight ζ and n crossings with black curves $\mathsf{b}_{i\in\{1,2,\ldots,n\}}$, with weights z_i as in figure 73(a). Originally g had n crossings with black curves and in turn, each black curve b_i have several intersections with gray curves. The lemma states that it can be added a black curve with weight z, but it will only have a crossing; therefore the partition function of Kuperberg for a manifold $\mathscr{M}$ with triangulation $\mathscr{T}$ (expression (16))

$$Z(\mathscr{M},\mathscr{T}) = \sum_{\text{conf}}\prod_{\text{f}}\prod_{\text{e}}\prod_{\text{o}} M_{abc}(\text{f})\Delta^{b_1 b_2\cdots b_k}(\text{e})S_x^y(\text{o}),$$

will be

$$Z(\mathscr{M},\mathscr{T}) = \sum_{\text{conf}}\prod_{\text{f}}\prod_{\text{e}}\prod_{\text{o}} M_{abc}(\text{f})N_{b_{k+1}}(\text{f}')\Delta^{b_1 b_2\cdots b_k b_{k+1}}(\text{e})S_x^y(\text{o}). \tag{33}$$

Note that the the differences between both partition functions are the extra face f' and the Δ associated to the hinges. $N(\text{f}')$ is the tensor associated with the new black curve and this has an element associated with the center z', which in general is different from the z associated with the original black curves. $\Delta^{b_1 b_2\cdots b_k b_{k+1}}$ implies to add another polygon to each hinge.

According to the mentioned above, the Wilson loops for a loop ℓ must be

$$\langle W(\ell)\rangle = \frac{1}{Z(\mathscr{M},\mathscr{T})}\sum_{\text{conf}}\prod_{\text{f}}\prod_{\text{e}}\prod_{\text{o}} W(\ell)M_{abc}(\text{f})N_{b_{k+1}}(\text{f}')\Delta^{b_1 b_2\cdots b_k b_{k+1}}(\text{e})S_x^y(\text{o}),$$

where $W(\ell) = \chi_r(U_\ell)$. χ_r are the characters and U_ℓ is the holonomy of links variables around the closed curve ℓ. Considering for simplicity a two-dimensional manifold $\mathscr{M}$ and supposing that the orientation of the loop is arbitrary. Let ℓ be a loop, with

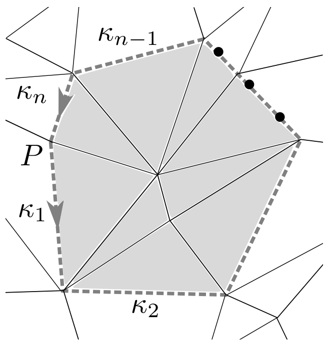

Figure 74. Loop with links κ_i.

origin at P and with the set of links $\kappa(\ell) = \{\kappa_1,\ldots,\kappa_n\}$ as it is shown in figure 74. Let G be the gauge group and we suppose that the lattice $\mathscr{M}$ is oriented. The holonomy over the loop ℓ is (see expression (1))

$$U_\ell = \prod_{\kappa_i\in\ell} g_{k_i}^{o_i(\ell,\kappa_i)},$$

with $o_i(\ell,\kappa_i) = \pm 1$ the relative orientation loop-link, and k_i the element representative to link κ_i. $\chi_r(U_\ell)$ is given by

$$\chi_r(U_\ell) = \chi_r\left(\prod_{\kappa_i\in\ell} g_{k_i}^{o_i(\ell,\kappa_i)}\right),$$

so, it is natural to define the covariant tensor $W^r_{k_1k_2\cdots k_n} \equiv \chi_r(U_\ell)$, so that the Wilson loops are written as

$$\langle W(\ell)\rangle = \frac{1}{Z(\mathscr{M},\mathscr{T})}\sum_{\text{conf}}\prod_{\text{f}} M_{abc}(\text{f})N_{b_{k+1}}(\text{f}')\prod_{\text{e}\notin\kappa(\ell)}\Delta^{b_1b_2\cdots b_kb_{k+1}}(\text{e}) \prod_{\kappa_j\in\kappa(\ell)}\Delta^{b_1b_2\cdots b_kb_{k+1}k_j}(\text{e})W^r_{k_1k_2\cdots k_n}\prod_{\text{o}}S^y_x(\text{o}), \tag{34}$$

where each covariant index $W^r_{k_1\cdots k_n}$ is contracted with the additional index k_j in $\Delta^{b_1b_2\cdots b_kb_{k+1}k_j}(\text{e})$ [FPTS12]. The meaning of the latter term is that links κ_i belonging to loop ℓ, would seem to add a polygon to the manifold $\mathscr{M}$, see figure 75, therefore

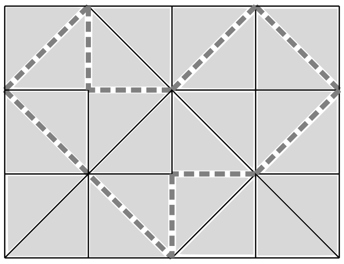

Figure 75. Loop in a regular triangular lattice.

we represent the loop with a dark gray color. Note that it is not necessary to locate the source of the loop because this is arbitrary. The polygon in figure 75 will have associated an element of the center

$$z_{\text{W}} = \sum_i z^i_{\text{W}}c_i \text{ where } c_i = \sum_{g\in\mathscr{C}_i}\phi_g,$$

and the index W denotes the weight associated to the Wilson loop. To find the elements z^i_{W} which expand the center, we make use of expression (27), noting that in our case, according with (35) the weight $M(g_i)$ is $\Delta^{b_1k_i}(\text{e})W^r_{k_i}$. Therefore,

$$z^i_{\text{W}} = \frac{1}{n}W^r_{k_i} = \frac{1}{n}\chi_r\left(\left(g_i^{o_i(\ell,k_i)}\right)^{-1}\right) = \frac{1}{n}\chi_r\left(g_i^{-o_i(\ell,k_i)}\right),$$

since we assume that the orientation of the loop over the lattice is arbitrary, we have

$$z^i_{\text{W}} = \frac{1}{n}\chi_r(g_i). \tag{35}$$

The last expression is a generalization of the paper [FPTS12], where $\mathbb{Z}_2$ was used as the only group considered for the three-dimensional case. As an example, for the dihedral group D_6 we obtain

$$\begin{aligned}
z_{\text{W}} &= \frac{1}{6}(\phi_1+\phi_a+\phi_{a^2}+\phi_b+\phi_{ab}+\phi_{a^2b});\ \text{for } r=1\\
z_{\text{W}} &= \frac{1}{6}\phi_1+\frac{1}{6}(\phi_a+\phi_{a^2})-\frac{1}{6}(\phi_b+\phi_{ab}+\phi_{a^2b});\ \text{for } r=2\\
z_{\text{W}} &= -\frac{1}{3}\phi_1+\frac{1}{6}(\phi_a+\phi_{a^2});\ \text{for } r=3.
\end{aligned}$$

In the case of $\mathbb{Z}_n$, the coefficients z^i_{W}, have the form

$$z^i_{\mathrm{W}} = \frac{1}{n}(\omega^r)^{k_i},$$

where $\omega = \mathrm{e}^{\frac{2\pi}{n}\mathrm{i}}$ and $r, k_i = \{0, 1, \dots, n-1\}$. Using again the faithful representation $r = 1$ to obtain (subsection 2.4)

$$z_{\mathrm{W}} = \frac{1}{n}\left(\phi_0 + \mathrm{e}^{\frac{2\pi}{n}\mathrm{i}}\phi_1 + \dots + \mathrm{e}^{\frac{2(n-1)\pi}{n}\mathrm{i}}\phi_{n-1}\right). \tag{36}$$

Lemma 4.2. The tensor related to the gray curve is given by the diagram 76(a). We

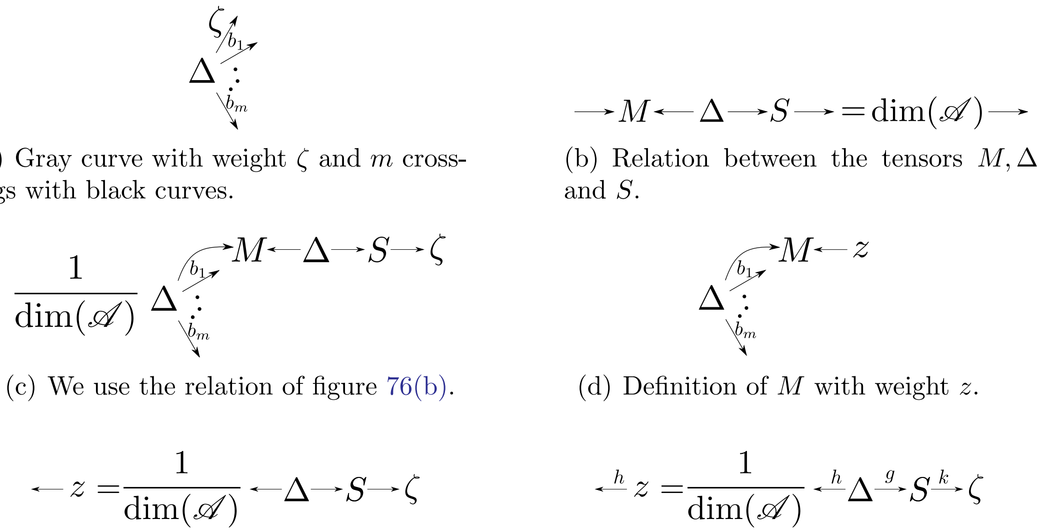

(a) Gray curve with weight ζ and m crossings with black curves.

(b) Relation between the tensors M, Δ and S.

(c) We use the relation of figure 76(b).

(d) Definition of M with weight z.

(e) Definition of z in figure 76(d).

(f) z written in terms of the coefficients.

FIGURE 76. Diagrammatic proof of lemma 4.2.

use the lemma 3.2 (figure 76(b)) for the inward arrows in ζ and we write the tensor explicitly as diagrams. Algebraically

$$z^h = \frac{1}{\dim(\mathscr{A})}\sum_{g,k}\Delta^{h,g}S^k_g\zeta_k$$

in the group algebra $\Delta^{h,g} = \delta(h,g)$ and $S^k_g = \delta(g, k^{-1})$, then

$$z^h = \frac{1}{\dim(\mathscr{A})}\sum_{g,k}\delta(h,g)\delta(g,k^{-1})\zeta_k = \frac{1}{\dim(\mathscr{A})}\zeta_{h^{-1}}.$$

□

In the three-dimensional case, the lemma states that it is equivalent to add another face to each hinge as stated earlier. However, for the two-dimensional case where each link has originally two faces glued to it (figure 77(a)) when one more face is added, we would obtain a three-dimensional model. The new face can be considered perpendicular to the plane, as shown in figure 77(b). Note that the colors of perpendicular faces are different from the original this is due that they have

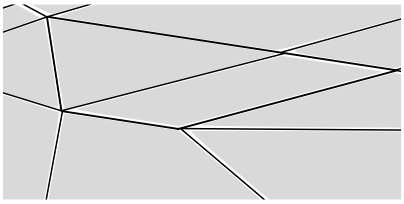

(a) Two-dimensional lattice. Links with weight gluing two polygons.

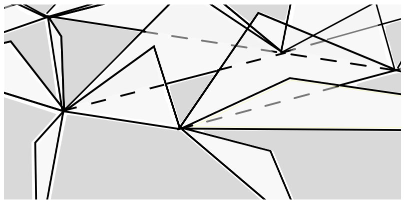

(b) Three-dimensional lattice. Links with weight gluing three polygons.

FIGURE 77. Equivalence between a two-dimensional lattice with weights in the links and a three-dimensional lattice without weight in the links.

a different weight associated (element of center). The original faces give the gauge fields and new polygons gives of the Higgs fields.

4.3. **Partition function and Wilson loops for a two-dimensional lattice.** Let us define the partition function for a two-dimensional lattice formed only by triangles (three links per triangle), figure 78(a). As it was stated, gauge fields are

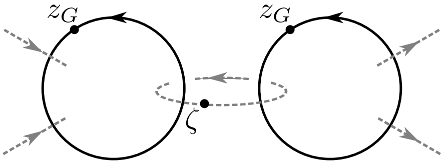

(a) Two-dimensional lattice. Edges with weight gluing two polygons.

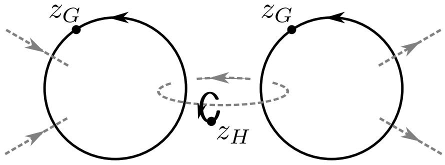

(b) Three-dimensional lattice. Edges without weight gluing three polygons.

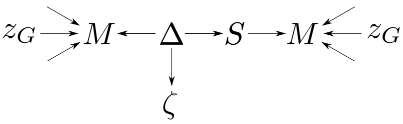

(c) Tensors figure 78(a).

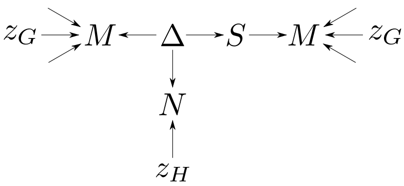

(d) Tensors figure 78(b)

FIGURE 78. Equivalence between a two-dimensional lattice with weights on the links and a three-dimensional lattice without weight on the links.

related to faces and matter fields to the links of triangulation. In the same way, faces and links are related to the elements z from the center and ζ of the cocenter respectively (as it is shown in figure 78(a), and the related tensorial diagram is shown in figure 78(c)). On the other hand, for the finite gauge group G we find that for the group algebra, the element z of center is provided by

$$z = \frac{1}{n}\sum_i M(g_i)c_i, \text{ where } c_i = \sum_{g\in\mathscr{C}_i}\phi_g.$$

This expression gives all the information related to the faces of the triangulation. However, the lemma 4.2 states that for the special case of the group algebra the information in the links is also provided by elements of the center of the group, figure 78(b). To distinguish between the elements of the center related to faces (gauge fields) and the links (Higgs field) we call z_G the elements of center associated with black curves (faces) and z_H the elements of center associated with the black curves which intersect only a gray curve (link), figure 78(b) (tensorial diagram 78(d)). For a manifold $\mathscr{M}$ without boundary, with triangulation $\mathscr{T}$, we note that each hinge has three glued faces. Therefore, the partition function of Kuperberg (33) in this instance will be

$$Z(\mathscr{M},\mathscr{T}) = \sum_{\text{conf}} \prod_{\text{f}} \prod_{\text{e}} \prod_{\text{o}} M_{abc}(\text{f}) N_{b_3}(\text{f}') \Delta^{b_1 b_2 b_3}(\text{e}) S_x^y(\text{o}). \tag{37}$$

For the case of Wilson loops, we draw a loop ℓ over the lattice, as in figure 75, and

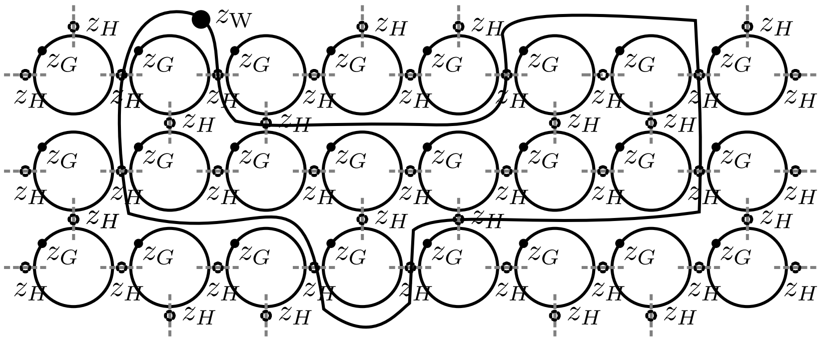

FIGURE 79. Representation in the language of colored curves of a two-dimensional manifold with loop ℓ. Each curve has an associated weight. All black curves have weights related to the center of algebra. Faces: z_G. The dotted black points related to links: z_H. The Wilson loop: z_W.

this will have the equivalent diagram in colored curves of figure 79. Note that in this diagram the weight associated with the loop ℓ is denoted by z_W and the orientation of each curve is not considered. Finally, in accordance with the mentioned above, the expected value of observables, Wilson loops, is given by

$$\langle W(\ell)\rangle = \frac{1}{Z(\mathscr{M},\mathscr{T})} \sum_{\text{conf}} \prod_{\text{f}} \prod_{\text{e}} \prod_{\text{o}} W(\ell) M_{abc}(\text{f}) N_{b_3}(\text{f}') \Delta^{b_1 b_2 b_3}(\text{e}) S_x^y(\text{o}). \tag{38}$$

4.4. **Calculation of the partition function and Wilson loops in the topological limits for $\mathbb{Z}_n$; detailed case, $\mathbb{Z}_2$.** So far, we showed the mathematical formalism needed to find partition functions over manifolds. Our goal is to calculate partition functions as general as possible form using the diagrammatic representation provided here. Let us recall that for the group $\mathbb{Z}_n$ with the group algebra we showed several useful properties such as the lemmas 3.16, 3.17, in addition each of the general moves 2.5 defined in section 2, were proved as lemmas (see lemmas 3.6 to 3.13) in section 3.

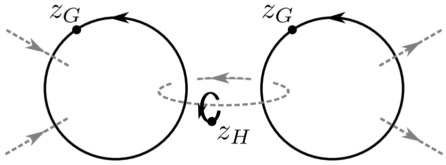

FIGURE 80. Two-dimensional lattice model.

In first instance we remember that the expression (30), which gives the center (for the gauge field z_G and for the matter field z_H) in terms of the elements of the group

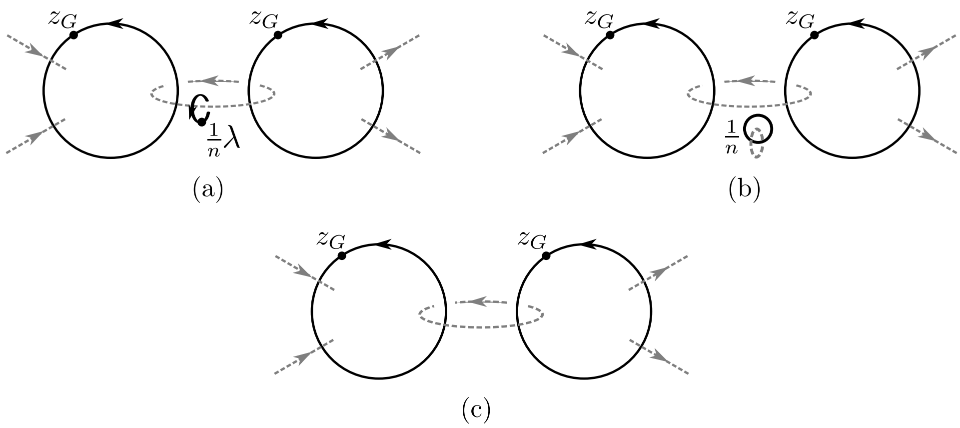

FIGURE 81. Two-dimensional gauge pure model.

$\mathbb{Z}_n$, is

$$z_{G,H} = \frac{1}{n}\sum_{h=0}^{n-1} \mathrm{e}^{\beta_{G,H}\cos\left(\frac{2h\pi}{n}\right)}\phi_h.$$

We note that for $\beta_{G,H} \to 0$, the element of the center will be $z_{G,H} = \frac{1}{n}\sum\limits_{h=0}^{n-1}\phi_h$, that is, the cointegral element divided by n. If we take $\beta_H \to 0$, the figure 80 is modified to figure 81(a), where λ is the cointegral element of algebra $\mathscr{A}$. Using the cointegral property, lemma 3.11, we obtain the figure 81(b). However, following the lemma 3.14 we know that isolated black and gray curves have as numerical value the dimension of algebra. Thus we obtain a gauge pure model, as expected [Kog79, YT07], see

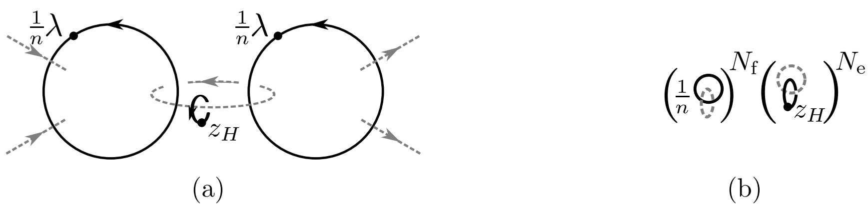

FIGURE 82. Representation of pure Higgs for two-dimensional case.

figure 81(c). On the other hand, for $\beta_G \to 0$, we have that the figure 80 will be modified by the figure 82(a). Using again the cointegral property we obtain the diagram 82(b), where N_{f} and N_{e} are the number of faces and links respectively. However, we know that a gray curve crossing just a black curve, has a numeric value which is equal to the dimension of algebra $\mathscr{A}$, then the factor 82(b) dependent on the number of faces is 1. For the term depending only on links, we see that tensors are provided in figure 83(a). Remember that $\phi_g \to \epsilon : \epsilon(\phi_g) = 1$ for all $g \in \mathsf{G}$. Since

(a) Tensors. (b) Use property of cointegral.

FIGURE 83. 83(a). Diagrammatic representation of tensors of a black curve with weight z_H and one gray curve. 83(b). Trivial tensors.

ϵ is a linear operation, the numerical value on the left part of the figure 83(b) in terms of the coefficients of the center is

$$\epsilon(z_H) = \frac{1}{n}\sum_{h=0}^{n-1} \mathrm{e}^{\beta_H \cos\left(\frac{2h\pi}{n}\right)}.$$

Thus, the numerical value of the partition function for a manifold $\mathscr{M}$ with triangulation $\mathscr{T}$ in pure Higgs case is

$$Z(\mathscr{M},\mathscr{T}) = \left(\sum_{h=0}^{n-1} \mathrm{e}^{\beta_H \cos\left(\frac{2h\pi}{n}\right)}\right)^{N_{\mathrm{e}}},$$

and this result coincides with Salinas [Sal10, page 91] where $\mathbb{Z}_2$ is the considered group. We obtain that the partition function explicitly depends on the number of links of triangulation, and now it is possible to state that the model is quasi-topological as defined in expressions (18) and (19).

In this paper, we observe the behavior of the partition function and Wilson loops for the group $\mathbb{Z}_2$ in the limits $\beta_{G,H} = 0^{\pm}, \beta_{G,H} = \pm\infty$, because as we will see, the partition functions in these situations can be calculated using moves over the colored curves, which means that the partition function is invariant or quasi-invariant topological. Thus, these limits are called topological limits of the theory. Note that the center for $\mathbb{Z}_n$ in the limit $\beta \to \infty$ is

$$\begin{aligned} z &= \frac{1}{n}\lim_{\beta\to\infty}\sum_{h=0}^{n-1} \mathrm{e}^{\beta\cos\left(\frac{2h\pi}{n}\right)}\phi_h \\ &= \frac{1}{n}\left(\sum_{h=1}^{n-1}\lim_{\beta\to\infty} \mathrm{e}^{\beta\cos\left(\frac{2h\pi}{n}\right)}\phi_h\right). \end{aligned}$$

The roots $\omega^h, h = 0,\dots,n-1$ are around the unitary circle. Thus, by taking $\cos\left(\frac{2h\pi}{n}\right)$ we have P positive values, negative values N and Z' null values (zeros), with $P + N + Z' = n$. Then, the center will be provided by

$$z = \frac{1}{n} P\gamma \sum_{h} \phi_h,$$

where $\gamma \to \infty$ and the sum is over h such that $\cos\left(\frac{2h\pi}{n}\right) > 0$.

Partition function for $\mathbb{Z}_2$. To obtain partition functions for $\mathbb{Z}_2$, we note that the two-dimensional model is represented in figure 84. Now, it is not necessary to orient the curves, since the relative orientation face-link is not required (the inverse element

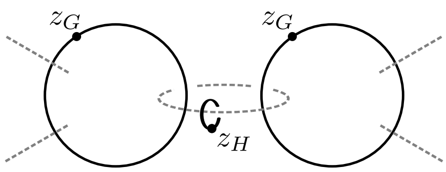

FIGURE 84. Two-dimensional gauge-Higgs model for $\mathbb{Z}_2$.

of one element of basis ϕ_g is itself). Note that the center of the group is provided by the gauge and Higgs fields as

$$z_{G,H} = \frac{1}{2} \sum_{h=0}^{1} \mathrm{e}^{\beta_{G,H} \cos(h\pi)} \phi_h = \sum_{g=0}^{1} \tilde{\gamma}_{G,H}^{g} \phi_g,$$

where the coefficients $\tilde{\gamma}_{G,H}^{g}$ are positive real numbers. Writing the term ϕ_g of the basis as $(0, \ldots, \underbrace{1}_{(g+1)\text{ th position}}, \ldots, 0)$, we have $z_{G,H} = (\tilde{\gamma}_{G,H}^{0}, \tilde{\gamma}_{G,H}^{1})$, with $\tilde{\gamma}_{G,H}^{0}$ and $\tilde{\gamma}_{G,H}^{1}$ the coefficients which expand the basis $\{\phi_0, \phi_1\}$. Let us calculate the partition functions for different z. For example, when $\beta_{G,H} = \pm\infty$, the centers will be given by

$$z_{G,H} = \begin{cases} \tilde{\gamma}_{G,H}^{0} \phi_0, & \text{if } \beta_{G,H} \to \infty \\ \tilde{\gamma}_{G,H}^{1} \phi_1, & \text{if } \beta_{G,H} \to -\infty \end{cases} = \begin{cases} (\tilde{\gamma}_{G,H}^{0}, 0), & \text{if } \beta_{G,H} \to \infty \\ (0, \tilde{\gamma}_{G,H}^{1}), & \text{if } \beta_{G,H} \to -\infty \end{cases}.$$

I.e., the centers will have the form $z_{G,H} = \tilde{\gamma}_{G,H}^{g} \phi_g$ where the Einstein sum notation is not used. Considering several cases for the centers:

- $z_H = \tilde{\gamma}_H^h \phi_h$: the model in figure 84, will be represented by figure 85(a). Since

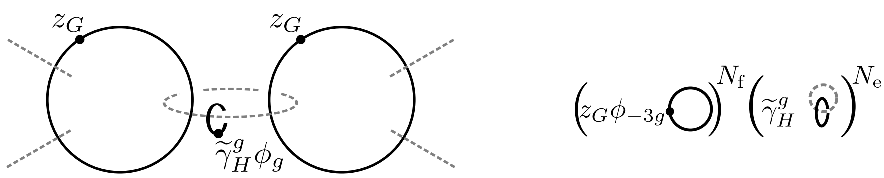

(a) (b)

FIGURE 85. Two-dimensional for $z_H = \tilde{\gamma}_H^h \phi_h$.

  the center is a homogeneous element multiplied by a constant, we use the lemma 3.17 in order to obtain the figure 85(b). Note that the weight of each curve associated with one "triangle", black curve, has a multiplicative factor ϕ_{-3h} due that this has three links. In $\mathbb{Z}_2$, the weight is $z_G\phi_{-3h} = z_G\phi_h$, therefore, the term associated to each black curve is

$$\operatorname{tr}(z_G\phi_h) = \sum_g \widetilde{\gamma}^g_G \operatorname{tr}(\phi_{g+h}) = 2\widetilde{\gamma}^g_G\delta(g+h,0) = 2\widetilde{\gamma}^g_G\delta(g,h).$$

On the other hand, the dependent factor of number of links is $2\widetilde{\gamma}^h_H$. Then, the partition function is

$$Z(\mathscr{M},\mathscr{T}) = (2\widetilde{\gamma}^g_G\delta(g,h))^{N_\mathrm{f}}(2\widetilde{\gamma}^h_H)^{N_\mathrm{e}}. \tag{39}$$

Calling $\gamma^{g,h}_{G,H} = 2\widetilde{\gamma}^{g,h}_{G,H}$ we find finally

$$Z(\mathscr{M},\mathscr{T}) = (\gamma^g_G)^{N_\mathrm{f}}(\gamma^h_H)^{N_\mathrm{e}}\delta(g,h).$$

I.e., the partition function is quasi-topological, see subsection 3.3 and expressions (18) and (19).

- $z_G = \widetilde{\gamma}^g_G\phi_g$ and $z_H = \frac{1}{2}(\phi_0+\phi_1)$: the model in figure 84 is a gauge pure model. This is represented by figure 81(c) for $\mathbb{Z}_n$ and by the figure 86(a) for $\mathbb{Z}_2$. Since the weights are homogeneous elements, we use the sliding move, lemma 3.16, having the figure 86(b). We note that the cointegral property can be used, lemma 3.11, to remove the black curve connected to the gray

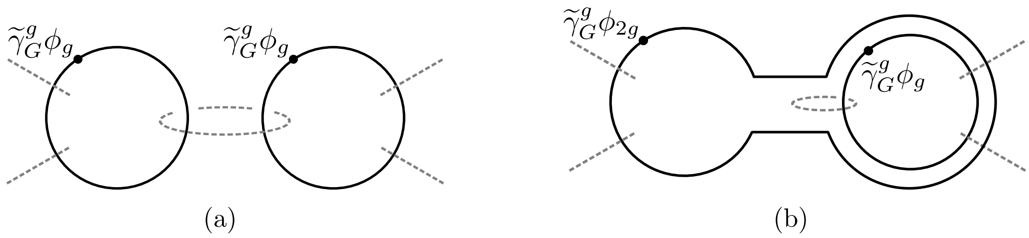

FIGURE 86. Gauge pure model with homogeneous elements like weights.

curve inside the greater closed curve. Now, the cointegral contributes with a factor of 2 and the constant $\widetilde{\gamma}^g_G$ is still present. So, each face contributes with a factor of $2\widetilde{\gamma}^g_G$. Since we have N_f faces, the partition function is

$$Z(\mathscr{M},\mathscr{T}) = (\gamma^g_G)^{N_\mathrm{f}}, \tag{40}$$

where $\gamma^g_G = 2\widetilde{\gamma}^g_G$. Once again, the partition function is quasi-topological.

- $z_G = \widetilde{\gamma}^g_G\phi_g$ and $z_H = \widetilde{\gamma}^0_H\phi_0 + \widetilde{\gamma}^1_H\phi_1$: we shall show the existence of a numeric value in terms of a numerical series, without find it explicitly. It was shown in [YTSM09] that if the Pachner move (2,2) is satisfied, the partition function has numeric value which corresponds to a numerical serie. Then, our porpuse is to show that it is satisfied the Pachner move (2,2). To achieve this we recall the Pachner move in figures 87(a) and 87(b). We note that in each case the link that is gluing both triangles has a vertical and horizontal position, respectively. The basic idea is to show the equivalence between both diagrams starting from the diagram 87(a) to diagram 87(b). Indeed, we apply sliding move of the curves with weight ϕ_g, similary to figure 86(b),

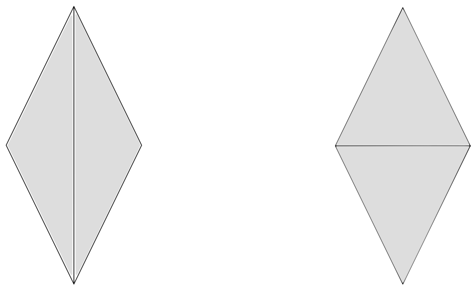

(a) (b)

FIGURE 87. Pachner move (2,2).

but with a general z_H. After this, we make sliding move of black curve with weight $z_H = \widetilde{\gamma}^0_H\phi_0 + \widetilde{\gamma}^1_H\phi_1$ over the right black curve and we note that we could remove this. We make similar moves when both triangles are glued by the horizontal link, and we would obtain that both final diagrams are equivalent.

Up to this point it was calculated the partition function for several elements of the center, which have the form $z = (\gamma^0, \gamma^1)$, where the γ^g are positive parameters. However, in general, it can be calculated the partition function for general elements which have the form $z = (\gamma^0, \gamma^1)$, where the γ^g are real parameters not necessarily positive, as was mentioned in subsection 3.4. This means that, as in the previous case we had elements of the center in the form $\gamma_{G,H}\phi_g$ for $\gamma_{G,H}$ positive; however, in the general case these coefficients can also be negative. In this way, we can also find partition functions when the coefficients have opposite sign, i.e., these could be calculated for an element of the center given by $\frac{1}{2}(1,-1)$. We shall show that, indeed, it can be found the partition function for elements of the center of the form $z_{G,H} = \frac{1}{2}(1,-1)$. In order to achieve this, we use the following lemma:

4.3. Lemma.
Let b *be a black curve with* n *crossings with gray curves,* $\{\mathsf{g}_i\}_{i\in 1,\ldots,n}$.

1. *The diagram of* b *with weight* $z = z_1 + z_2$ *is the sum of individual diagrams of* b *with weight* z_1 *and the same black curve* b *with weight* z_2.
2. *The diagram of* b *with weight* $z' = \alpha z$ *with* $\alpha \in \mathbb{C}$ *is equal to* b *with weight* z *multiplied by* α.

Proof. The proof is due to the linearity of the trace. We have for b with n crossings with gray curves g, $\mathrm{tr}(z\phi_{a_1}\cdots\phi_{a_n}) = \mathrm{tr}(z_1\phi_{a_1}\cdots\phi_{a_n}) + \mathrm{tr}(z_2\phi_{a_1}\cdots\phi_{a_n})$. For the second part, we know that $\mathrm{tr}(\alpha z\phi_{a_1}\cdots\phi_{a_n}) = \alpha\mathrm{tr}(z\phi_{a_1}\cdots\phi_{a_n})$. □

Considering the previously lemma, it can be shown the following result:

4.4. Lemma.
We consider $\mathbb{Z}_2$ *with* ϕ_0 *and* ϕ_1 *the basis of the group algebra. Let* C_1 *and* C_2 *be two black closed curves with weights* $\lambda' = \phi_0 - \phi_1$ *and* $z = \alpha^0\phi_0 + \alpha^1\phi_1$ $(\alpha^0, \alpha^1 \in \mathbb{C})$ *respectively, figure 88(a). The curve* C_1 *is replaced by the curve* C_1' *with weight* λ'. *The new curve* C_2' *is an isotopy of* C_2 *with weight* $z^- = \alpha^0\phi_0 - \alpha^1\phi_1$. *The curve* C_1' *(resp.* C_2'*) has the same orientation of* C_1 *(resp.* C_2*), figure 88(b).*

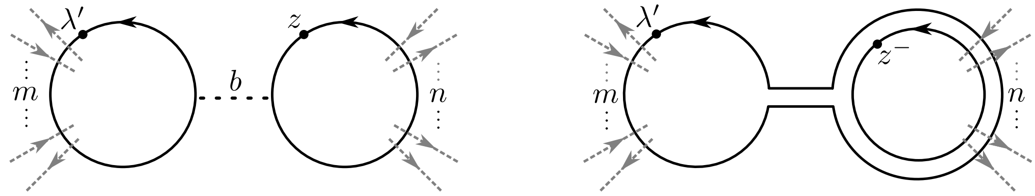

(a) *Two black curves connected by a ribbon.* (b) *Sliding.*

FIGURE 88. *88(a). The black curve C_1 (resp. C_2) has m (resp. n) crosses with gray curves (resp. black curves). After sliding the final curve C_1' (resp. C_2') has $m+n$ (resp. n) crossings with gray curves (resp. black curves).*

Proof. The point of the proof is to separate the right curve as the sum of two graphs. The first has weight $\alpha^0\phi_0$ and the second $\alpha^1\phi_1$. Then we apply sliding move under homogeneous elements, lemma 3.16, and we note that the second graph will have weight $\phi_1\lambda' = -\lambda'$. We apply linearity and we obtain the desired result. □

The lemma above will be very useful in the calculation of Wilson loops for $\mathbb{Z}_2$. However, for the moment we use it to calculate partition functions. We consider the first case in which $z_G = \frac{1}{2}(\phi_0 - \phi_1) = \frac{1}{2}\lambda'$, figure 89(a). Then we make use of lemma 4.4 to obtain the figure 89(b), where λ is the cointegral. Finally we use the cointegral property to remove curves with weight $\frac{1}{2}\lambda$, which contribute to a numeric value of $\frac{1}{2}\mathrm{tr}(\phi_0+\phi_1) = 1$. We note that we have a black curve with weight $z_H = \tilde{\gamma}_H^0\phi_0 + \tilde{\gamma}_H^1\phi_1$

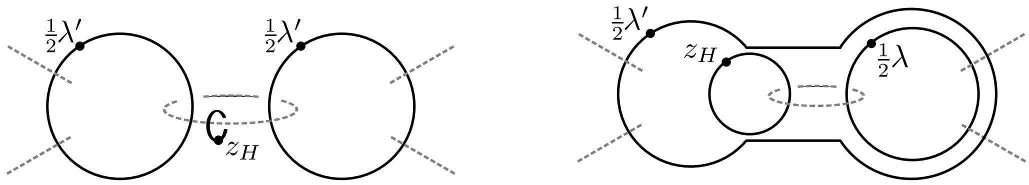

(a) (b)

FIGURE 89. Black curves relationed with the faces, these have weight $z_G = \lambda'$.

connected to a gray curve, which contributes with a numeric value $\epsilon(z_H) = \gamma_H^0 + \gamma_H^1$ multiplied by 2, see figure 83(b) (pure Higgs model). The important fact to note is that the sliding move eliminates a link, so we can apply the sliding moves in the whole lattice, and the end we will end up with a black curve with weight $\frac{1}{2}\lambda'$, and numerical factor $\frac{1}{2}\mathrm{tr}(\phi_0 - \phi_1) = 1$. So, we obtain that for $z_G = \frac{1}{2}(1,-1)$ and $z_H = (\tilde{\gamma}_H^0, \tilde{\gamma}_H^1)$ the partition function is

$$Z(\mathscr{M}, \mathscr{T}) = 2^{N_e}\left(\tilde{\gamma}_H^0 + \tilde{\gamma}_H^1\right)^{N_e}. \tag{41}$$

This result coincides with the Higgs pure model, $z_G = \frac{1}{2}(1,1)$, for $\mathbb{Z}_2$.

So far, we found explicitly the partition function for several limits, however we need to state their physics meaning. Indeed, we wrote the model in terms of the

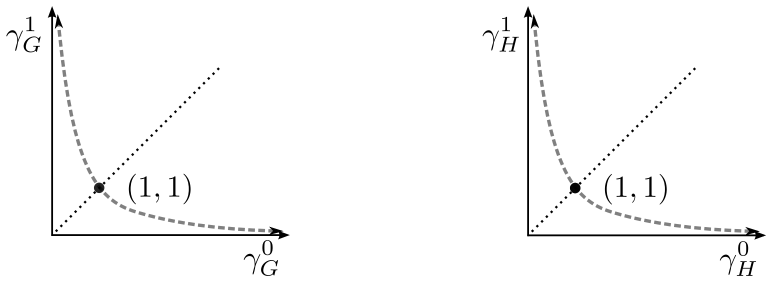

(a) Gauge parameters. (b) Higgs parameters.

FIGURE 90. Regions where the partition function was calculated for coupling constants $\beta_{G,H}$ reals and positive parameters γ. These are represented by the continuous and pointed lines.

coefficients $\gamma_{G,H}$, see remark 4.1 of subsection 4.1. For the particular case of $\mathbb{Z}_2$, we have that the coefficients describing the model are relationed by the equation of the hyperbola $\gamma^0_{G,H}\gamma^1_{G,H} = 1$, see figures 90(a) and 90(b). However, as it was mentioned, this is equivalent to write the center of the group as $z_{G,H} = (\gamma^0_{G,H}, \gamma^1_{G,H})$. In the gauge pure case, $z_H = (1,1)$, Wegner found its value, and several methods can be used to obtain it [Weg71, YT07, Aza13]. This result is

$$Z(\mathscr{M},\mathscr{T}) = 2^{N_{\mathrm{e}}}(\cosh(\beta_G)^{N_{\mathrm{f}}} + \sinh(\beta_G)^{N_{\mathrm{f}}}), \tag{42}$$

which can be thought as quasi-topological, due that it depends on details of triangulation, however, it does not satisfies the condition of expression 18. The pointed line in figure 90(a) represents the limit when $\beta_G \to 0^{\pm}$ and we note that for values above this line, we have the paramagnetic case ($\beta_G \to -\infty$). On the other hand, for values

z_G \ z_H	$\gamma_H(1,0)$	$\gamma_H(0,1)$	$\frac{1}{2}(1,1)$	(γ^0_H,γ^1_H)
$\gamma_G(1,0)$	$(\gamma^0_G)^{N_{\mathrm{f}}}(\gamma^0_H)^{N_{\mathrm{e}}}$	0	$(\gamma^0_G)^{N_{\mathrm{f}}}$	$\bigstar$
$\gamma_G(0,1)$	0	$(\gamma^1_G)^{N_{\mathrm{f}}}(\gamma^1_H)^{N_{\mathrm{e}}}$	$(\gamma^1_G)^{N_{\mathrm{f}}}$	$\bigstar$
$\frac{1}{2}(1,1)$	$(\gamma^0_H)^{N_{\mathrm{e}}}$	$(\gamma^1_H)^{N_{\mathrm{e}}}$	1	$(\gamma^0_H+\gamma^1_H)^{N_{\mathrm{e}}}$
(γ^0_G,γ^1_G)	$(\gamma^0_G)^{N_{\mathrm{f}}}(\gamma^0_H)^{N_{\mathrm{e}}}$	$(\gamma^1_G)^{N_{\mathrm{f}}}(\gamma^1_H)^{N_{\mathrm{e}}}$	Ξ	✠

TABLE 2. Partition functions for differents $\gamma_{G,H} \geqslant 0$.

below this line we have the ferromagnetic case ($\beta_G \to \infty$) [FPTS12, Aza13]. In the case for β_H, the meaning in figure 90(b) is similar. Topological limits are represented by the axis $\gamma^0_{G,H}$ (as an element of the center $z_{G,H} = \gamma_{G,H}(1,0)$) and $\gamma^1_{G,H}$ (as an element of the center $z_{G,H} = \gamma_{G,H}(0,1)$), and are $\beta_{G,H} \to \infty$ and $\beta_{G,H} \to -\infty$ respectively. We note that the parameters are positive and these are consistent with the literature [Kog79, Sei82, MMS79]. The table 2 shows the results for several values of the positive parameters $\gamma^{g,h}_{G,H}$. In the table 2, the symbol $\bigstar$ denots the existence of a possible numeric value in power series, which was not explicitly calculated. The

z_G \ z_H	$\gamma_H(1,0)$	$\gamma_H(0,1)$	$\frac{1}{2}(1,1)$	$\frac{1}{2}(1,-1)$	(γ_H^0, γ_H^1)
$\gamma_G(1,0)$	✓	✓	✓	✓	✶
$\gamma_G(0,1)$	✓	✓	✓	✓	✶
$\frac{1}{2}(1,1)$	✓	✓	✓	✓	✓
$\frac{1}{2}(1,-1)$	✓	✓	✓	✓	✓
(γ_G^0, γ_G^1)	✓	✓	✓	✠	✠

TABLE 3. Partition function for differents $\gamma_{G,H}$.

symbol Ξ represents the expression of the partition function calculated by Wegner, (42). On the other hand, the symbol ✠ makes reference to the points where it was not possible to find a numeric value; this corresponds to the general case of the gauge-Higgs model. We note that other topological limits could be calculated and we made this explicitly; now, the parameters $\gamma_{G,H}^{g,h}$ are reals, positive and negative. The table 3 contains different cases of parameters $\gamma_{G,H}^{g,h}$, and the symbol ✓ is used

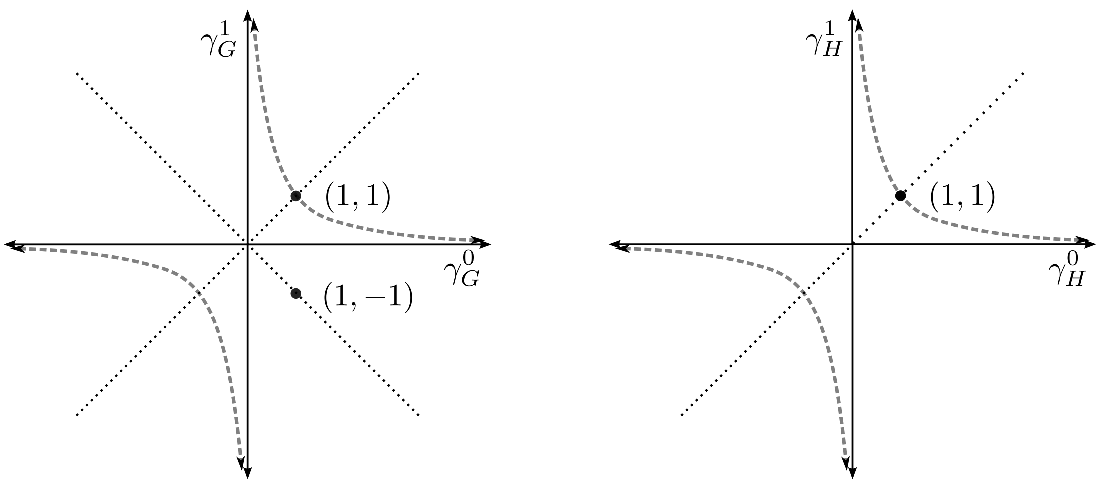

(a) Gauge parameters. (b) Higgs parameters.

FIGURE 91. Regions where the partition function is calculable. These are represented by solid and dotted lines.

to denote those cases where the numeric values of the partition function were calculated. The symbol ✶ denots the existence of a possible numeric value in power series, and we use the symbol ✠ to denote those cases where it was not possible to obtain any numeric value. The graphs are represented in 91(a) and 91(b).

Wilson loops for $\mathbb{Z}_2$. Following the expression (36), in the case of $\mathbb{Z}_2$, the weight associate to the loop ℓ will be [FPTS12]

$$z_{\mathrm{W}} = \frac{1}{2}(\phi_0 - \phi_1). \tag{43}$$

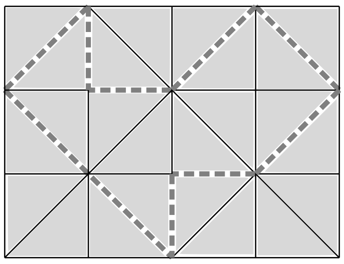

FIGURE 92. Loop in a regular triangular lattice.

As it was stated, in terms of colored curves with weights, the figure 92 is represented by the figure 93, and as previously mentioned, each curve has a weight associated to it. Only black curves belonging to links are represented by dotted black points and weights z_H. We may note that the new curves with weight z_{W}, seems to intersect these points but we know that two curves of the same color can not cross, which

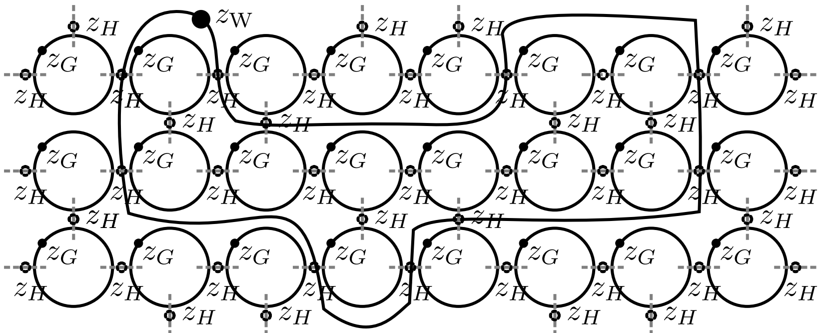

FIGURE 93. Representation in the language of colored curves of a two-dimensional manifold with loop ℓ. Each curve has an associated weight. All black curves have weights related to the center of algebra. Faces: z_G. The dotted black points related to links: z_H. The Wilson loop: z_{W}.

would be contradictory. In fact, these geometrical objects do not intersect, and the diagram is showed in that way for simplicity. A part of the diagram 93 corresponds to figure 94. Knowing the form of z_{W}, we make several choices for the weights $z_{G,H}$,

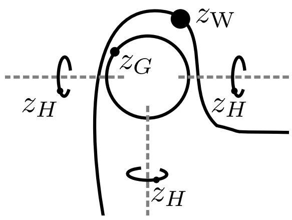

FIGURE 94. Lattice with Wilson loop.

as we did in the case of partition functions. Let us first vary the element of the center z_H, related to the matter field. First, the topological limits $z_H = \widetilde{\gamma}_H^h \phi_h$, with $\widetilde{\gamma}_H^0$ and $\widetilde{\gamma}_H^1$ limits for $\beta_H = \pm\infty$, respectively. Second in $\beta_H = 0$, that is, $z_H = \frac{1}{2}(\phi_0 + \phi_1)$:

- $z_H = \tilde{\gamma}^h_H \phi_h$: the diagram is shown in figure 95(a). Since the center is a

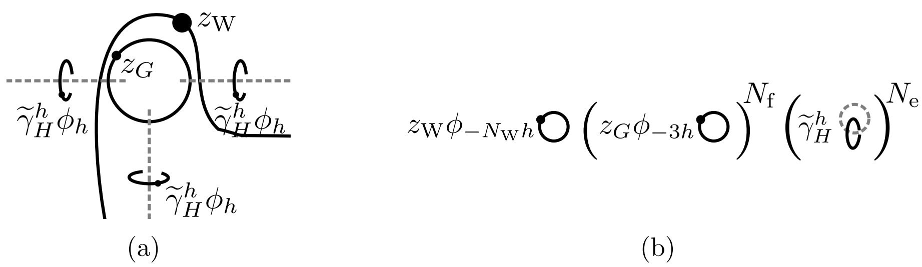

Figure 95. Diagram corresponding to the calculating of Wilson loops for $z_H = \tilde{\gamma}^h_H \phi_h$.

homogeneous element multiplied by a constant, we use the lemma 3.17 to obtain the figure 95(b). Note that the weight of each curve associated to one triangle, has a factor ϕ_{-3h} due that it has three links glued to it. For the Wilson loop, the factor which multiplies the weight is $\phi_{-N_W h}$, where N_W is the number of links where the loop is crossing. Since we are using the group $\mathbb{Z}_2$, the weights are $z_G\phi_{-3h} = z_G\phi_h$ and $z_W\phi_{-N_W h} = z_W\phi_{N_W h}$, respectively. Thus, the term associated to each face is

$$\operatorname{tr}(z_G\phi_h) = \sum_g \tilde{\gamma}^g_G \operatorname{tr}(\phi_{g+h}) = 2\tilde{\gamma}^g_G \delta(g+h,0) = 2\tilde{\gamma}^g_G\delta(g,h)$$

and the loop

$$\operatorname{tr}(z_W\phi_{N_W h}) = \frac{1}{2}(\operatorname{tr}(\phi_0\phi_{N_W h}) - \operatorname{tr}(\phi_1\phi_{N_W h})) = \delta(0, N_W h) - \delta(1, N_W h).$$

Note that for $h = 0$, the numeric value is 1. For $h = 1$, the numeric value depends on whether N_W is even or odd. For N_W even, we have again 1. For N_W odd, we have -1. This is summarized as follows:

$$\operatorname{tr}(z_W\phi_{N_W h}) = \begin{cases} 1, & \text{if } h = 0, \text{ for all } N_W \\ (-1)^{N_W}, & \text{if } h = 1, \text{ for all } N_W, \end{cases}$$

where the factor depending on the number of links is $2\tilde{\gamma}^h_H$. Calling $\gamma^{g,h}_{G,H} = 2\tilde{\gamma}^{g,h}_{G,H}$ we have that the numerator in (35) is

$$\begin{cases} (\gamma^g_G)^{N_f}(\gamma^h_H)^{N_e}\delta(g,h), & \text{if } h = 0, \text{ for all } N_W \\ (-1)^{N_W}(\gamma^g_G)^{N_f}(\gamma^h_H)^{N_e}\delta(g,h), & \text{if } h = 1, \text{ for all } N_W. \end{cases}$$

With (39) we obtain that the Wilson loops are given by

$$\langle W(\ell)\rangle = \begin{cases} (-1)^{gN_W}, & \text{if } g = h, \text{ for all } N_W \\ \text{undefined}, & \text{in other cases.} \end{cases}$$

- $z_H = \frac{1}{2}(\phi_0 + \phi_1)$: the diagram is shown in 96(a), this weight is the cointegral element divided 2. We can extract each curve with this weight, by using the cointegral property, lemma 3.11. The numerical factor which contributes

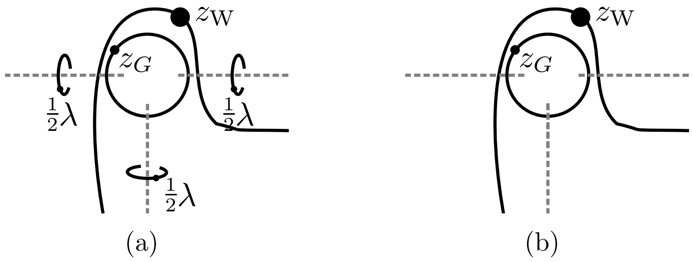

FIGURE 96. Diagram corresponding to the calculation of Wilson loops for $z_H = \frac{1}{2}\lambda$.

to the weight of the links is 2 divided into 2, i.e., we have to calculate the Wilson loops in the case of a pure gauge model, figure 96(b). However, in [GP96], Gambini and Pullin showed that, for high temperatures, $\beta_G \ll 1$, the behavior has the form

$$\langle W(\ell)\rangle = \mathrm{e}^{-f(\beta_G)\mathrm{area}(\ell)} \tag{44}$$

where $f(\beta_G) = -\ln(\tanh(\beta_G))$ and $\mathrm{area}(\ell)$ is the number of elementary plaquetes inside of the loop ℓ. For low temperatures, $\beta_G \gg 1$, the dependence of $\langle W(\ell)\rangle$ is in relation to the perimeter of the loop [OHZ06], and the methods of this paper lead us to the same result. We take $\beta = 0$ and $\beta = \infty$, for the limit of high and low temperatures respectively:

$\beta_G = 0$ If $z_G = \frac{1}{2}(\phi_0 + \phi_1)$, by the cointegral property we can extract all black curves relationed with the faces of triangulation. Now, the loop will cross N_W links. So, the loop will have N_W gray curves crossing it. The curves for the loop do not cross, and these taken from the diagram and

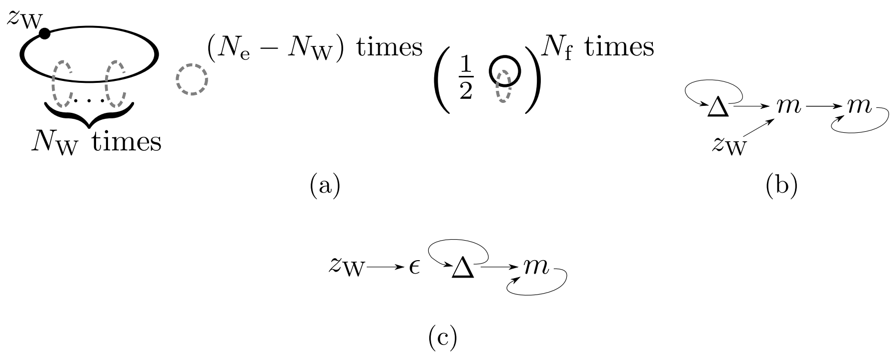

FIGURE 97. Diagram corresponding to the calculation of Wilson loops for $z_G = z_H = \frac{1}{2}\lambda$.

have numerical factor 2, as it is shown in figure 97(a). Using again the cointegral property we extract one by one the gray curves until one of them is missing. Finally we have a black curve with weight $z_W = \frac{1}{2}(\phi_0 - \phi_1) = \frac{1}{2}\lambda'$ crossed by one gray curve, and this tensor is represented in figure 97(b). We use again the cointegral property and we obtain the tensor of figure 97(c), where $z_{\mathrm{W}} \to \epsilon$ contributes as: $\epsilon(z_{\mathrm{W}}) = \frac{1}{2}(\epsilon(\phi_0) - \epsilon(\phi_1)) = 0$, therefore the Wilson loop is simply 0. Note that $\beta_G = 0$ in expression (44) is also zero.

$\beta_G = \pm\infty$ If $z_G = \widetilde{\gamma}^g_G \phi_g$, we make the move sliding, lemma 4.4, over each face. We know that the weight of each face will change as well, originally $z_G = \widetilde{\gamma}^g_G \phi_g$, figure 98(a), after sliding is $z^-_G = (-1)^g \widetilde{\gamma}^g_G \phi_g$, figure 98(b); we can do this under each face. At the end, we have that the faces

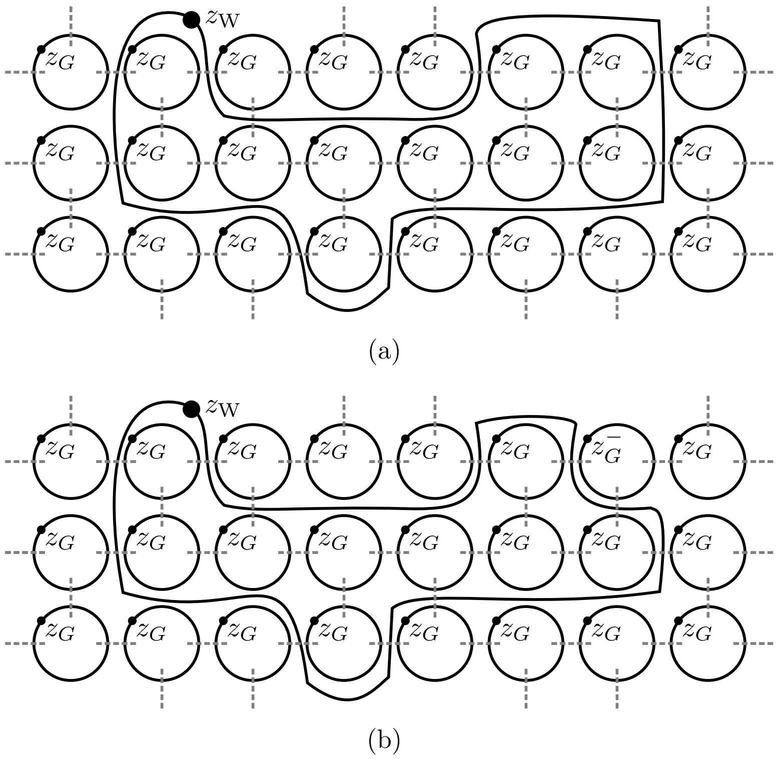

Figure 98. Diagram corresponding to the calculation of Wilson loops for $z_G = \widetilde{\gamma}^g_G \phi_g$ and $z_H = \frac{1}{2}\lambda$.

inside the loop will change their weight if $\beta = -\infty$, or $g = 1$. The fact is that we can factor the signal $N_{\mathrm{f.W}}$ times, where $N_{\mathrm{f.W}}$ is the number of faces within the Wilson loop. Wilson loops have the same value of the partition function (40), except for the factor $(-1)^{N_{\mathrm{f.W}}}$. Found so the Wilson loop has a value

$$\langle W(\ell)\rangle = (-1)^{gN_{\mathrm{f.W}}}.$$

This expression would appear to have the form of the area's law to high temperature limits, $\beta_G = 0$. However, we note from figures 98(a) and 98(b) that for every face that adds (removes) inside the loop, the loop will cross a link more (less). So it actually can be written Wilson loops as

$$\langle W(\ell)\rangle = (-1)^{gN_{\mathrm{W}}},$$

which has the form of perimeter's law [FPTS12].

Now, for z_H fixed, we vary the element of the center z_G, associated with the gauge fields. Within the topological limits $z_G = \widetilde{\gamma}^g_G\phi_g$, with $\widetilde{\gamma}^0_G$ and $\widetilde{\gamma}^1_G$ limits as $\beta_G = \pm\infty$, respectively. After, for $\beta_G = 0$, i.e. for $z_G = \frac{1}{2}(\phi_0 + \phi_1)$. Finally for $z_G = \frac{1}{2}(\phi_0 - \phi_1)$:

- $z_G = \widetilde{\gamma}^g_G\phi_g$: The diagram is shown in figure 99(a). Even without finding

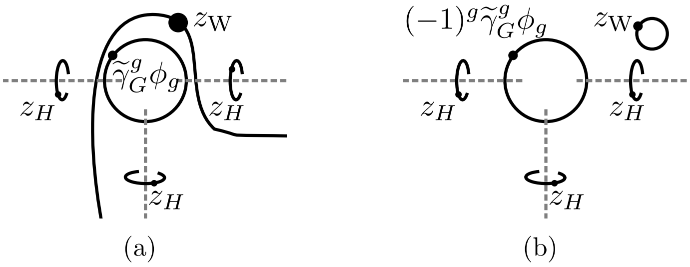

FIGURE 99. Diagram corresponding to the calculation of Wilson loops for $z_G = \widetilde{\gamma}^g_G\phi_g$.

  explicitly the partition function in this situation, the argument is the same as for the limits $\beta_G = \pm\infty$ from the previous part, in which the center a homogeneous element do sliding move, lemma 4.4, under each face. We know that the weight of each face will change as well: originally $z_G = \widetilde{\gamma}^g_G\phi_g$, figure 99(a), after sliding move is $z_G^- = (-1)^g\widetilde{\gamma}^g_G\phi_g$, figure 99(b). But we note that the isolated black curve has numeric value 1 and we factor signals. The Wilson loops have the same numerical value of the partition function, if it is not zero, except for the factor $(-1)^{gN_W}$, then

$$\langle W(\ell)\rangle = \frac{(-1)^{gN_W}}{Z(\mathscr{M},\mathscr{T})} Z(\mathscr{M},\mathscr{T}) = (-1)^{gN_W}.$$

- $z_G = \frac{1}{2}(\phi_0 + \phi_1)$: the diagram is represented in figure 100(a). By the cointegral property black curves relationed to the faces can be extracted from the diagram. The links which do not intersect the loop leave the leave the dia-

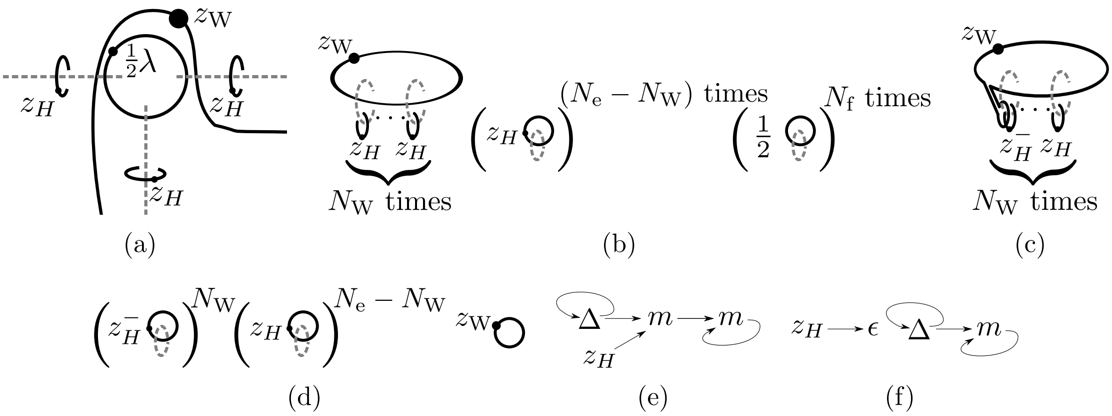

FIGURE 100. Diagram corresponding to the calculation of Wilson loops for $z_G = \frac{1}{2}\lambda$.

gram, the others remain therein as shown in figure 100(b). We make sliding move of the loop with weight $z_{\mathrm{W}} = \frac{1}{2}(\phi_0 - \phi_1)$, over each black curve with weight $z_H = \widetilde{\gamma}^0_H\phi_0 + \widetilde{\gamma}^1_H\phi_1$, figure 100(c) (The links which do not intersect the loop leave the diagram, the others remain therein as shown in figure 100(b)). After sliding move the weights will change to $z^-_H = \widetilde{\gamma}^0_H\phi_0 - \widetilde{\gamma}^1_H\phi_1$. Making two point move by applying the move sliding the following $N_{\mathrm{W}} - 1$ black curves, we have the figure 100(d). Now, the numeric value of one black curve with weight, glued with a gray curve, is calculated using the tensor represented in 100(e) and 100(f). For the curves with weight z_H the numeric value is two times $\epsilon(z_H) = \widetilde{\gamma}^0_H + \widetilde{\gamma}^1_H$ and for the curves with weight z^-_H is two times $\epsilon(z^-_H) = \widetilde{\gamma}^0_H - \widetilde{\gamma}^1_H$. Then, the Wilson loop using (41) is

$$\langle W(\ell)\rangle = \frac{2^{N_{\mathrm{W}}}\left(\widetilde{\gamma}^0_H - \widetilde{\gamma}^1_H\right)^{N_{\mathrm{W}}} 2^{N_{\mathrm{e}}-N_{\mathrm{W}}}\left(\widetilde{\gamma}^0_H + \widetilde{\gamma}^1_H\right)^{N_{\mathrm{e}}-N_{\mathrm{W}}}}{2^{N_{\mathrm{e}}}\left(\widetilde{\gamma}^0_H + \widetilde{\gamma}^1_H\right)^{N_{\mathrm{e}}}} = \frac{\left(\widetilde{\gamma}^0_H - \widetilde{\gamma}^1_H\right)^{N_{\mathrm{W}}}}{\left(\widetilde{\gamma}^0_H + \widetilde{\gamma}^1_H\right)^{N_{\mathrm{W}}}},$$

for $\widetilde{\gamma}^0_H \neq -\widetilde{\gamma}^1_H$.

- $z_G = \frac{1}{2}(\phi_0 - \phi_1)$: The diagram is shown in figure 101(a) and we use the sliding move to the loop on each face. The weight of each face is $z_G = \frac{1}{2}\lambda'$, and it is the weight of the loop as well. By lemma 4.4, we know that the weights on each side will change to $z^-_G = \frac{1}{2}\lambda$. At the end of the process we have figure 101(b). By cointegral property the black curves related to faces can be extracted from the diagram. After disconnecting the $N_{\mathrm{f.W}}$ faces inside

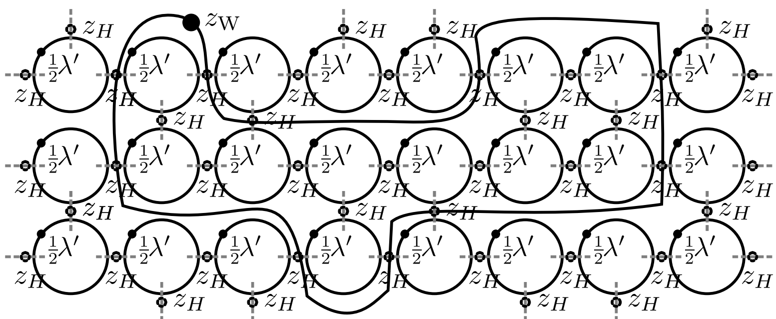

(a)

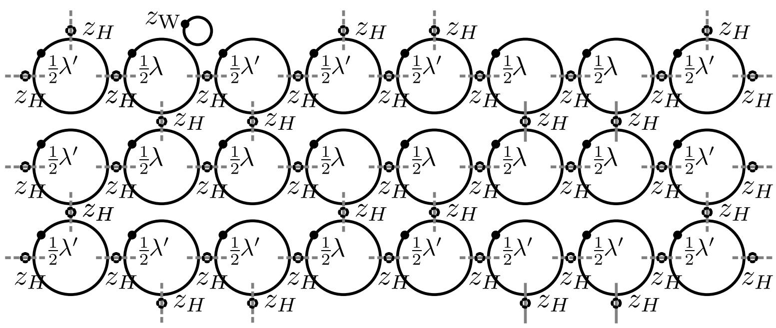

(b)

FIGURE 101. Diagram corresponding to the calculation of Wilson loops for $z_G = \frac{1}{2}\lambda'$.

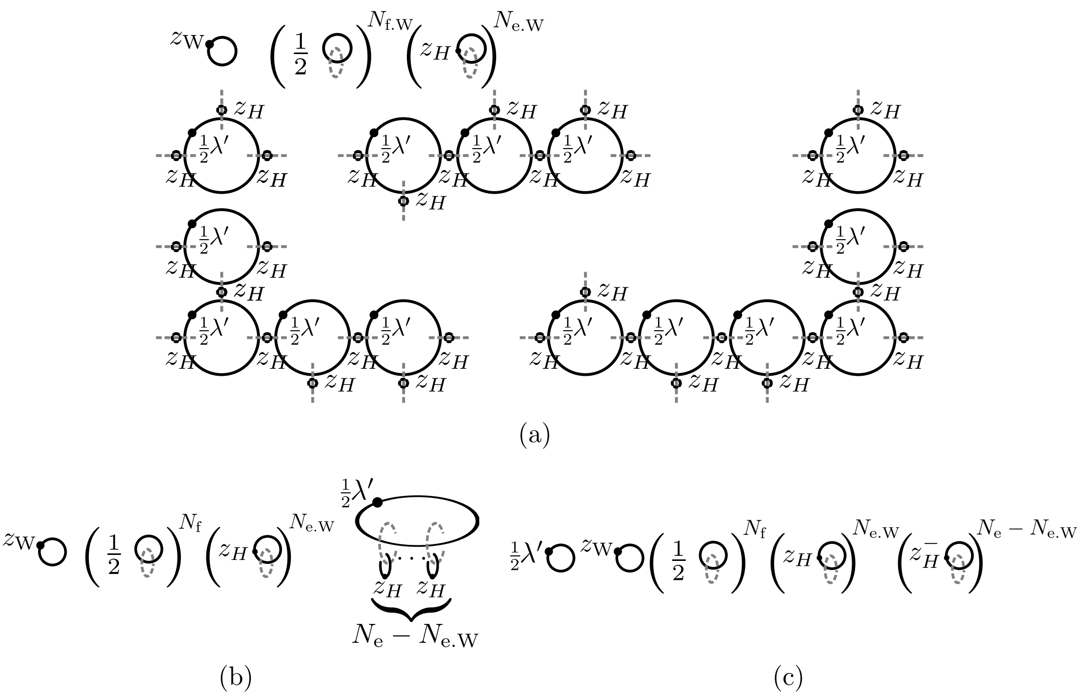

FIGURE 102. Diagram corresponding to the calculation of Wilson loops for $z_G = \frac{1}{2}\lambda'$.

the loop, we note that the $N_{\mathrm{f.W}}$ links within the loop connecting the faces are isolated, as it is shown in figure 102(a). Now, we could choose one face f and do sliding move under each face glued to it via a link. Certainly, the black curve with weight $z_G = \frac{1}{2}\lambda'$, will change to be $z_G^- = \frac{1}{2}\lambda$. Then, we can extract that curve, and we make sliding move until extracting all black curves. However, note that each time we apply the sliding move the face f will have more and more links crossing it. At the end we have figure 102(b), where $N_{\mathrm{e}} - N_{\mathrm{e.W}}$. Finally, we make again sliding move as in figure 100(c) until arriving at figure 102(c). Recalling from left to right the weights of each of the curves in figure 102(c): $\frac{1}{2}2 = 1$, for the first three; $2(\widetilde{\gamma}_H^0 + \widetilde{\gamma}_H^1)$ and $2(\widetilde{\gamma}_H^0 - \widetilde{\gamma}_H^1)$ for the last two set of curves. The value of Wilson loops using (41) is

$$\begin{aligned}\langle W(\ell)\rangle &= \frac{2^{N_{\mathrm{e.W}}}\left(\widetilde{\gamma}_H^0 + \widetilde{\gamma}_H^1\right)^{N_{\mathrm{e.W}}} 2^{N_{\mathrm{e}}-N_{\mathrm{e.W}}}\left(\widetilde{\gamma}_H^0 - \widetilde{\gamma}_H^1\right)^{N_{\mathrm{e}}-N_{\mathrm{e.W}}}}{2^{N_{\mathrm{e}}}\left(\widetilde{\gamma}_H^0 + \widetilde{\gamma}_H^1\right)^{N_{\mathrm{e}}}} \\ &= \frac{\left(\widetilde{\gamma}_H^0 - \widetilde{\gamma}_H^1\right)^{N_{\mathrm{e}}-N_{\mathrm{e.W}}}}{\left(\widetilde{\gamma}_H^0 + \widetilde{\gamma}_H^1\right)^{N_{\mathrm{e}}-N_{\mathrm{e.W}}}},\end{aligned}$$

since $N_{\mathrm{W}} = N_{\mathrm{e}} - N_{\mathrm{e.W}}$, the result is $\langle W(\ell)\rangle = \frac{\left(\widetilde{\gamma}_H^0 - \widetilde{\gamma}_H^1\right)^{N_{\mathrm{W}}}}{\left(\widetilde{\gamma}_H^0 + \widetilde{\gamma}_H^1\right)^{N_{\mathrm{W}}}}$ and it is satisfied for $\widetilde{\gamma}_H^0 \neq -\widetilde{\gamma}_H^1$. As expected, the result is quasi-topological and depends on the usual form of the Wilson loops.

Previously, we analyze the meaning of partition functions using this to also study the values found for Wilson loops. However, this becomes more difficult in this latter

$z_G \backslash z_H$	$\gamma_H(1,0)$	$\gamma_H(0,1)$	$\frac{1}{2}(1,1)$	$\frac{1}{2}(1,-1)$	(γ_H^0, γ_H^1)
$\gamma_G(1,0)$	1	undefined	1	1	1
$\gamma_G(0,1)$	undefined	$(-1)^{N_W}$	$(-1)^{N_W}$	$(-1)^{N_W}$	$(-1)^{N_W}$
$\frac{1}{2}(1,1)$	1	$(-1)^{N_W}$	0	undefined	$\frac{(\gamma_H^0-\gamma_H^1)^{N_W}}{(\gamma_H^0+\gamma_H^1)^{N_W}}$
$\frac{1}{2}(1,-1)$	1	$(-1)^{N_W}$	0	undefined	$\frac{(\gamma_H^0-\gamma_H^1)^{N_W}}{(\gamma_H^0+\gamma_H^1)^{N_W}}$
(γ_G^0, γ_G^1)	1	$(-1)^{N_W}$	✠	✠	✠

TABLE 4. Numeric values of Wilson loops for differents $\gamma_{G,H}$.

case, because there are three possible values of the center of the center of algebra. Certainly, the values of the γ, for Wilson loops which could have some physical meaning, correspond to real positive numbers. In most of cases it was confirmed the perimeter's law. However, there is a "physical" case where the expected value of Wilson loop is zero. It ocurred when the coupling constant β_G was zero in a pure gauge model, $\beta_H = 0$, which coincides with Wilson in relation with the confinament of quarks [Wil74]. Other values of Wilson loops were considered undefined since we obtain divergences when performing their explicit calculation. In the case where the parameters γ could have any real value, there were found numeric values which can be found in table 4. Inside of it, the symbol ✠ is used to denote those points for which it was not possible to obtain any value for Wilson loops. Figures representing the numeric values of Wilson loops in topological limits, are shown in figures 103(a) and 103(b).

The description based in curves here discussed is important due that it may be used to characterize models satisfying topological properties. In [BPT13], the weight on curves describes anyonic excitations in the lattice, such as the Kitaev's toric code [Kit03], in this work the transfer matrix is represented in terms of curves, and there are also being studied generalizations for other models. Matter fields are introduced in the vertex of the lattice without using a representation different from regular representation, in order to describe the dynamics of $(1+1)$ and $(2+1)$ models, with matter fields. Finally, we observe that the methods using curves as well as thoser showed here, can be useful to study phases of matter, thus as in other parallel works, for example [LW06, BMD08, DK13], which use also graphs to understand the behavior and properties of dynamical of models.

5. OUTLOOK

We presented in this paper a review of the basic concepts of LGT in two and three dimensions for finite groups. In order to do this, we recall the basic definitions

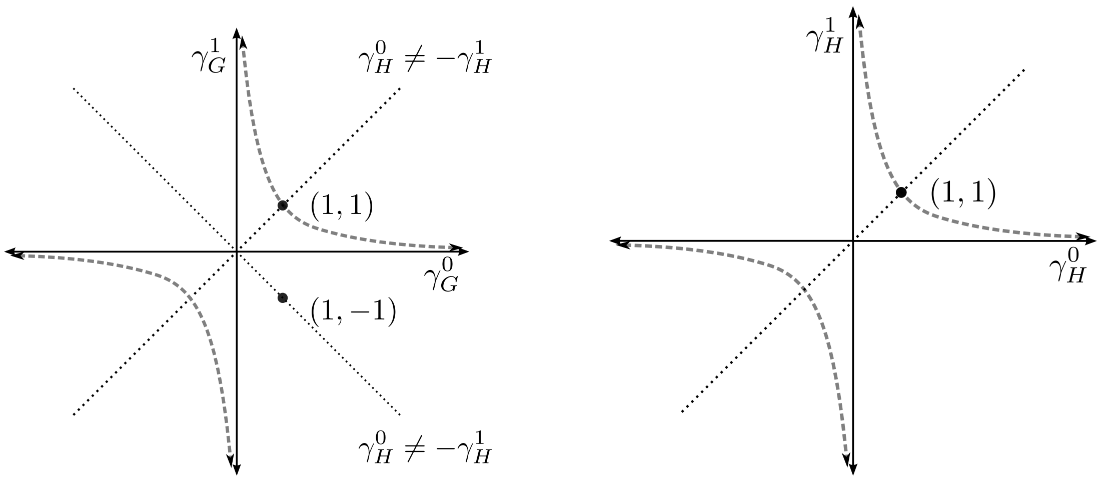

(a) Gauge parameters. (b) Higgs parameters.

FIGURE 103. Regions where the expected value, Wilson loops, were calculated. The real parameters γ are represented by continuous lines and pointed lines.

of gauge transformations for gauge and Higgs fields in a lattice, and we define a gauge-Higgs action model for the $\mathbb{Z}_n$ case, which can be generalized for any finite group when the unitary gauge is chosen. The latter recalls the colored-Heegaard diagrams, for a two-dimensional and three-dimensional discretized manifold, respectively, where the curves must satisfy five different moves in order to be deformed, and also to obtain equivalent colored-Heegaard diagrams.

On the other hand, we remember LTFT for two and three dimensions, and we show topological invariance in a two-dimensional theory, where we state the Pachner moves, (1,3) and (2,2), using colored curves, where there are gauge and Higgs fields associated with black and gray curves respectively. We define the partition function and the Wilson loops for a topological and quasi-topological theory for a special kind of tensors M, Δ and S, which are intimately related with Hopf algebras, and use the fact that the physical information is related with the center and cocenter of the Hopf algebra used. The procedure is similar for the three-dimensional case, and can be generalized for higher dimensions, taking the corresponding Pachner moves in each dimension.

We also show that the information of a gauge pure model can be described using the elements of center z of the gauge group considered. For this purpose, it was used the group algebra, and we show that all the information of the gauge-Higgs model can be described only by z. This is performed to specify that the partition function and Wilson loops with matter fields, it is equivalent to add one more face to the triangulation, however this latter will have a different weight. This lead us to provide a general Wilson loop's weight for a finite group. Finally, we calculate the partition function and Wilson loops in topological limits for the special case of $\mathbb{Z}_2$, in a two-dimensional lattice, where we conclude the following results: the trivial dependence on the triangulation for the partition function, the dependence on the area's or perimeter's laws for Wilson loops, and a topological dependence on real parameters γ_H^0 and γ_H^1 for the Higgs pure case.

In the end, we hope that methods used here, about describing topological invariance using curves, may be useful in order to find topological limits without solving a specific model for any compact group. Furthermore, the approach in this work may be useful to understand topological theories, as well study dynamical of observables in condensed matter, using a different representation of the regular representation to describe matter fields, and classify the topological phases of models.

Acknowledgement

N.J.B. Aza thanks to Miguel Bernabé-Ferreira for fruitfull discussions, and Paulo Teotônio-Sobrinho for his assistance with the perspective of the work. He also thanks to CAPES for supporting this work. The authors thank to Michele Fontanini for his iluminating ideas, and also to USP, Brazil and U of Manitoba, Canada.

References

[Ale01] Virelizier Alexis, *Algèbres de Hopf graduées et fibrés plats sur les 3-variétés*, Ph.D. thesis, Institut de Recherche Mathématique Avancée, 2001. (Cited in pages 12, 13, 15, 20, 25 and 28.)

[Aza13] N.J.B. Aza, *Topological Limits in the Gauge-Higgs Model with $\mathbb{Z}_2$ Symmetry in a Two-dimensional Lattice*, Master's thesis, Universidade de São Paulo, November 2013. (Cited in pages 3, 11, 12 and 62.)

[BDHK13] Benjamin Bahr, Bianca Dittrich, Frank Hellmann, and Wojciech Kaminski, *Holonomy spin foam models: Definition and coarse graining*, Phys. Rev. D **87** (2013), 044048. (Cited in page 5.)

[BDR11] Benjamin Bahr, Bianca Dittrich, and James P. Ryan, *Spin foam models with finite groups*. (Cited in pages 2, 5 and 8.)

[Ber12] M.J. Bernabe-Ferreira, *Discrete Field Theories and Topological Models*, Master's thesis, Universidade de São Paulo, 2012. (Cited in pages 3, 12, 13, 19, 34 and 37.)

[Bha81] Gyan Bhanot, *High-temperature expansion along the self-dual line of three-dimensional $Z(2)$ spin-gauge theory*, Phys. Rev. D **23** (1981), 1811–1814. (Cited in page 7.)

[BJM10] A.P. Balachandran, G. Jo, and G. Marmo, *Group Theory and Hopf Algebra: Lectures for Physicists*, World Scientific, 2010. (Cited in page 20.)

[BMD08] H. Bombin and M. A. Martin-Delgado, *Family of non-Abelian Kitaev models on a lattice: Topological condensation and confinement*, Phys. Rev. B **78** (2008), 115421. (Cited in page 71.)

[Bou97] D. V. Boulatov, *Quantum Deformation of Lattice Gauge Theory*, Communications in Mathematical Physics **186** (1997), 295–322. (Cited in pages 3 and 11.)

[BPT13] M. J. Bernabé Ferreira, P. Padmanabhan, and P. Teotonio-Sobrinho, *2D Quantum Double Models From a 3D Perspective*, ArXiv e-prints (2013). (Cited in pages 3, 11, 12, 14, 20, 27, 37, 41 and 71.)

[CFS94] Stephen-wei Chung, Masafumi Fukuma, and Alfred Shapere, *Structure of Topological Lattice Field Theory in Three Dimensions*, International Journal of Modern Physics A **09** (1994), no. 08, 1305–1360. (Cited in pages 2, 4, 16, 19, 20 and 27.)

[CKS98] J. Scott Carter, Louis H. Kauffman, and Masahico Saito, *Structures and Diagrammatics of Four Dimensional Topological Lattice Field Theories*, Advances in Math. 146, 1998, pp. 980602–3. (Cited in pages 2, 18, 19 and 20.)

[CO83] Michael Creutz and Masanori Okawa, *Generalized Actions in $\mathbb{Z}_p$ Lattice Gauge Theory*, Nuclear Physics B **220** (1983), no. 2, 149–166. (Cited in page 7.)

[Cre80] Michael Creutz, *Phase Diagrams for Coupled Spin-Gauge Systems*, Phys. Rev. D **21** (1980), 1006–1012. (Cited in pages 9 and 11.)

[DH12] Bianca Dittrich and Philipp A Höhn, *Canonical simplicial gravity*, Classical and Quantum Gravity **29** (2012), no. 11, 115009. (Cited in pages 2 and 19.)

[DK13] Bianca Dittrich and Wojciech Kaminski, *Topological lattice field theories from intertwiner dynamics*. (Cited in page 71.)

[DW90] Robbert Dijkgraaf and Edward Witten, *Topological gauge theories and group cohomology*, Communications in Mathematical Physics **129** (1990), no. 2, 393–429 (English). (Cited in page 2.)

[Fer14] Alysson Ferreira Morais, *A Tensorial Approach to Study of Dualities between Spin Models in the Lattice*, Master's thesis, Universidade de São Paulo, 2014. (Cited in page 45.)

[FHK94] M. Fukuma, S. Hosono, and H. Kawai, *Lattice topological field theory in two dimensions*, Communications in Mathematical Physics **161** (1994), 157–175. (Cited in pages 2, 4, 16, 19, 20 and 26.)

[FM83] Klaus Fredenhagen and Mihail Marcu, *Charged States in $\mathbb{Z}_2$ Gauge Theories*, Communications in Mathematical Physics **92** (1983), no. 1, 81–119 (English). (Cited in page 3.)

[FPTS12] Miguel J. B. Ferreira, Victor A. Pereira, and Paulo Teotonio-Sobrinho, *Quasi-Topological Quantum Field Theories and $\mathbb{Z}_2$ Lattice Gauge Theories*, International Journal of Modern Physics A **27** (2012), no. 23, 1250132. (Cited in pages 3, 11, 37, 52, 62, 63 and 67.)

[GP96] R. Gambini and J. Pullin, *Loops, Knots, Gauge Theories and Quantum Gravity*, Cambridge Monographs on Mathematical Physics Series, Cambridge University Press, 1996. (Cited in pages 3, 6, 10 and 66.)

[GS96] Martí Ruiz-Altaba Gómez César and Germán Sierra., *Quantum Groups in Two-Dimensional Physics*, Cambridge University Press, 1996. (Cited in page 20.)

[GSW87a] M.B. Green, J.H. Schwarz, and E. Witten, *Superstring Theory: Volume 1, Introduction*, Cambridge Monographs on Mathematical Physics, Cambridge University Press, 1987. (Cited in page 2.)

[GSW87b] ———, *Superstring Theory: Volume 2, Loop Amplitudes, Anomalies and Phenomenology*, Cambridge Monographs on Mathematical Physics, Cambridge University Press, 1987. (Cited in page 2.)

[Ham89] M. Hamermesh, *Group Theory and Its Application to Physical Problems*, Dover Books on Physics Series, Dover Publications, 1989. (Cited in page 45.)

[ID91] C. Itzykson and J.M. Drouffe, *Statistical Field Theory: Volume 1, From Brownian Motion to Renormalization and Lattice Gauge Theory*, Cambridge Monographs on Mathematical Physics, Cambridge University Press, 1991. (Cited in pages 7 and 9.)

[Iwa95] Junichi Iwasaki, *A definition of the Ponzano-Regge quantum gravity model in terms of surfaces*, J. Math. Phys **36** (1995), 6–10. (Cited in page 2.)

[JL01] G. James and M. Liebeck, *Representations and Characters of Groups*, Cambridge mathematical textbooks, Cambridge University Press, 2001. (Cited in pages 7, 10, 40, 45, 46 and 47.)

[Joh] Jesse Johnson, *Notes on Heegaard Splittings*. (Cited in pages 2, 12, 13 and 29.)

[Jon87] V.F.R. Jones, *Hecke algebra representations of braid groups and link polynomials*, Annals Math. **126** (1987), 335–388. (Cited in page 2.)

[Kit03] A.Yu. Kitaev, *Fault-tolerant quantum computation by anyons*, Annals of Physics **303** (2003), no. 1, 2–30. (Cited in page 71.)

[Kog79] John B. Kogut, *An Introduction to Lattice Gauge Theory and Spin Systems*, Rev. Mod. Phys. **51** (1979), 659–713. (Cited in pages 3, 11, 56 and 62.)

[KR99] L. H. Kauffman and D. E. Radford, *On Two Proofs for the Existence and Uniqueness of Integrals for Finite-Dimensional Hopf Algebras*, ArXiv Mathematics e-prints (1999). (Cited in pages 20, 21 and 23.)

[Kup91] Greg Kuperberg, *Involutory Hopf algebras and 3-manifold invariants*, International Journal of Mathematics **02** (1991), no. 01, 41–66. (Cited in pages 2, 4, 14, 20, 21, 22, 23, 27 and 28.)

[Kup96] ______, *Non-involutory Hopf algebras and* 3*-manifold invariants*, Duke Mathematical Journal **84** (1996), no. 1, 83–129. (Cited in pages 2 and 20.)

[LR88] Richard G Larson and David E Radford, *Finite dimensional cosemisimple Hopf algebras in characteristic 0 are semisimple*, Journal of Algebra **117** (1988), no. 2, 267–289. (Cited in pages 20 and 22.)

[LR95] R.G. Larson and D.E. Radford, *Semisimple Hopf Algebras*, Journal of Algebra **171** (1995), no. 1, 5–35. (Cited in page 20.)

[LW05] Michael A. Levin and Xiao-Gang Wen, *String-net condensation: A physical mechanism for topological phases*, Phys. Rev. B **71** (2005), 045110. (Cited in page 3.)

[LW06] ______, *Detecting Topological Order in a Ground State Wave Function*, Phys. Rev. Lett. **96** (2006), 110405. (Cited in pages 3 and 71.)

[MMS79] R. Marra and S. Miracle-Sole, *On the statistical mechanics of the gauge invariant Ising model*, Communications in Mathematical Physics **67** (1979), no. 3, 233–240 (English). (Cited in page 62.)

[Mor83] K. Moriyasu, *An Elementary Primer for Gauge Theory*, World Scientific, 1983. (Cited in page 8.)

[OHZ06] Jaan Oitmaa, Chris Hamer, and Weihong Zheng, *Series Expansion Methods for Strongly Interacting Lattice Models*, Cambridge University Press, May 2006. (Cited in pages 9, 10 and 66.)

[Pac78] Udo Pachner, *Bistellare Äquivalenz kombinatorischer Mannigfaltigkeiten*, Archiv der Mathematik **30** (1978), no. 1, 89–98 (German). (Cited in pages 2, 18 and 19.)

[Pac91] ______, *P.L. homeomorphic manifolds are equivalent by elementary shellings*, Eur. J. Comb. **12** (1991), no. 2, 129–145. (Cited in pages 2 and 18.)

[PS97] V. V. Prasolov and A. B. Sossinsky, *Knots, Links, Braids and 3-Manifolds: An Introduction to the New Invariants in Low-Dimensional Topology*, Amer Mathematical Society, 1997. (Cited in page 2.)

[Reb83] C. Rebbi, *Lattice Gauge Theories and Monte Carlo Simulations*, World Scientific, 1983. (Cited in page 11.)

[Reg61] T. Regge, *General relativity without coordinates*, Il Nuovo Cimento (1955-1965) **19** (1961), 558–571, 10.1007/BF02733251. (Cited in page 2.)

[Rob05] Oeckl Robert, *Discrete Gauge Theory - From Lattices to TQFT*, Imperial College Press, 8 2005. MR MR2174961 (Cited in pages 2, 5, 8 and 18.)

[Sal10] S. Salinas, *Introduction to Statistical Physics*, Graduate Texts in Contemporary Physics, Springer, 2010. (Cited in pages 3 and 57.)

[Sav80] Robert Savit, *Duality in field theory and statistical systems*, Rev. Mod. Phys. **52** (1980), 453–487. (Cited in page 11.)

[Sei82] E. Seiler, *Gauge theories as a problem of constructive quantum field theory and statistical mechanics*, Lecture notes in physics, Springer-Verlag, 1982. (Cited in pages 3, 7 and 62.)

[Tun85] W.K. Tung, *Group Theory in Physics*, World Scientific, 1985. (Cited in page 11.)

[TV92] V.G. Turaev and O.Y. Viro, *State sum Invariant of 3-Manifolds and Quantum* $6j$*-Symbols*, Topology **31** (1992), no. 4, 865–902. (Cited in page 2.)

[Weg71] F. J. Wegner, *Duality in Generalized Ising Models and Phase Transitions without Local Order Parameters*, Journal of Mathematical Physics **12** (1971), 2259–2272. (Cited in pages 3, 5, 11 and 62.)

[Wen03] Xiao-Gang Wen, *Quantum Orders in an Exact Soluble Model*, Phys. Rev. Lett. **90** (2003), 016803. (Cited in page 3.)

[Wen04] ______, *Quantum Field Theory of Many-body Systems: From the Origin of Sound to an Origin of Light and Electrons*, Oxford Graduate Texts, Oxford University Press, USA, 2004. (Cited in page 3.)

[Wil74] Kenneth G. Wilson, *Confinement of Quarks*, Phys. Rev. D **10** (1974), 2445–2459. (Cited in pages 3, 5 and 71.)

[Wit88] Edward Witten, *2 + 1 dimensional gravity as an exactly soluble system*, Nuclear Physics B **311** (1988), no. 1, 46–78. (Cited in page 2.)

[Wit89] ______, *Quantum field theory and the Jones polynomial*, Communications in Mathematical Physics **121** (1989), no. 3, 351–399 (English). (Cited in page 2.)

[Wit91] ______, *On quantum gauge theories in two dimensions*, Communications in Mathematical Physics **141** (1991), 153–209, 10.1007/BF02100009. (Cited in page 5.)

[Yok05] N. Yokomizo, *Discrete Quasi-Topological Field Theories and Three Dimensions*, Ph.D. thesis, Universidade de São Paulo, 2005. (Cited in page 3.)

[YT07] Nelson Yokomizo and Paulo Teotonio-Sobrinho, $GL(2,\mathbb{R})$ *dualities in generalised* $\mathbb{Z}_2$ *gauge theories and Ising models*, Journal of High Energy Physics **2007** (2007). (Cited in pages 3, 11, 56 and 62.)

[YTSB07] Nelson Yokomizo, Paulo Teotonio-Sobrinho, and Joao C.A. Barata, *Topological low-temperature limit of Z(2) spin-gauge theory in three dimensions*, Phys.Rev. **D75** (2007), 125009. (Cited in page 37.)

[YTSM09] Nelson Yokomizo, Paulo Teotonio-Sobrinho, and Carlos Molina, *On two-dimensional Quasitopological Field Theories*, International Journal of Modern Physics A **24** (2009), no. 32, 6105–6121. (Cited in pages 3 and 59.)

USP, Universidade de São Paulo
E-mail address: njavierbuitragoa@gmail.com

Departament of Physics and Astronomy - University of Manitoba
E-mail address: fdorestyf@gmail.com